AD-A074 773 METEOROLOGY INTERNATIONAL INC MONTEREY CALIF F/G 4/2
DEVELOPMENT OF A SYNOPTIC CLIMATOLOGY OF TROPOSPHERIC REFRACTIV--ETC(U)
SEP 77 M J CUMING, F G CATON, P P KALINYAK N00228-76-C-3139
UNCLASSIFIED MII-M-226 NEPRF-TR-77-06 NL

| OF |
AD
A074773

END
DATE
FILMED
11-79
DDC

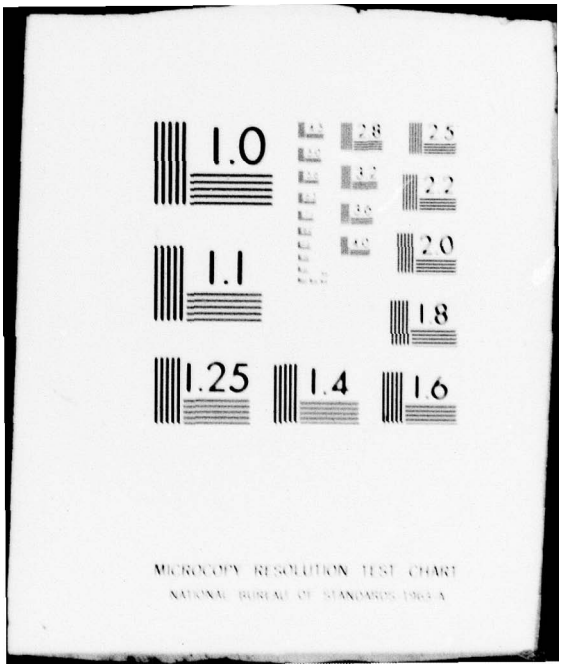
1.0
1.1
1.25
1.4
1.6
2.8
3.2
3.6
4.0
2.5
2.2
2.0
1.8
MICROCOPY RESOLUTION TEST CHART
NATIONAL BUREAU OF STANDARDS 1963-A

LEVEL III

NEPRF TR 77-06

Project M-226 FINAL REPORT
September 1977

DEVELOPMENT OF A SYNOPTIC CLIMATOLOGY OF TROPOSPHERIC REFRACTIVE CONDITIONS FOR THE EASTERN PACIFIC OCEAN OFF THE WEST COAST OF THE UNITED STATES

Task Three: The Assessment of Refractive Structures from Typical Synoptic Patterns

by

Michael J. Cuming
Francis G. Caton
Paul P. Kalinyak

Performed for:

The Commanding Officer
Naval Environmental Prediction Research Facility
Monterey, California 93940

Performed under Contract No. N00228-76-C-3139

METEOROLOGY INTERNATIONAL INCORPORATED

Monterey, California 93940

UNCLASSIFIED

SECURITY CLASSIFICATION OF THIS PAGE (When Data Entered)

(19) TR-77-06

REPORT DOCUMENTATION PAGE

READ INSTRUCTIONS BEFORE COMPLETING FORM

(18) 1. REPORT NUMBER: NEPRF Technical Report 77-06 ✓

2. GOVT ACCESSION NO.

3. RECIPIENT'S CATALOG NUMBER

(6) 4. TITLE (and Subtitle): DEVELOPMENT OF A SYNOPTIC CLIMATOLOGY OF TROPOSPHERIC REFRACTIVE CONDITIONS FOR THE EASTERN PACIFIC OCEAN OFF THE WEST COAST OF THE UNITED STATES. Task Three: The Assessment of Refractive Structures from Typical Synoptic Patterns. A073341

5. TYPE OF REPORT & PERIOD COVERED

6. PERFORMING ORG. REPORT NUMBER: M-226 ✓

7. AUTHOR(s):
(10) Michael J. Cuming
Francis G. Caton
Paul P. Kalinyak

8. CONTRACT OR GRANT NUMBER(s)
(15) N00228-76-C-3139 ✓

9. PERFORMING ORGANIZATION NAME AND ADDRESS
Meteorology International Incorporated ✓
205 Montecito Avenue
Monterey, California 93940
227 450

10. PROGRAM ELEMENT, PROJECT, TASK AREA & WORK UNIT NUMBERS

11. CONTROLLING OFFICE NAME AND ADDRESS
Commander, Naval Air Systems Command
Department of the Navy
Washington, D. C. 20361

(11) 12. REPORT DATE
September 77

13. NUMBER OF PAGES
82

14. MONITORING AGENCY NAME & ADDRESS (if different from Controlling Office)
Naval Environmental Prediction Research Facility
Monterey, CA 93940

15. SECURITY CLASS. (of this report)
UNCLASSIFIED

15a. DECLASSIFICATION/DOWNGRADING SCHEDULE

16. DISTRIBUTION STATEMENT (of this Report)

(12) 84

Approved for public release: distribution unlimited.

17. DISTRIBUTION STATEMENT (of the abstract entered in Block 20, if different from Report)

(14) NEPRF-M-226 (9) Final rept.

18. SUPPLEMENTARY NOTES

19. KEY WORDS (Continue on reverse side if necessary and identify by block number)

Refractive Index
Eastern Pacific Ocean
Pattern Characteristics
Climatology
Synoptic Patterns
Synoptic Parameters

20. ABSTRACT (Continue on reverse side if necessary and identify by block number)

The work required to develop a synoptic climatology of refractive conditions which significantly affect the tropospheric propagation of electromagnetic waves off the west coast of the United States is to be carried out under three tasks. This Report, for Task Three, describes methods and techniques developed and utilized by associating synoptic patterns and synoptic parameters with refractive conditions for the area 29° N-51° N, 120° W-140° W.

227 450

DD FORM 1 JAN 73 1473 EDITION OF 1 NOV 65 IS OBSOLETE

dcg

dcg

UNCLASSIFIED

SECURITY CLASSIFICATION OF THIS PAGE (When Data Entered)

TABLE OF CONTENTS

		Page
1.	INTRODUCTION	1
2.	THE DATA BASE OF REFRACTIVE CONDITIONS	3
	2.1 Introduction	3
	2.2 The Data Base of Upper-Air Soundings	3
	2.3 The Classification of Refractive Profiles by Continuous Parameters	3
	2.4 The Data Base of S and D Values	7
3.	THE DATA BASE OF SYNOPTIC ANALYSES	10
	3.1 Scale-and-Pattern Spectra Decompositions	10
	3.2 The Available Data Base of Synoptic Analyses	11
4.	THE RAPID ANALOGUE SELECTION SYSTEM	12
	4.1 Introduction	12
	4.2 Basic Concepts of RASS	12
	4.3 Construction of the RASS Data Base for Zones 1-5	14
	4.4 Assessment of the RASS Capability to Compare and Score Synoptic Patterns	16
5.	THE DEPENDENCE OF REFRACTIVE STRUCTURE ON THE PREVAILING SYNOPTIC SITUATION	23
	5.1 Introduction	23
	5.2 Synoptic Types and Refractive Structure	24
	5.3 Discussion of Results	44
6.	THE DEPENDENCE OF REFRACTIVE STRUCTURE ON CONCURRENT SYNOPTIC PARAMETERS	49
	6.1 Introduction	49
	6.2 Method	52

Page

6.3 Results 53

6.3.1 The Dependence of Parameter D on Contour Height. 53

6.3.2 The Dependence of Parameter D on Wind Speed and Direction 57

6.4 Discussion of Results 79

7. CONCLUSIONS AND RECOMMENDATIONS 81

8. REFERENCES 82

1. INTRODUCTION

The Naval Environmental Prediction Research Facility (NEPRF) has collected a data base of upper-air soundings recorded by radar picket ships off the west coast of the United States; the data base relates to the period October 1956 through June 1965, and to the area 29°-51°N, 120°-140°W. Under the terms of Contract No. N00228-76-C-3139, this data base was to be used to develop a synoptic climatology of tropospheric refractive conditions for that area, and to establish a more general capability for assessing refractive structures from synoptic patterns.

Technical Report No. TR 2-77 (MII) dated April 1977 [1] presents the monthly climatologies of refractive conditions developed in accordance with Task One of the contract, together with measures of the persistence and transition probabilities developed in accordance with Task Two. The development of the capability for assessing refractive structures from typical synoptic patterns, addressed by Task Three of the contract, is the subject of this Technical Report.

Sections 2 and 3 provide a brief account of the data bases of refractive structure and synoptic patterns available for this study. Section 4 describes in outline the techniques utilized for matching patterns and includes a demonstration of the effectiveness of the system even when applied to small-scale synoptic disturbances. Section 5 presents the results of utilizing this synoptic-pattern matching capability in conjunction with the data bases in order to select synoptic situations having a high probability of trapping. No such "typical" situations could be found and it is concluded that the space and time resolutions provided by the two data bases--particularly that of refractive structure--are insufficient to allow any relationship to be established even though the capability for doing so now exists. An alternative approach was therefore made, establishing statistical relationships between

refractive structure and synoptic parameters such as contour height and wind speed and direction. The results obtained are given in Section 6 and it is concluded that such techniques are capable of providing operationally significant information and are worthy of further study.

2. THE DATA BASE OF REFRACTIVE CONDITIONS

2.1 Introduction

Technical Report No. TR 2-77 (MII) discusses in detail the data base of upper-air soundings available for Tasks 1, 2 and 3. A brief review of this data base is given in Section 2.2 below. Similarly, Section 2.3 briefly recounts the technique developed during the performance of Tasks 1 and 2 for the classification of refractive profiles by continuous parameters.

2.2 The Data Base of Upper-Air Soundings

After the elimination of duplicates and demonstratably erroneous reports, there remained 6922 upper-air soundings recorded by radar picket ships during the period October 1956 through June 1965 within the area 29°-51°N, 120°-140°W. The geographical distribution of these soundings is shown in Fig. 1. In order to detect latitudinal variations of refraction conditions (a requirement of Tasks 1 and 2), the profiles in the data base were separated into latitude zones. The demarcation latitudes selected (29.0°N, 34.5°N, 37.5°N, 41.0°N) are shown on Fig. 1; the number of profiles recorded in each latitude zone is given along the ordinate.

2.3 The Classification of Refractive Profiles by Continuous Parameters

Parameter S has been designed to be a measure of the strength of surface ducting, or, if no surface duct exists, to be a measure of the proximity to surface ducting.

The definition of parameter S is

$$S \equiv \frac{10^7}{c} \frac{1}{H_\star} \left(v_{r,i} - v_{r,o} \right) \quad , \text{ provided } v_{r,i} > v_{r,o} \qquad (1)$$

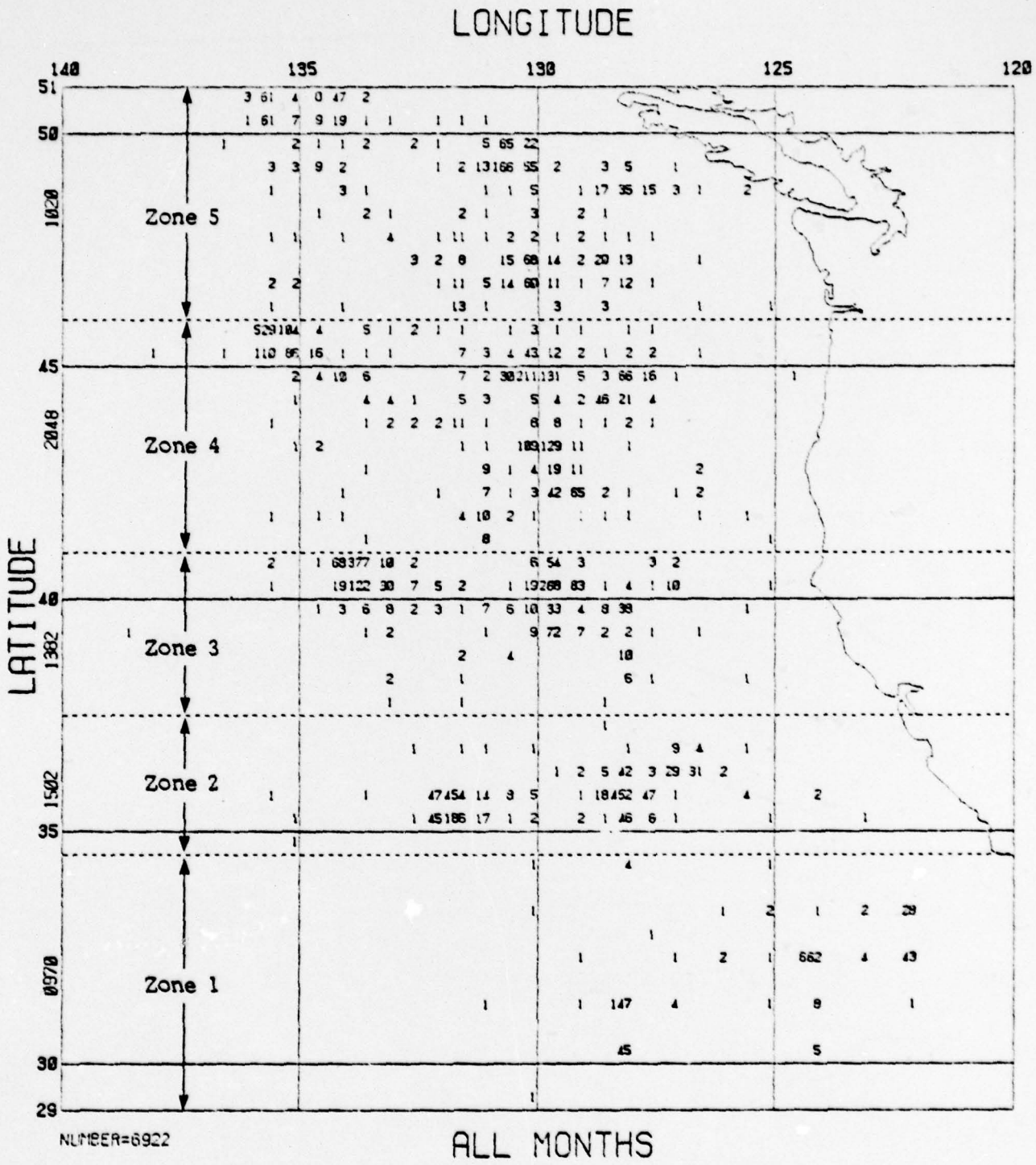

Figure 1. Geographical Distribution of Radiosonde Reports: All Months October 1956-June 1965

where $v_{r,o}$ is the surface value of the modified speed profile, v_r, and $v_{r,i}$ is the maximum value in the profile above the surface. H_* is a specified scaling height. The extension of the definition in the base of no surface duct, i.e., if $v_{r,o}$ is the maximum speed in the profile, is given by

$$S \equiv \frac{10^7}{c}\left(\frac{v_{r,i} - v_{r,o}}{H_i}\right)_{max} , \quad \text{where } v_{r,i} < v_{r,o} \qquad (2)$$

and H_i is the height of level i. This extension gives a measure of the proximity of the profile to a surface duct situation. This negative extension of S is not necessarily related to the bottom layer defined by the first reported level ($i = 1$) above the surface; the maximum may occur for $i = 2$ or higher.

The total tropospheric ducting parameter D is similar to S except that it need not be surface based:

$$D \equiv \frac{10^7}{c}\left(v_{r,j} - v_{r,i}\right)_{max} , \quad \text{provided } v_{r,j} > v_{r,i} \text{ and } j > i . \qquad (3)$$

For no ducting:

$$D \equiv \frac{10^7}{c}\left(\frac{v_{r,j} - v_{r,i}}{H_j - H_i}\right)_{max} , \quad \text{where } v_{r,j} < v_{r,i} . \qquad (4)$$

Table 1 shows the relationships between various measures of refractivity, including the S and D parameters, together with the terminology used for referring to discrete categories of refractive conditions.

Table 1

Relationship between values of the S and D parameters and other standard measures of refractivity

Vertical Derivative/ Parameter	Trapping/Ducting			Super-Refraction		Normal (N)	Sub-Refraction
	Strong (DS)	Moderate (DM)	Weak (DW)	Strong (SS)	Weak (SW)		
S	← 0.79	↔ 0.40	↔	0 ↔	-0.40	↔ -0.79	→
D	← 0.79	↔ 0.40	↔	0 ↔	-0.40	↔ -0.79	→
$\frac{10^7}{c}\frac{dv_r}{dH}$	←		→	0 ↔		-0.79 ↔ -1.57	→
$\frac{10^7}{c}\frac{dv}{dH}$	←		→	1.57 ↔		0.79 ↔ 0	→
$\frac{dN}{dH}$	←		→	-1.57 ↔		-0.79 ↔ 0	→
$\frac{dM}{dH}$	←		→	0 ↔		0.79 ↔ 1.57	→

The S and D parameters, calculated in accordance with Eqs. (1) through (4), are a measure of the most positive/least negative values. As a consequence no values of S and D corresponding to sub-refractive conditions were ever observed.

Every profile provides a value for S and a value for D. Because D is determined from the whole profile, whereas S is only applicable to the surface, the values of S and D will coincide if the base of the most positive/least negative layer is at the earth's surface. However, if this layer is aloft, then the profile will give different values for S and D.

2.4 The Data Base of S and D Values

Values of the S and D parameters were calculated for each of the 6922 profiles in the data base of upper-air soundings. This derived data base of S and D parameters has been used in the performance of all three Tasks of the current project.

Investigation of the relationships between refractive structure (as measured by S and D) and the synoptic patterns prevailing at the time the profile was recorded required, of course, a correspondence between the data base of profiles and the data base of synoptic analyses--only those profiles could be used for which the corresponding-in-time synoptic analysis was available. This requirement reduced the number of usable profiles (for certain aspects of Task 3) from 6922 to about 4320.

Figures 2 and 3 show values of the S and D parameters in each of the 5 latitude zones for two years selected from the total period (October 1956 to June 1965); only those values are given for which corresponding synoptic analyses are available. Figure 2 (1960) shows the "best" year of data coverage, whereas Fig. 3 (1963) shows a "typical" year. The obvious limitations of the available data base are discussed in the Sections for which these limitations are significant.

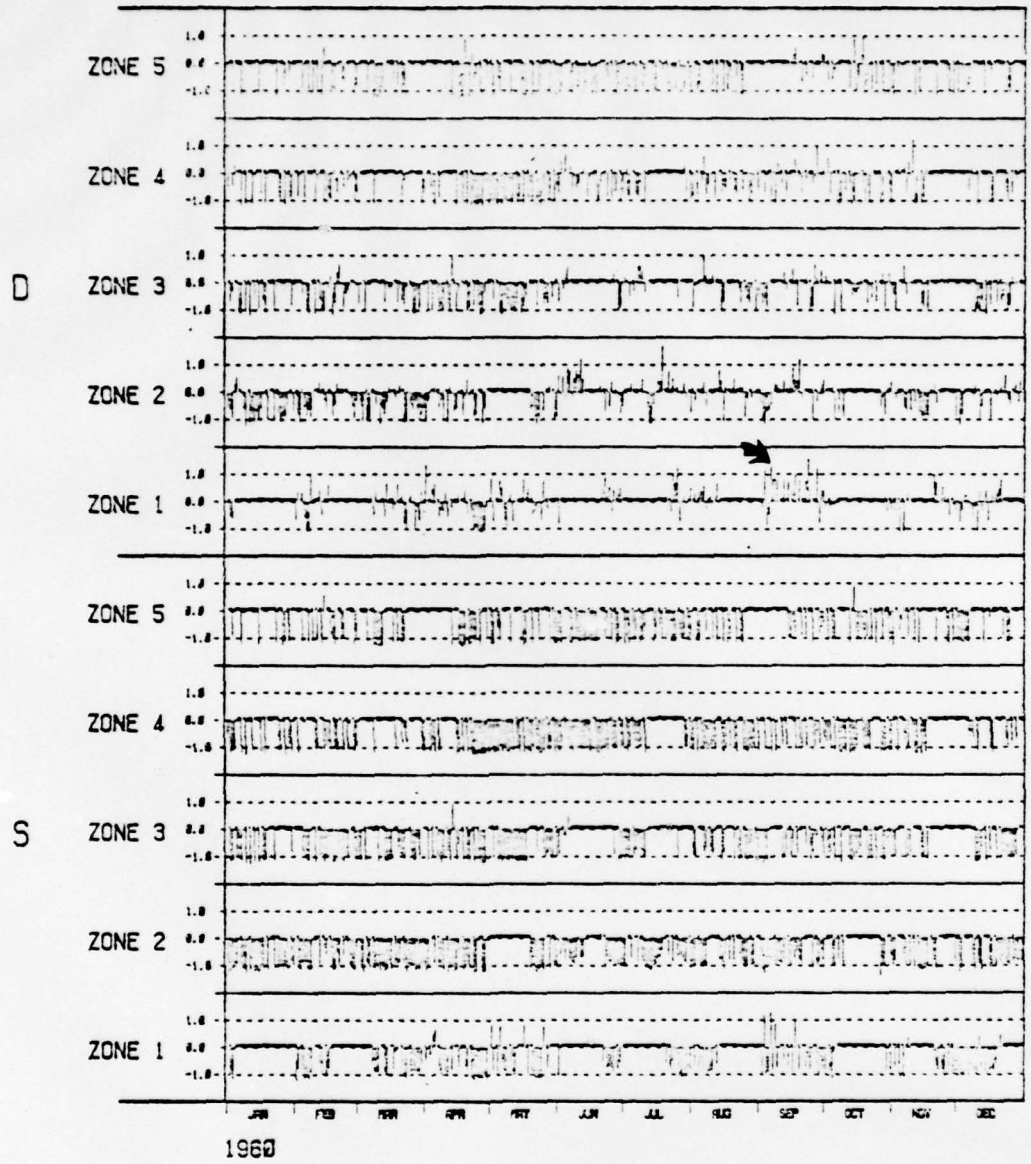

(crosses denote no profile available)

Figure 2. Chronological Distribution of the S and D Parameters for Zones 1-5

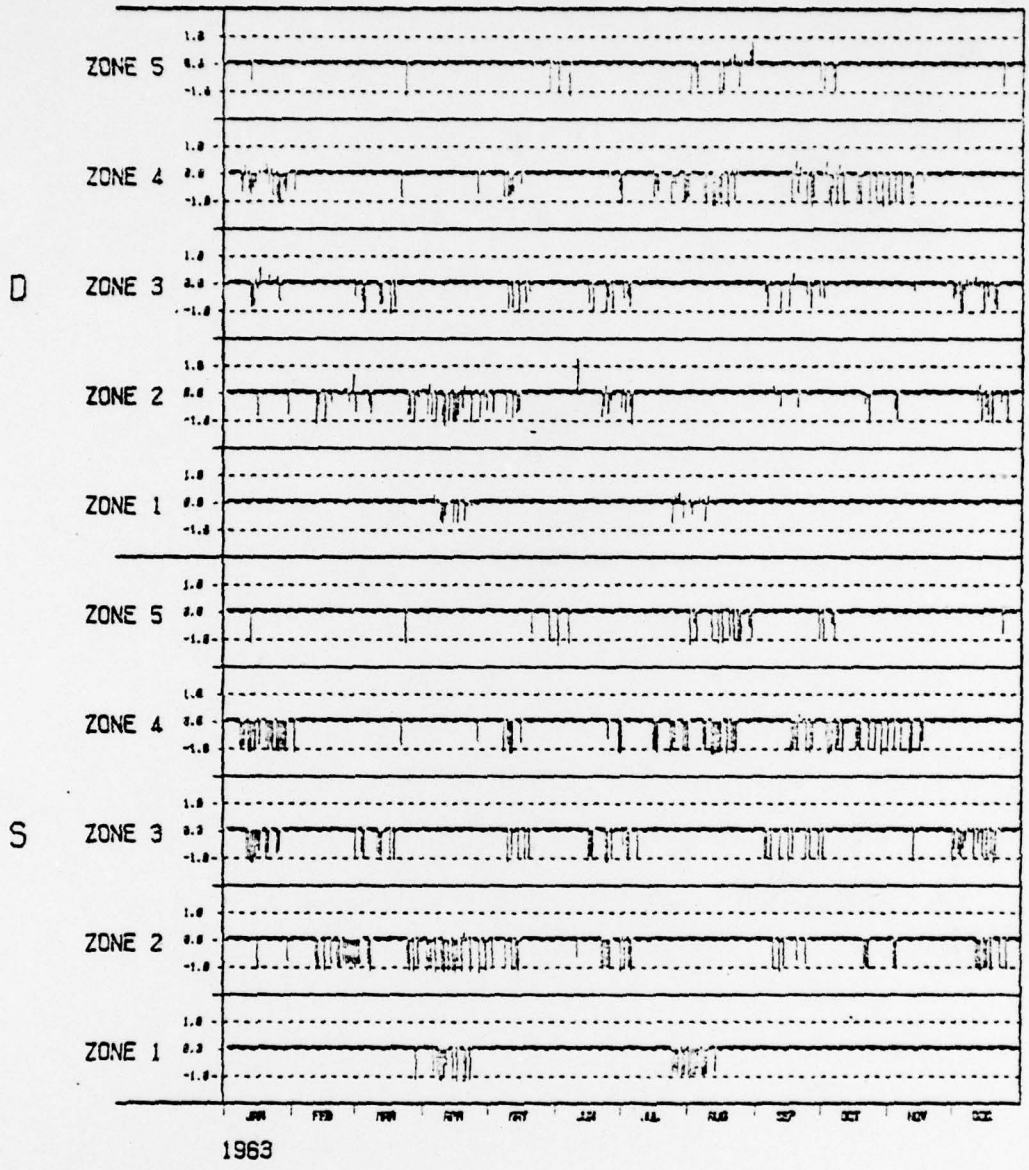

(crosses denote no profile available)

Figure 3. Chronological Distribution of the S and D Parameters for Zones 1-5

3. THE DATA BASE OF SYNOPTIC ANALYSES

3.1 Scale-and-Pattern Spectra Decompositions

Two of the fundamental concepts in the interpretation of meteorological fields are those of pattern and scale. In 1963, MII developed an objective technique [2] for separating any geophysical field into recognizable patterns, or features, evident in the field, so that their relative contributions to the total can be quantitatively represented.

Using the 500-mb field (HT) as an example, this may be decomposed into additive component ranges-of-scale expressed by:

$$HT = SD + SR$$

$$= SD + SL + SV$$

where SD is the Disturbance range-of-scale component,

SR is the Residual range-of-scale component,

SL is the Long-wave range-of-scale component,

SV is the Planetary Vortex.

By definition, $SR = SL + SV$.

The concepts of scale-and-pattern spectra and decomposition have many applications to environmental studies, analyses and forecasts; these concepts have been used in this project.

3.2 The Available Data Base of Synoptic Analyses

The available archived records consist of six component fields for the whole of the Northern Hemisphere for each date-time group. These are the three component-range-of-scale (SV, SL and SD) fields for the 500-mb and 1000-mb height fields. An additional three thickness fields, one for each scale component, are produced from the 500-mb and 1000-mb isobaric fields as differences. Each of these nine fields is expressed by a 63x63 array of grid-point values. (Part of this array is shown in Fig. 4, page 15.) The 30 years of available history of once daily and twice daily coverage is summarized as follows:

JAN 1946 - MAR 1955	once daily	(12Z)
APR 1955 - MAR 1960	twice daily	(00Z and 12Z)
APR 1960 - DEC 1964	once daily	(12Z)
JAN 1965 - DEC 1975	twice daily	(00Z and 12Z)

Matching the date-time groups of the recorded upper-air soundings (Section 2.2) with those of the archived fields produced the 4320 cases (Section 2.4) for which both S and D values and analyses were available.

4. THE RAPID ANALOGUE SELECTION SYSTEM

4.1 Introduction

In June 1976 MII was awarded Contract No. N00228-76-C-3189 to continue with the development of a Rapid Analogue Selection System (RASS) on behalf of NEPRF. This development is the subject of a separate report [3] and so only a brief outline of the pertinent features will be presented here, together with those modifications made to RASS for application to Task 3 of this project.

4.2 Basic Concepts of RASS

Analogue selection is based on an ability to recognize significant degrees of similarity between an event selected from recorded meteorological history and all the other recorded events. The selected event is referred to as the "baseday". [For forecasting purposes the baseday is, of course, the current synoptic pattern. However any synoptic pattern from the recorded history may be chosen as baseday.]

Having chosen the baseday, a comparison is then made, one at a time, with all other recorded synoptic events and a score assigned to each "analogue candidate". Those events similar (in meteorologically-significant pattern characteristics) to the baseday achieve a higher score than events which are dissimilar. Thus the score, or "match coefficient", is a measure of the degree of similarity. Those analogue candidates reaching an acceptable level of similarity are recognized as "analogues" of the baseday.

The MII Rapid Analogue Selection System is based on a bit coding of all recorded synoptic events expressed in terms of their nine component

fields[1]--the 3 ranges-of-scale (SV, SL, SD) for the 500-mb and 1000-mb levels, and the 500-1000-mb thickness for each range-of-scale. The bit coding methodology developed takes into account the variations in resolution required by the three different scales of atmospheric disturbance. Each synoptic event is represented by a bit string and, by comparing the bit string for a baseday with that for any analogue candidate, a count of the number of matching bits provides an absolute measure of the degree of similarity between the two synoptic events. The comparison is made in stages and an analogue candidate which fails to maintain a predetermined rate of scoring is automatically rejected at that stage. This screening process markedly reduces the time required to search the 30 years of available history for the top-scoring analogues. In addition weight factors can be applied to the actual score at each stage. These weights can be adjusted (tuned) to emphasize any desired feature or combination of features (i.e., range-of-scale, level, thickness, resolution) of the synoptic situations being compared.

Analogue selection based on the total hemisphere can only be useful in the broadest terms because of the great variability in synoptic patterns occurring simultaneously over the hemisphere. Experience has shown that, on the synoptic scale, the range of variabilities is so great that the available data base of meteorological history (30 years) is insufficient to provide analogues unless the selection criteria are made so coarse that synoptic-scale disturbances play little part in determining analogue selection. To choose analogues for synoptic-scale disturbances the analogue selection system must have the ability to "focus" on a specified region, making no attempt to match irrelevant external events. This capability is a feature of RASS and has

[1]See Sections 3.1 and 3.2.

been tested and evaluated by application to the Greater Mediterranean region [3].

The regional focus capability of RASS is accomplished by dividing the 63x63 elements of the hemispheric array into modules. Thus, for example, to represent the SD range-of-scale at full resolution,[2] the hemispheric array is divided into non-overlapping modules of 4x4 elements. To represent the SL range-of-scale modules of 8x8 are used, and the SV range-of-scale utilizes modules of 12x12. To focus on a geographical region the appropriate SD, SL and SV modules covering that region are chosen. (Note that modules from <u>different</u> ranges-of-scale <u>do</u> overlap, thus providing SD, SL and SV coverage for the region.)

4.3 Construction of the RASS Data Base for Zones 1-5

To cover the area of interest (Zones 1-5 as shown on Fig. 1) only one module for each of the three ranges-of-scale was required. The selected modules are shown in Fig. 4, together with the approximate locations of the radar picket ships.

During the course of RASS development the available 30-year history of synoptic analyses for the Northern Hemisphere was converted to the bit-string representation outlined in Section 4.2. This RASS data base was used to construct a data subset covering the period October 1956-June 1965 for the three modules shown on Fig. 4. This data subset was, of course, in the RASS bit-string format.

---

[2] RASS allows three degrees of resolution for each of the three ranges-of-scale, this being accomplished by combining basic full-resolution modules.

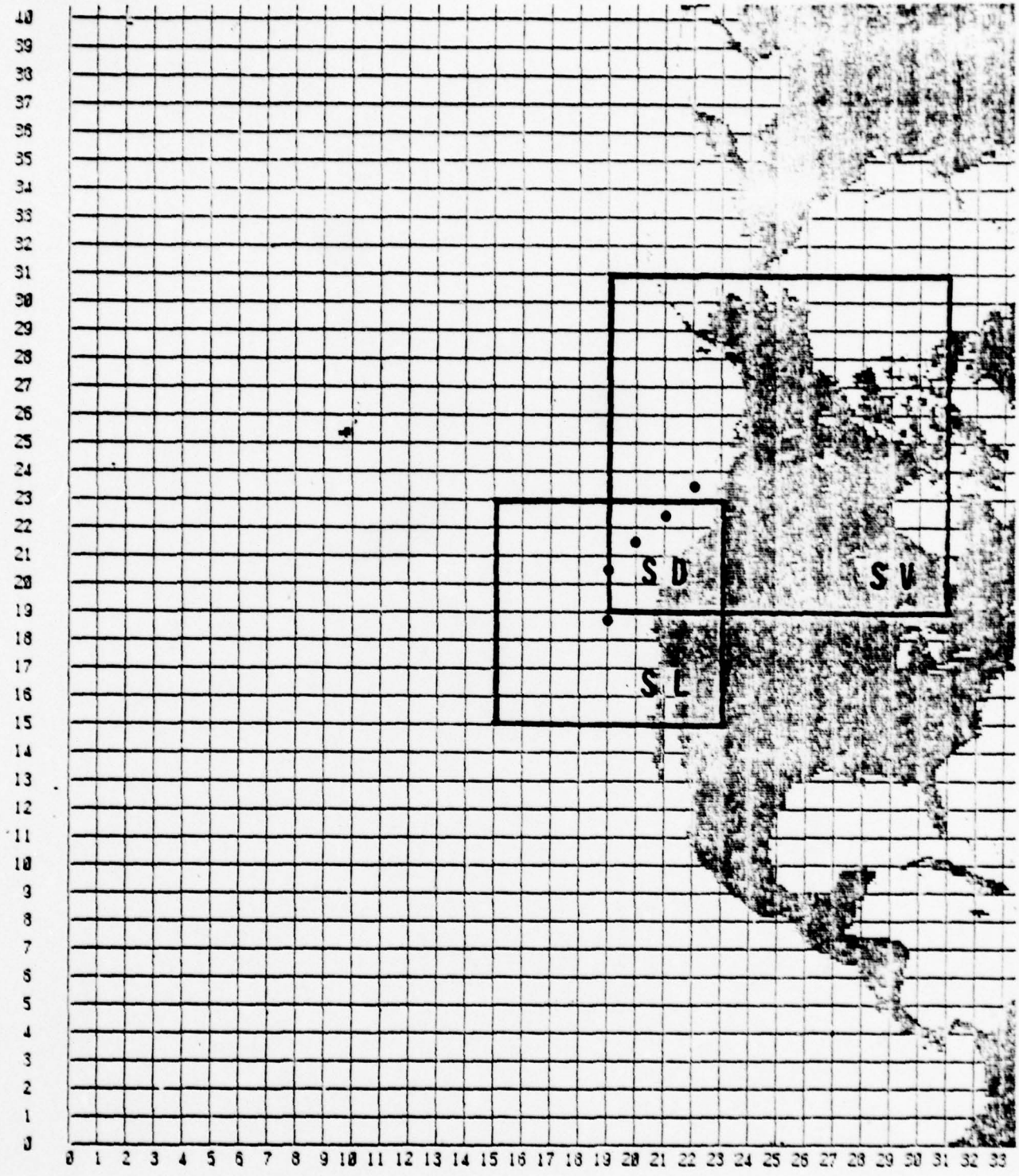

Figure 4. Part of the 63x63 Northern Hemisphere Polar Stereographic Grid showing the 3 Modules (SV, SL, SD) used for Pattern Matching. The dots lying in or near the SD module show the approximate mean location of the radar picket ships.

Once this data subset had been constructed, the capability then existed, using RASS, to compare and score any two synoptic patterns affecting Zones 1-5. Assessing the effectiveness of this capability, a necessary prerequisite to its use in linking synoptic patterns and refractive conditions, is described in Section 4.4.

4.4 Assessment of the RASS Capability to Compare and Score Synoptic Patterns

Previous experience with RASS has been confined to analogue selection based on comparatively large regions[3] requiring several modules for the adequate representation of the various scales of atmospheric disturbance. As can be seen from Fig. 4, only one module for each range-of-scale is required to cover the area of interest and its was decided therefore, before proceeding further, to test and assess the effectiveness of RASS when using the very small region of focus demanded by this project.

When matching the nine component fields of a chosen baseday situation against the corresponding nine component fields of an analogue candidate, in general the smaller the scale of atmospheric disturbances represented by a particular component field the more "difficult" it is to find a good match. The reason for this, of course, is that for a fixed area, the range of variabilities that can be encompassed by the area depends inversely on the characteristic wavelength of the atmospheric disturbances involved. Thus the most difficult test of the effectiveness of any analogue selection system is to base it on the 1000-mb SD scale of atmospheric disturbance.

As explained in Section 4.2, RASS scoring and ranking is based on a count of the matching bits between the bit string representing the baseday

---

[3]The smallest region of focus studied in any detail prior to this project is the Greater Mediterranean [3].

situation and the bit string representing the analogue candidate. This count provides an absolute measure of the degree of pattern similarity between the two situations. In general it is more convenient to use the "match coefficient" which expresses the number of matching bits as a fraction of the total number of bits used to represent each situation. Thus a match coefficient of 1.00 implies a "perfect" match.

Figure 5 shows part of the full hemispheric analysis of the SD_{1000} field for 12Z on 6 September 1960. The region of focus used in analogue selection is outlined, corresponding to the single SD module shown on Fig. 4. Using this analysis as baseday and basing the scores of analogue candidates entirely on the degree of SD pattern similarity within this single module, the RASS data base of synoptic situations was searched for the best match. This was found to be the 00Z analysis of 5 August 1958, shown in Fig. 6, with a match coefficient of 0.95. Other selections were made with match coefficients of 0.92 and 0.87; these are shown in Figs. 7 and 8 respectively. Note the (visual) dependence of pattern similarity on the match coefficient and the effectiveness of the focusing capability--no attempt is made by the system to match patterns outside the selected area. Figure 9 shows an analysis with a match coefficient of 0.60, this chart being selected to demonstrate the effect of a "poor" match. Although pressure remains relatively high to the north, note the effect on the orientation of pressure gradient. A match coefficient tending toward zero would, of course, show relatively high pressure to the south.

It is concluded that RASS, as modified for this particular project, is an extremely effective tool for selecting matching patterns on even the SD scale of atmospheric disturbance. How this capability was utilized and linked to the data base of refractive conditions is described in Section 5.

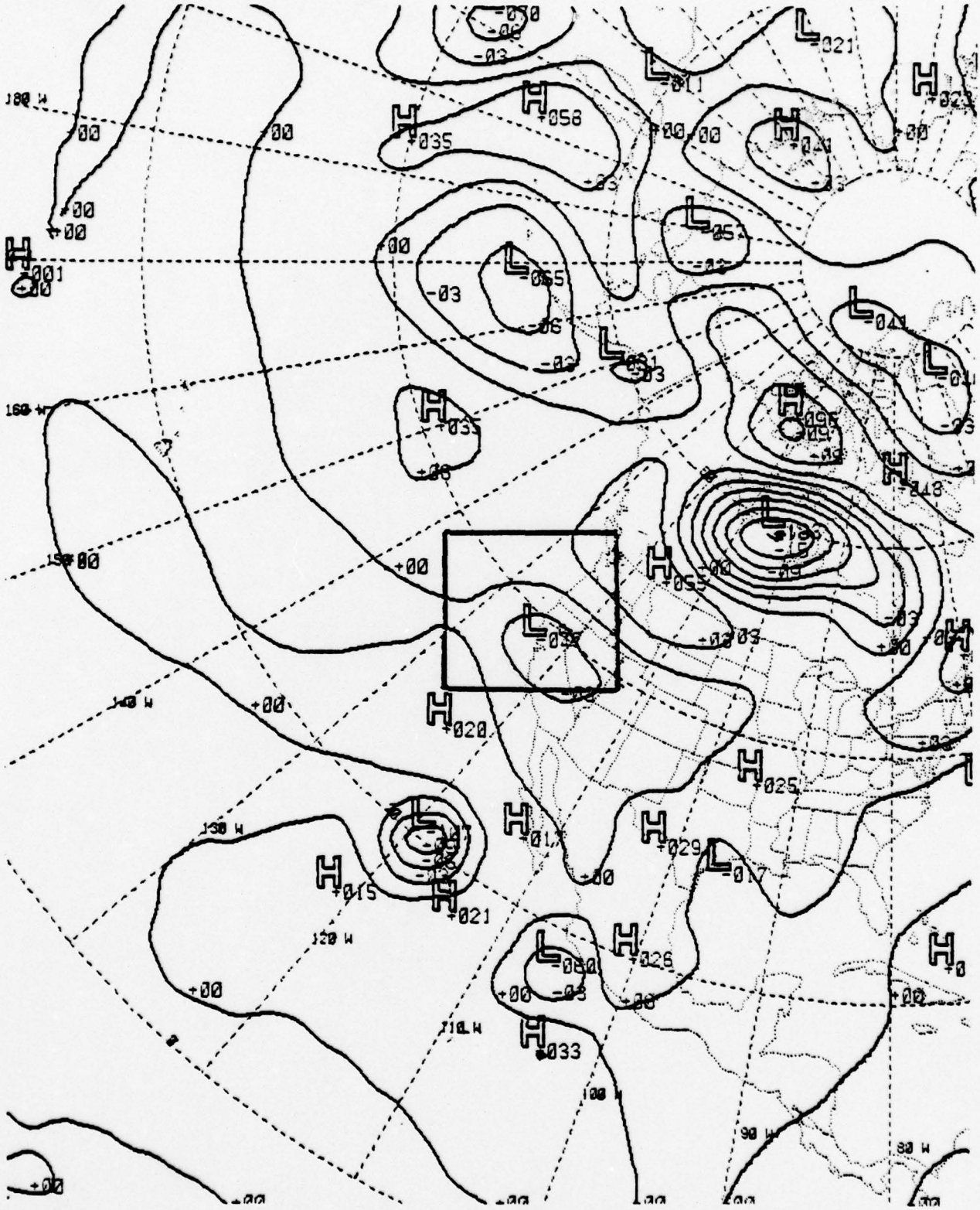

Figure 5. SD_{1000} Analysis for 12Z 6 September 1960.
Baseday used for analogue selection (match coefficient = 1.00).

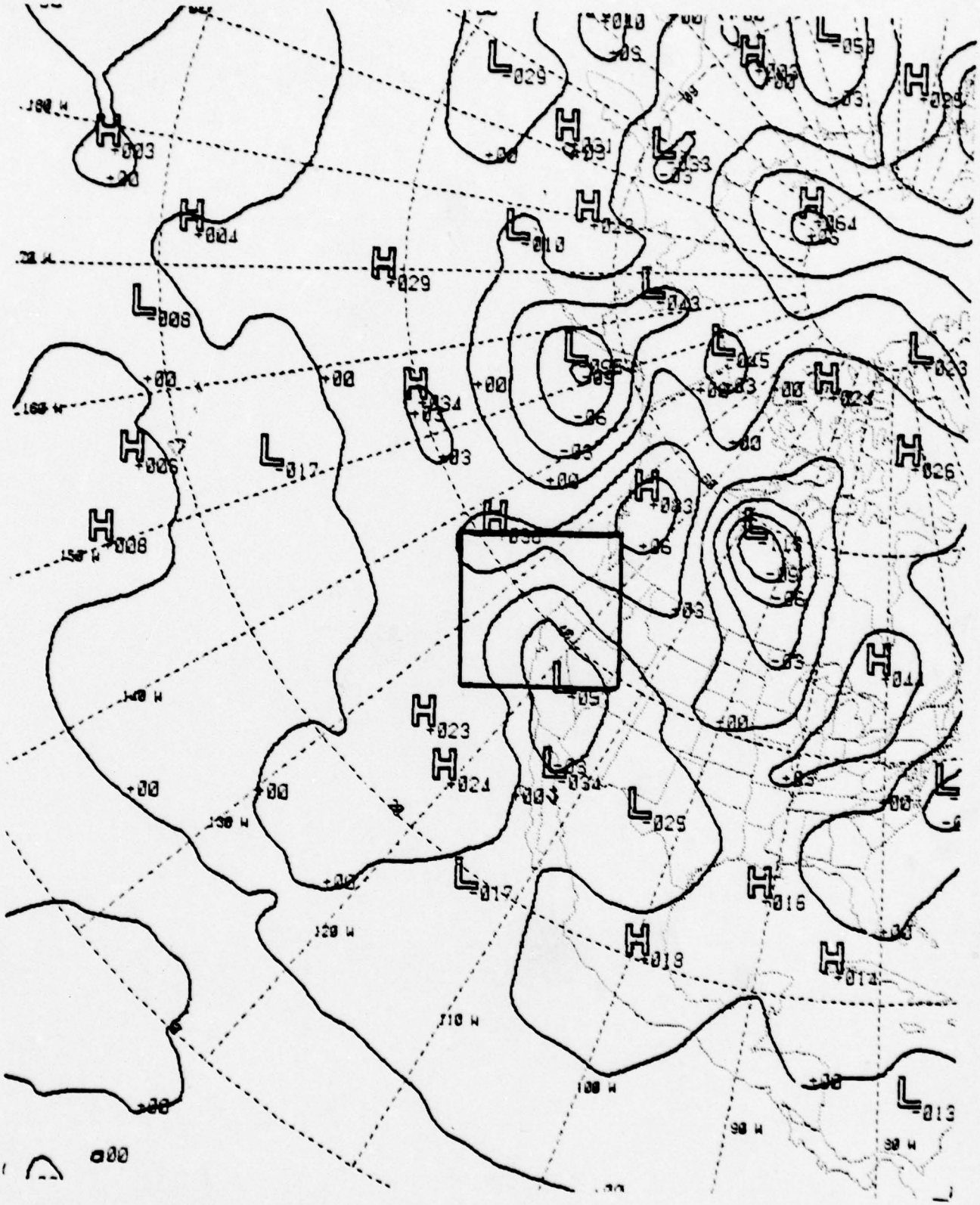

Figure 6. SD_{1000} Analysis for 00Z 5 August 1958.
Match coefficient 0.95 with Fig. 5 as baseday.

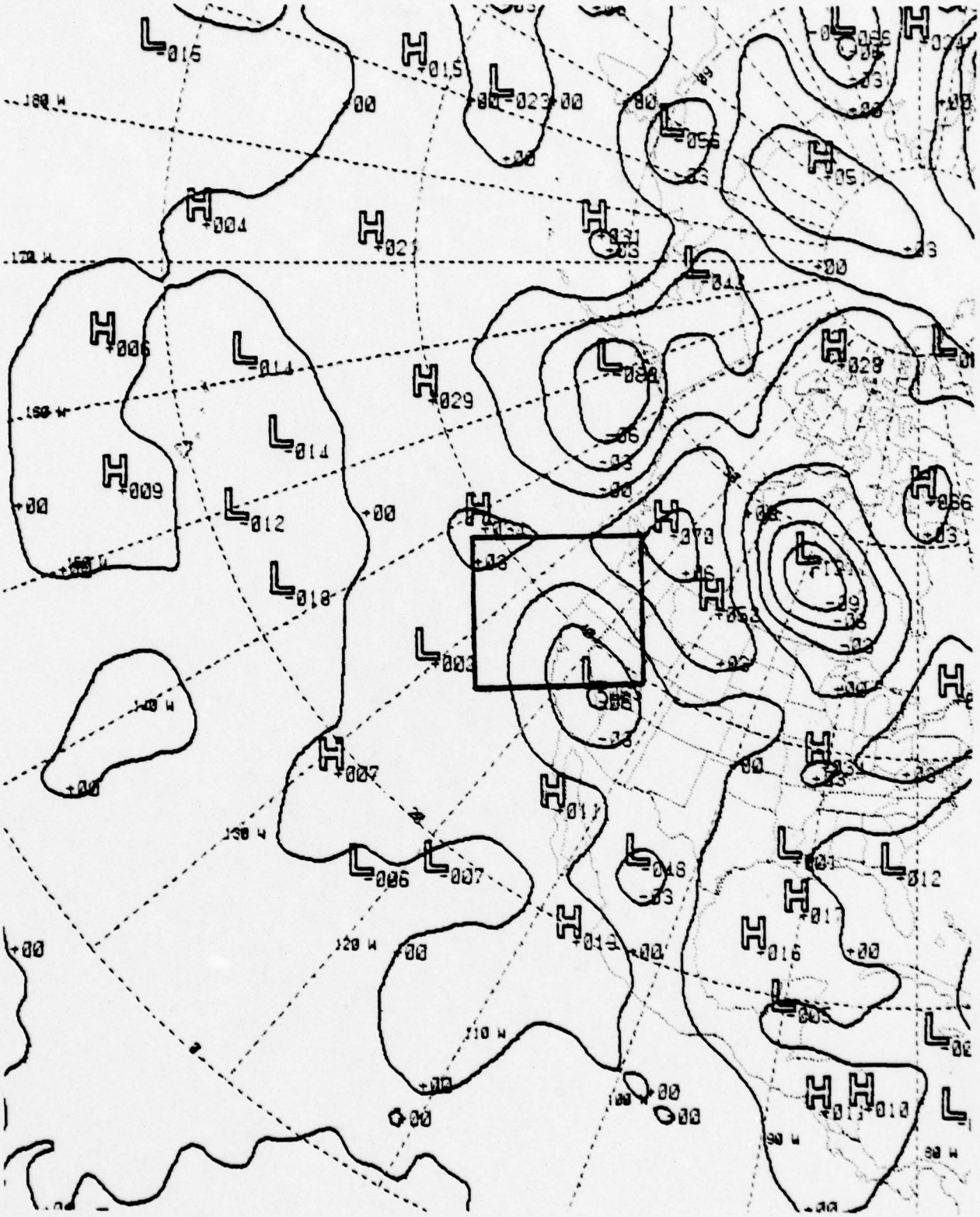

Figure 7. SD_{1000} Analysis for 12Z 5 August 1958.
Match coefficient 0.92 with Fig. 5 as baseday.

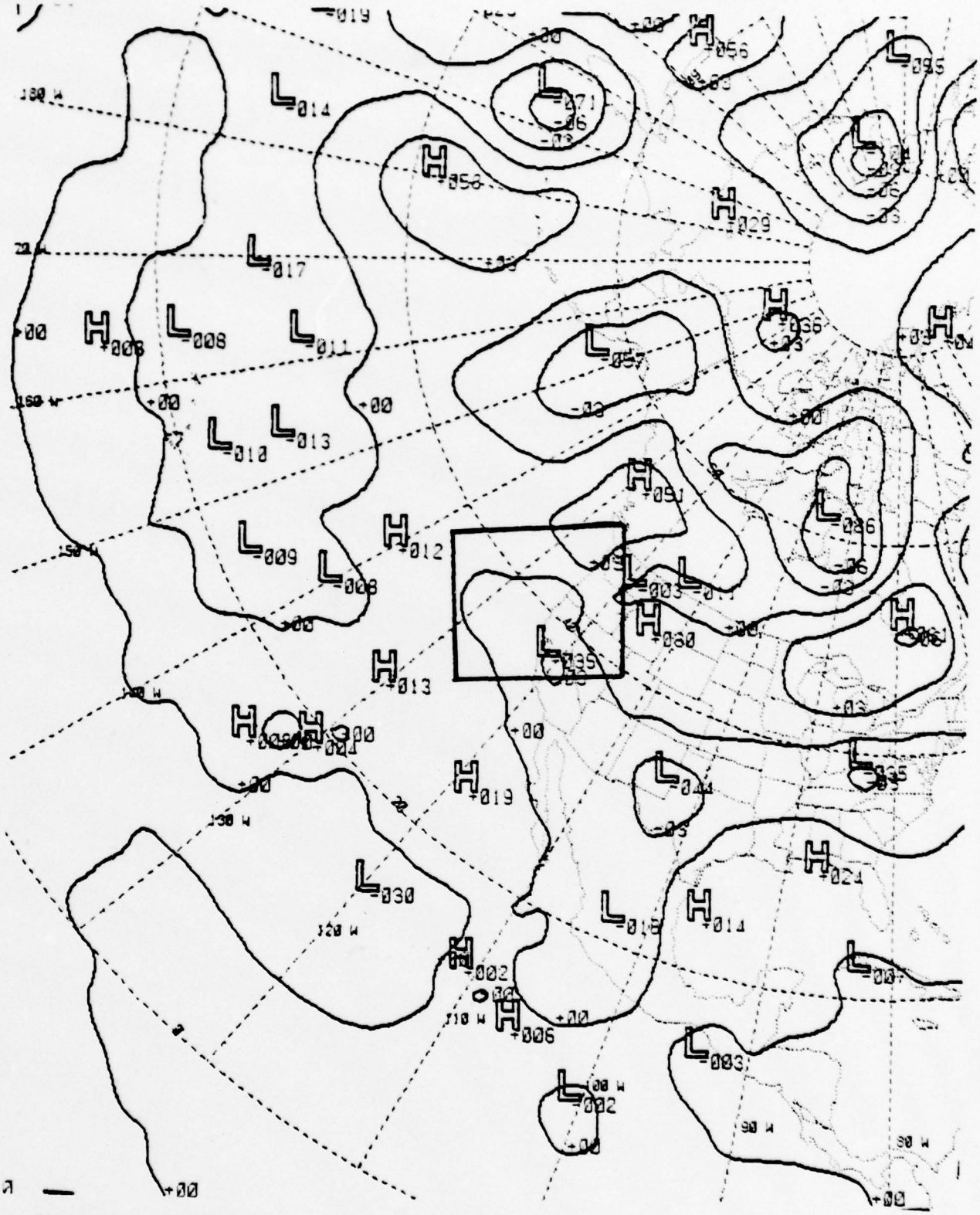

Figure 8. SD_{1000} Analysis for 00Z 1 August 1958.
Match coefficient 0.87 with Fig. 5 as baseday.

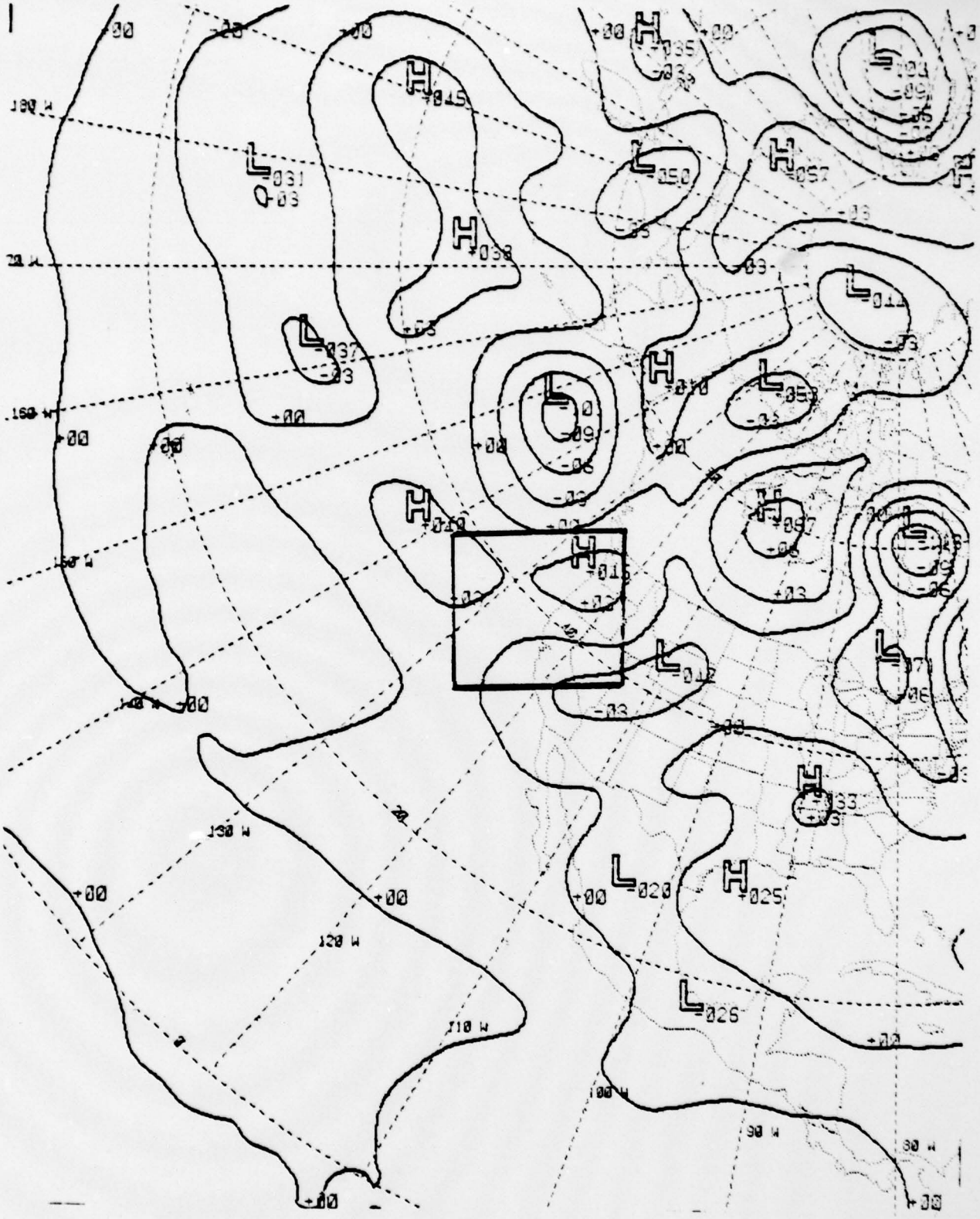

Figure 9. SD_{1000} Analysis for 12Z 15 June 1960.
Match coefficient 0.60 with Fig. 5 as baseday.

5. THE DEPENDENCE OF REFRACTIVE STRUCTURE ON THE PREVAILING SYNOPTIC SITUATION

5.1 Introduction

By this stage in the performance of the overall project we had:

a. Prepared a data base of refractive conditions in the form of S and D parameters;

b. Modified the Rapid Analogue Selection System to use the appropriate region of focus;

c. Prepared a data base of synoptic situations in the RASS bit-coded format for the region of focus;

d. Demonstrated the ability of RASS to select from the data base those synoptic patterns most closely resembling those of a chosen baseday.

Given these preparations it then became possible to investigate whether or not a significant relationship exists between a particular type of synoptic situation and the associated refractive structure.

For reference purposes it is convenient to postulate an idealized approach, thus:

a. Select a particular refractive structure--for example, an unusually high value of D;

b. Using the concurrent synoptic situation as baseday, utilize the regionalized capabilities of RASS to score and rank the other situations in the data base;

c. Compare the refractive structures of the analogue candidates with the refractive structure of the baseday to determine significant facets of similarity. (Thus, for example, if the

refractive profiles associated with the higher-scoring situations were to exhibit values of the D parameter which, like the baseday, also were unusually high, then the baseday synoptic situation would define a "synoptic type", the occurrence of which could be associated with a high probability of trapping.)

The difficulty in this approach became apparent when attempts were made to select basedays having pronounced trapping on the scale of the available synoptic patterns. Inspection of Figs. 2 and 3 shows that the variability of the refractive conditions is of a smaller scale in space and time. It became inevitable that the above ideal approach would have to give way to more-statistical treatments.

5.2 Synoptic Types and Refractive Structure

Representing a synoptic situation by the gridded fields of three basic parameters--the 1000-mb height, 500-mb height and 500-1000-mb thickness--conceals, of course, much of the variability associated with that particular state-of-the-atmosphere. Nevertheless it is generally accepted that such a representation enables a synoptic situation to be meaningfully defined for the purposes of meteorological forecasting. RASS uses the component fields (SV, SL, SD) of each of these three basic parameters to represent the synoptic situation in a bit-coded format. The bit code is produced by considering certain ranges of values of the component fields, and, in this process, some of the variability present in the field of the basic parameters is also lost.

However, in spite of this loss of represented variability in passing from an actual synoptic situation to its full-resolution bit-coded format, no two synoptic situations have ever been found which have a matching coefficient close to 1.0 for all nine component fields. Thus based on

evidence to date, ALL synoptic situations are unique, even after part of the atmospheric variability has been discarded by the processes described above.

A "synoptic type" may be regarded as a synoptic situation which, within acceptable limits of similarity, occurs with some regularity. In the past, synoptic types have been determined qualitatively by visual inspection of large numbers of synoptic charts with the objective of discovering, for example, synoptic patterns which regularly affect an area of interest and which can be associated with a particular type of weather phenomena.[1] (In effect, of course, the attempt to establish synoptic types is an analogue approach to weather forecasting.) Usually the selection of synoptic types is based on one level in the atmosphere, sea-level pressure being the most common choice, although some classifications attempt to take a broad-brush account of an upper-level flow such as that at 500mb. Weather typing methodologies of a descriptive/qualitative nature suffer from a major defect--they have to be so broadscale that they fail to encompass the meteorologically significant facets of the situation.

It has long been known that ducting is more likely to occur in certain broadscale synoptic situations than in others. For example, ducting is frequently associated with a subsidence inversion in a warm high-pressure area, and an example of this situation is the Pacific anticyclone that normally covers the oceanic region shown in Fig. 1.

Although trade inversion characteristics vary greatly in space and time [5], in general the atmospheric circulation is such that the subsidence

---

[1] A good example of weather typing is provided by Weather in the Mediterranean [4].

effects are most marked in the eastern region of the anticyclone, producing a strong inversion that usually lies at about 500 to 1500m above sea level [6]. Figures 10, 11 and 12 are taken from a detailed study of the inversion over the eastern North Pacific Ocean by Neiburger *et al.* [7]. Figure 10, the average height of the inversion base during summer months, shows that the height in general increases toward the north and to the west. Figure 11 shows a cross-section of mean temperature between San Francisco and Honolulu; note the decrease of inversion intensity and the increase of inversion height toward the west. Figure 12 shows the percentage of observations (available to Neiburger) with no inversions during the months June-September.

The great variability in space and time of inversion characteristics (and the concomitant variability of ducting occurrences) takes place within the framework of the synoptic type that affects most of the region of interest for most of the time--i.e., the Pacific anticyclone. As an example of the variability of the D parameter than can occur within apparently similar synoptic situations, Figs. 13 through 16 show the 1000-mb and 500-mb charts for 12Z 26 JAN 65 and 00Z 27 JAN 65. Shown on these charts are the locations and values of the D parameters obtained concurrently with these charts. In all cases the picket ships are located near the center of an anticyclone at 1000-mb under a 500-mb ridge. Note that the more southerly D value has changed from -0.46 to +0.43 in 12 hours (i.e., from weak super-refraction to moderate ducting) while the charts for 00Z 27 JAN 65 show +0.43 for the southerly ship and -0.83 for the ship about 250 miles to the north. Similar variabilities were found within other situations and sequences. No reasons based on visually-determined differences between these charts can be established and supported for explaining the observed variations of the D parameter.

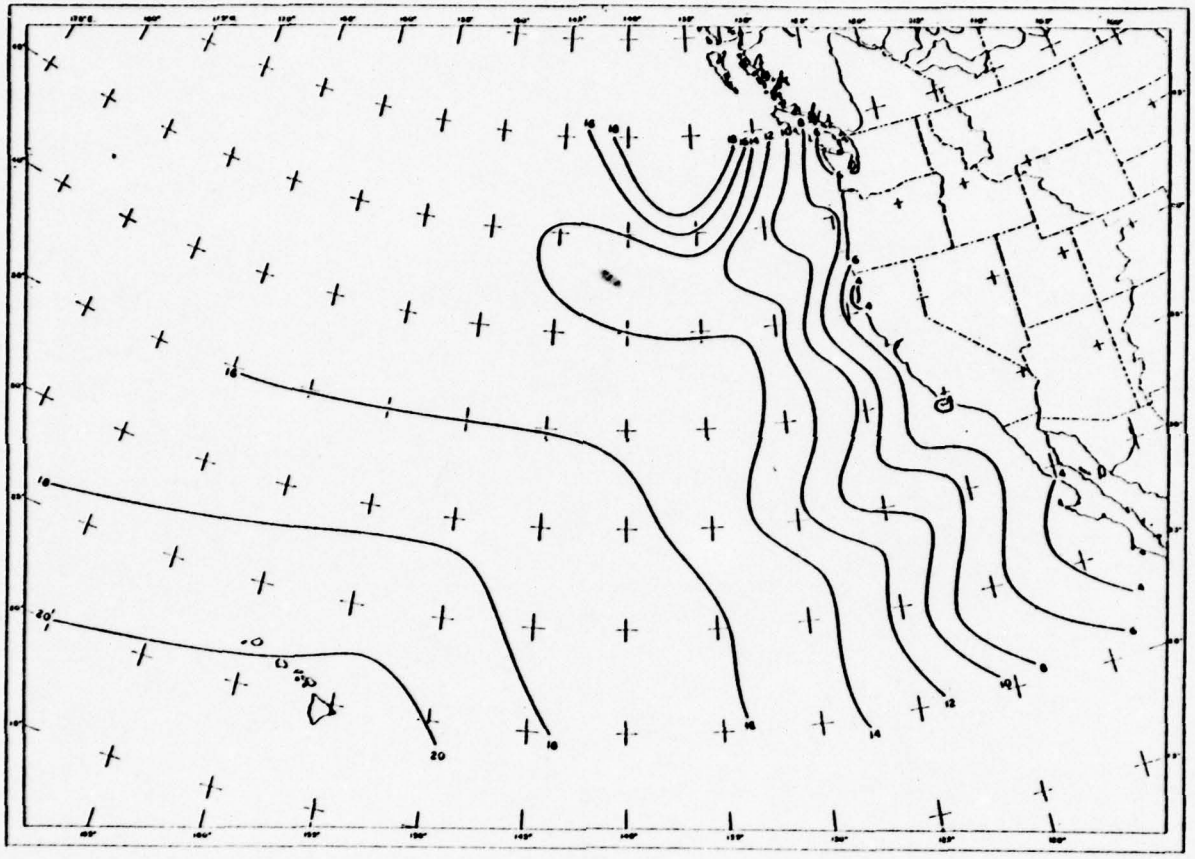

Figure 10. Average Height of Inversion Base during Summer (hundreds of meters). [7]

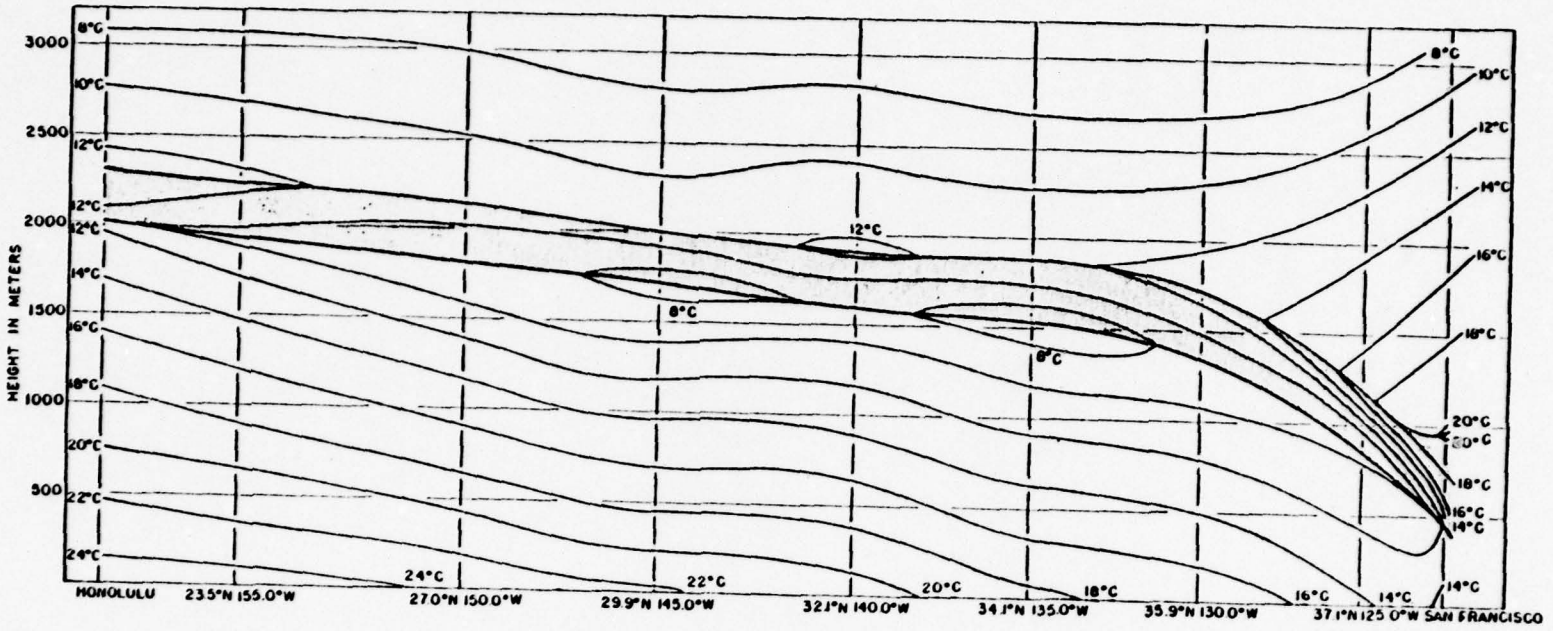

Figure 11. Cross Section Showing Average Temperature (°C) between San Francisco and Honolulu in Summer; Inversion Layer Shaded. [7]

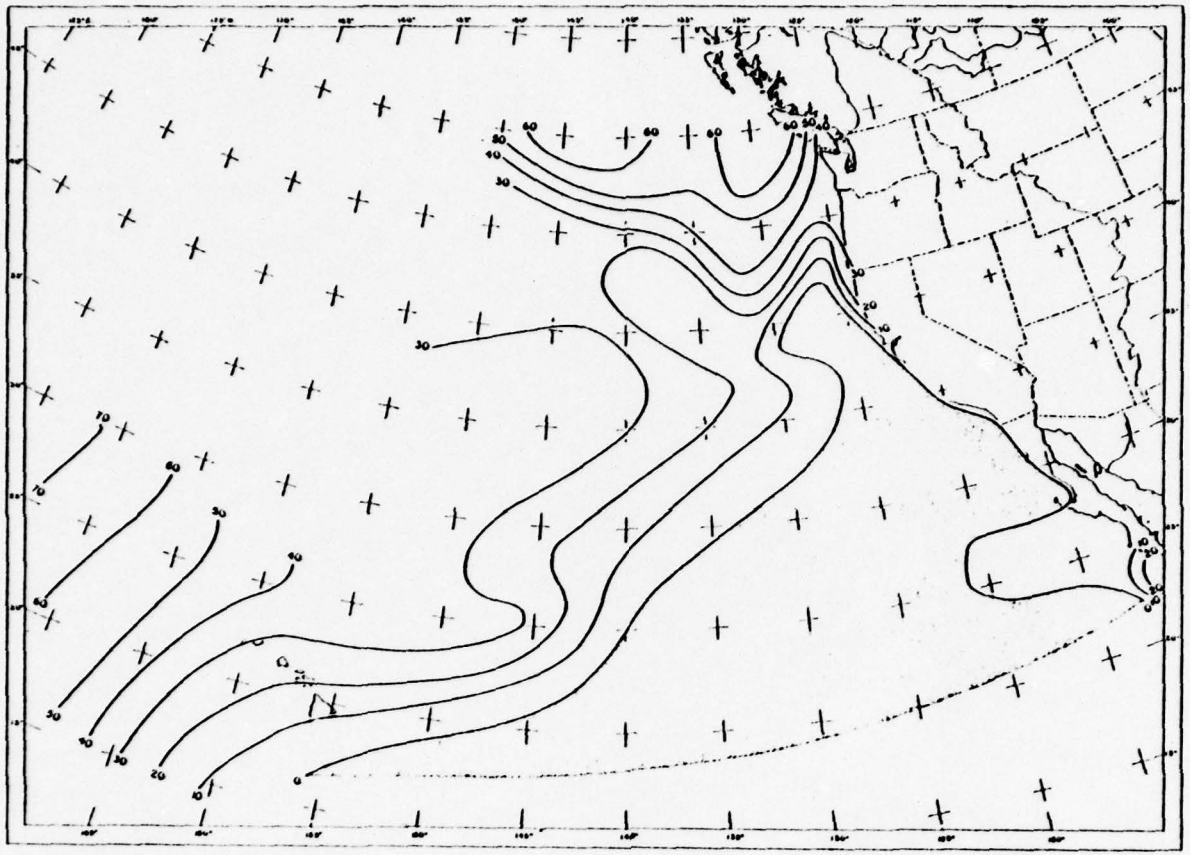

Figure 12. Percentage of Observations with No Inversions during the Months June-September. [7] Note that within the shaded area all observations showed the inversion to be present.

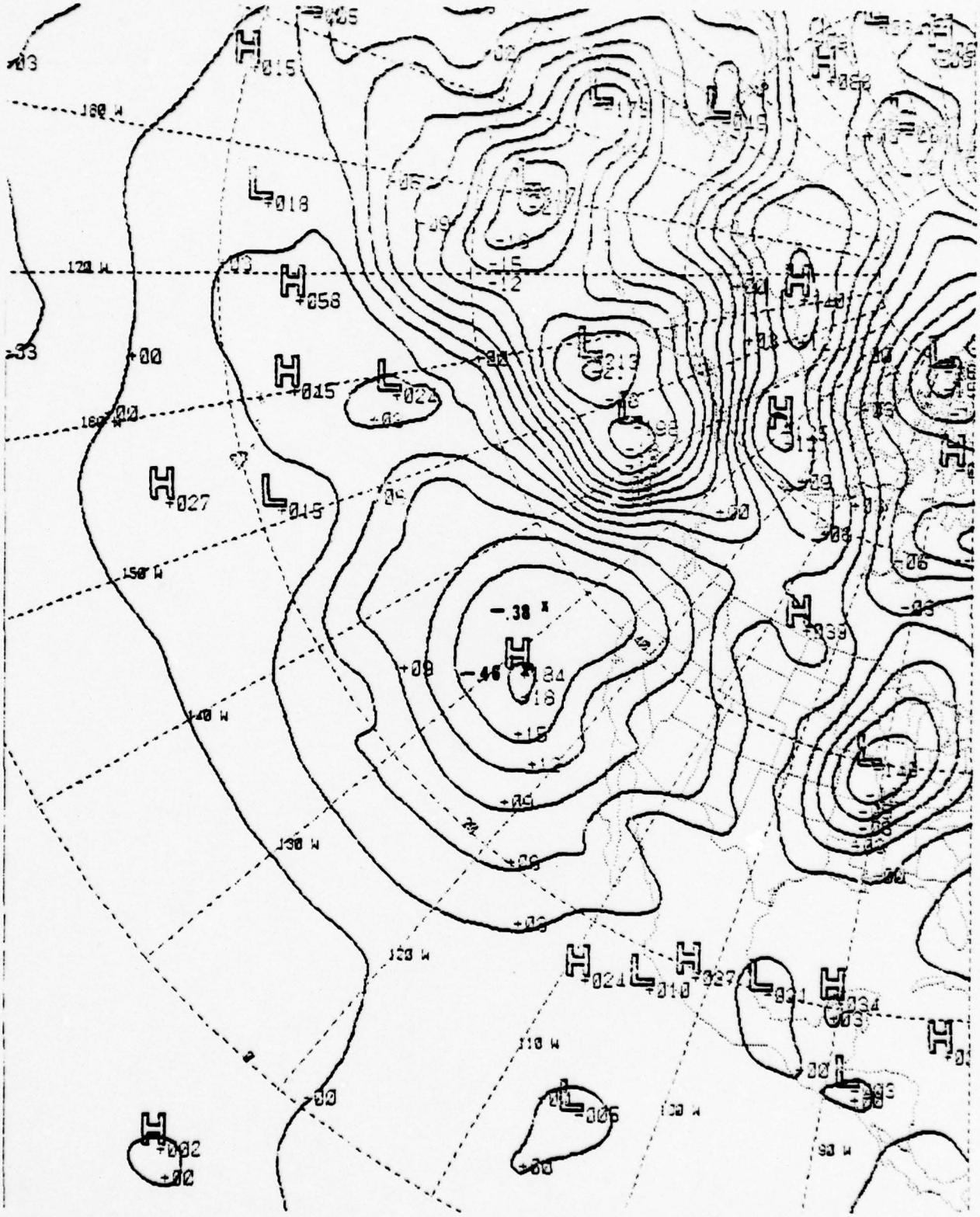

Figure 13. 1000-mb Analysis for 12Z 26 January 1965. Also shown are locations and values of the D parameter derived from concurrent radiosonde reports.

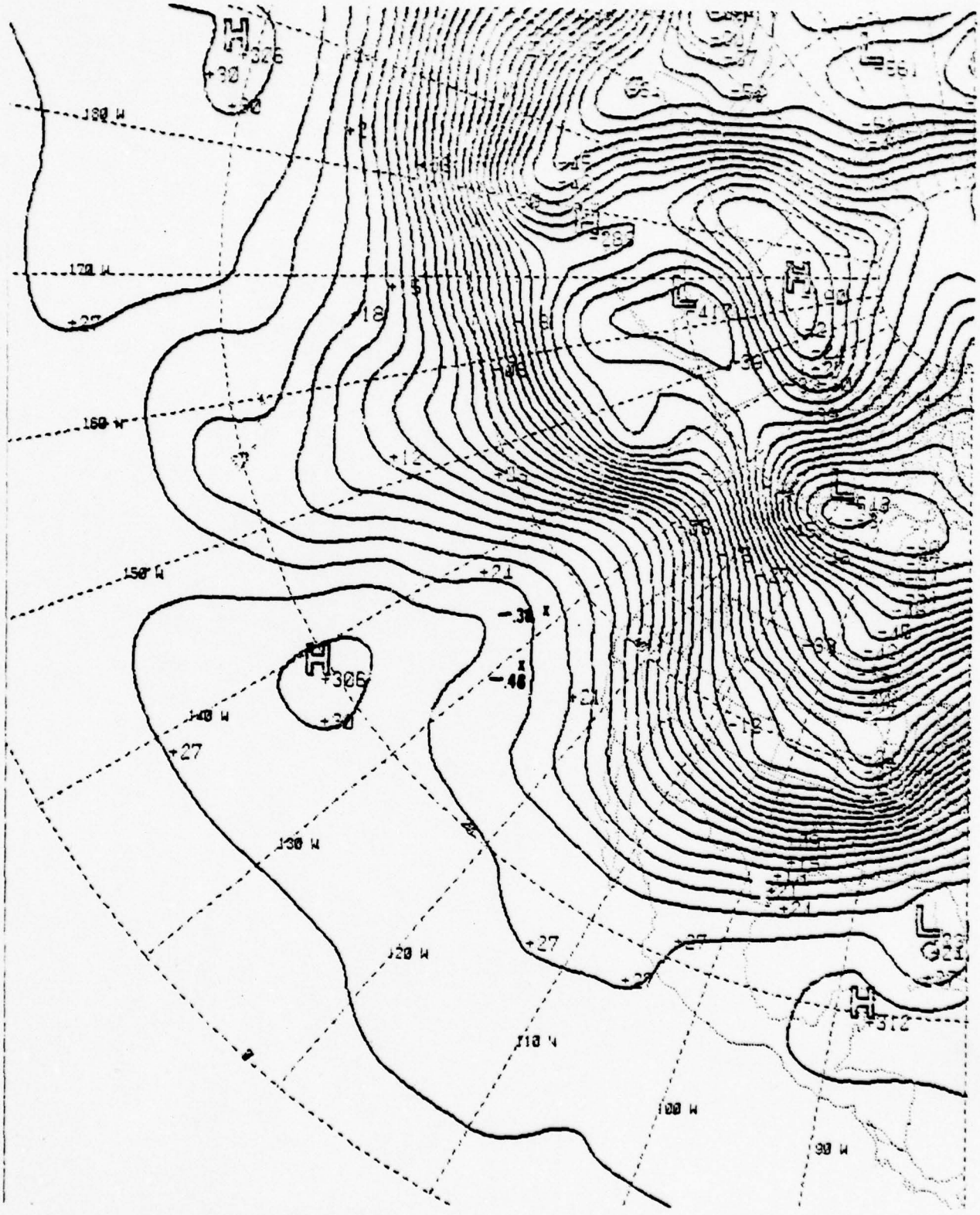

Figure 14. 500-mb Analysis for 12Z 26 January 1965. Also shown are locations and values of the D parameter derived from concurrent radiosonde reports.

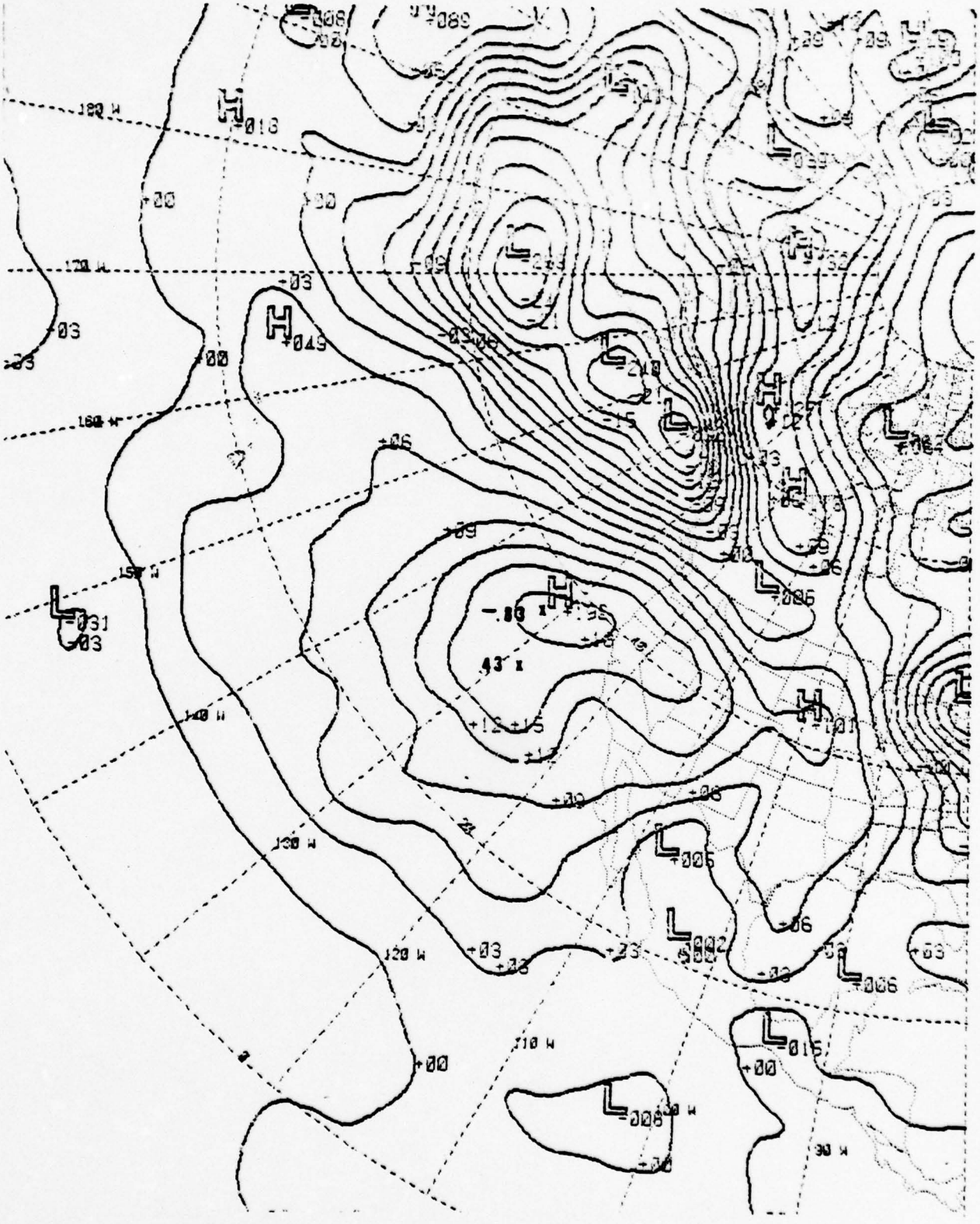

Figure 15. 1000-mb Analysis for 00Z 27 January 1965. Also shown are locations and values of the D parameter derived from concurrent radiosonde reports.

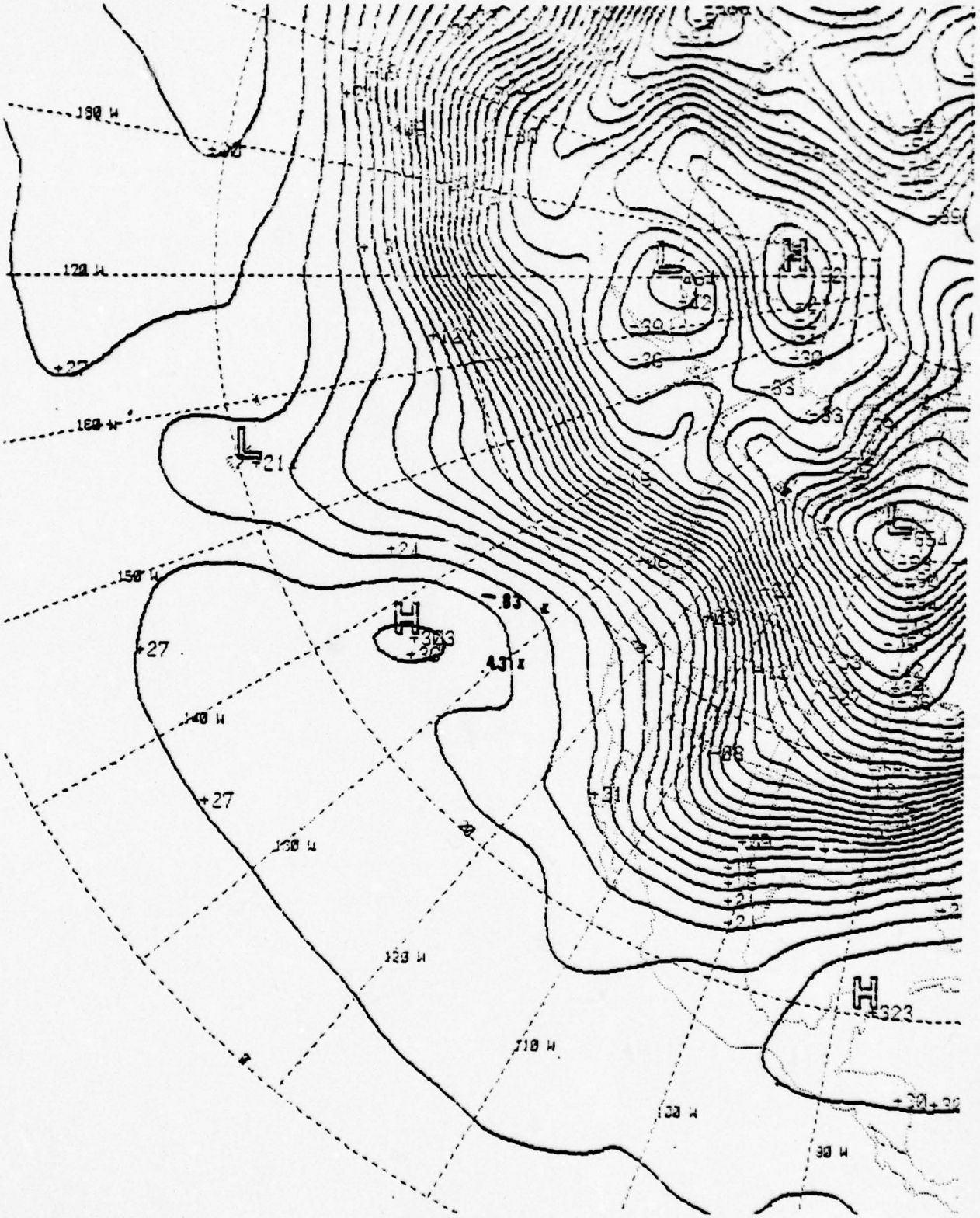

Figure 16. 500-mb Analysis for 00Z 27 January 1965. Also shown are locations and values of the D parameter derived from concurrent radiosonde reports.

At full resolution, RASS identifies every synoptic situation as unique. It does, however, provide a numerical measure (the matching coefficient) of the degree of pattern similarity between any two synoptic situations. Two methods (or a combination of both) can be used to provide quantitatively-selected synoptic types:

a. Using full resolution and a chosen baseday, score all other situations in the data base. Those analogue candidates with a matching coefficient exceeding a given value then define a synoptic type distributed around the baseday situation. If the baseday is an unusual situation then only a small number of acceptable analogues will be found; if the baseday is a common situation then a larger number of acceptable analogues will be found.

b. A similar procedure may be followed using the reduced resolution capabilities of RASS. In this case the matching coefficient would be high for (slightly) dissimilar patterns.

In this project only method a. was used; it is not known whether or not the two procedures would result in essentially the same set of acceptable analogues.

It will be noted that every baseday defines a synoptic type, RASS determining the number of situations from the total data base which fall within the specified limits of pattern similarity determined by the chosen acceptance/rejection level of the matching coefficient. To detect the most frequently occurring types would involve matching every situation against every other situation. For the 4320 situations in the RASS data base associated with this project, about 9.3×10^6 matching calculations would be required--this has not been attempted.

Referring now to the idealized approach postulated in Section 5.1, the establishment of a synoptic type associated with ducting was attempted. The first baseday chosen was 12Z, 6 September 1960 (see Section 4.4) with a D value of +1.277 in Zone 1; the date and D value are marked with an arrow on Fig. 2. This baseday was compared with all other synoptic situations in eight years of the data base (January 1958 to December 1965) using the regionalized capabilities of RASS applied to the SD, SL and SV modules shown in Fig. 4. A sample of the results is given in Figs. 17 and 18.

Figure 17 shows, for 1958, the match coefficients for each of the nine component fields. A TOTAL match coefficient is also given, this being derived from all nine component fields using weighting factors of unity throughout--i.e., each component field contributes equally towards the final score, no emphasis being placed on any particular synoptic feature or combination of features (see Section 4.2). Figure 18 shows a similar sequence for 1960. For this sample of two years, two analyses per day were available for the first 15 months, then one per day for the remaining 9 months (see Section 3.2); the reduction in the frequency of analyses is evident on Fig. 18. The "perfect match" on Fig. 18 results from the baseday being matched against itself. Note that "good" matches occur less frequently the smaller the scale of atmospheric disturbance. This is further illustrated by Table 2 which shows, for each component field and for the total field, the date-time group and matching coefficient of the relevant top ten analogues. The analogues for the SD scale of atmospheric disturbance were obtained by matching the SD fields only (as in Section 4.4), the SL scale analogues were obtained by matching the SL field only, and so on.

Following the idealized approach, the next stage in determining if the baseday <u>type</u> is associated with high D values is to compare the top analogues given in Table 2 with the data base of S and D parameters;

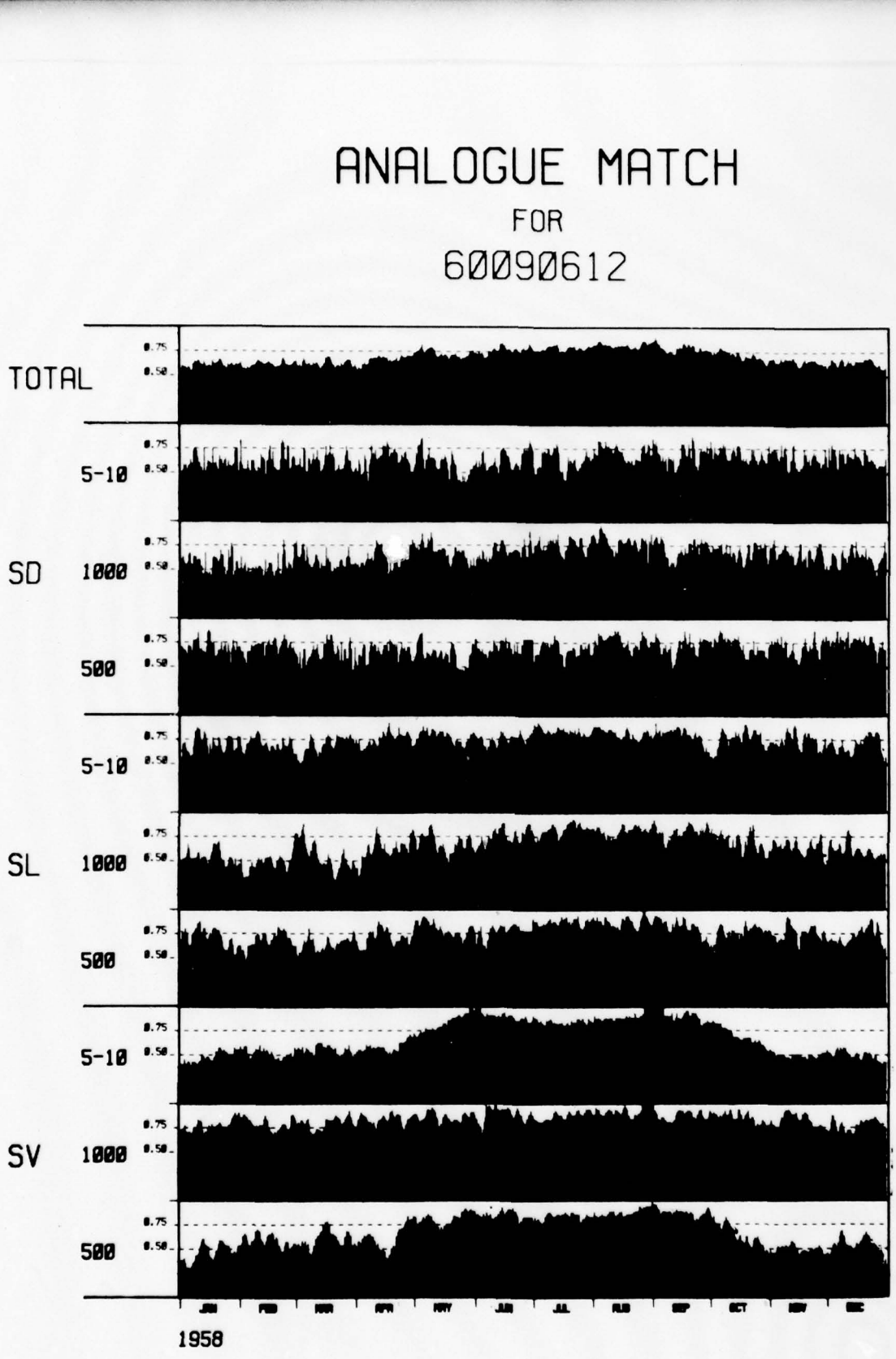

Figure 17. Match Coefficients for the Nine Component Fields and the Total Field for 1958 using 12Z 6 September 1960 as Baseday.

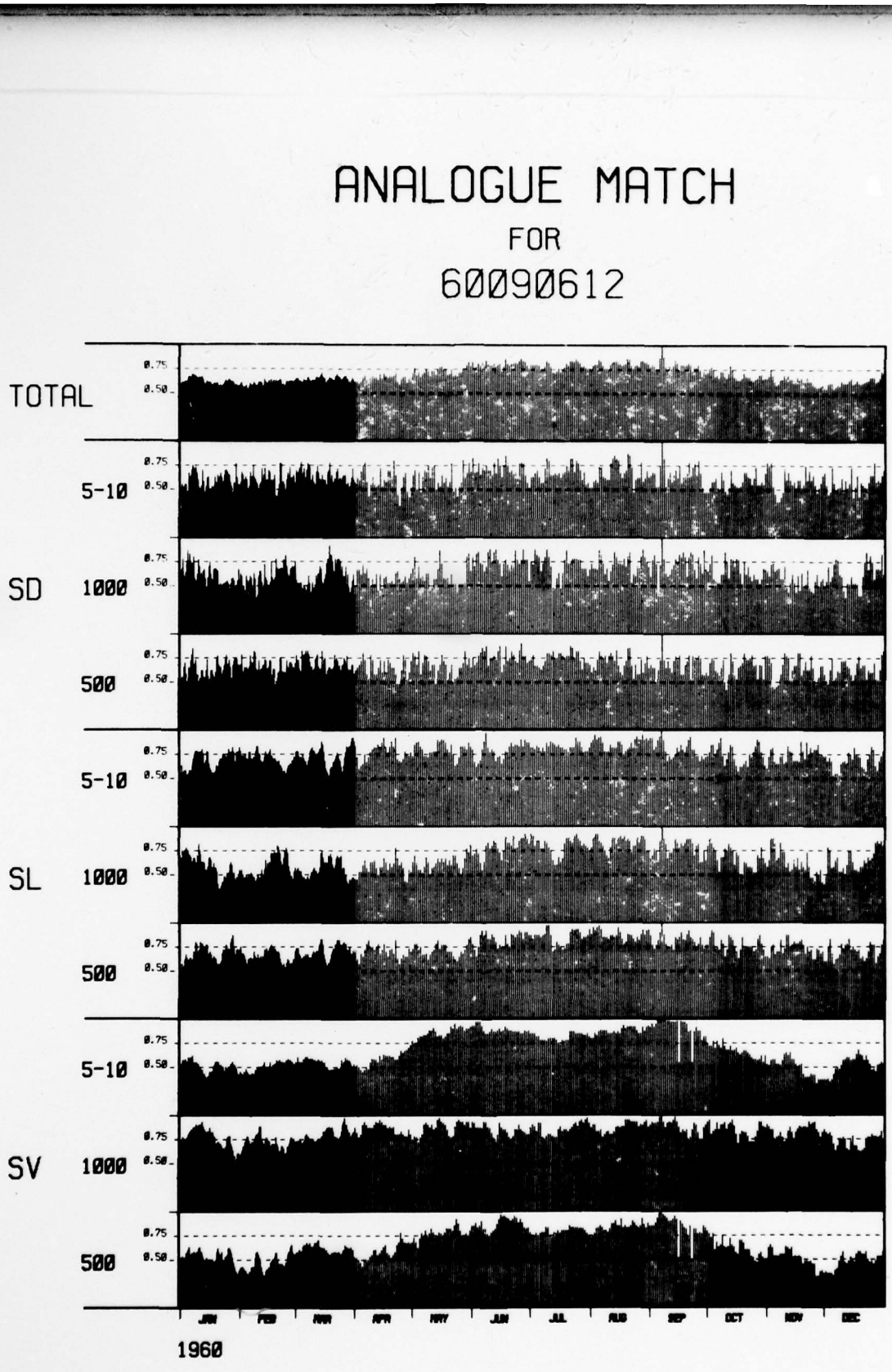

Figure 18. Match Coefficients for the Nine Component Fields and the Total Field for 1960 using 12Z 6 September 1960 as Baseday.

Table 2

The top ten analogues for 12Z 6 September 1960 for each component field and the total field. For each selection the date-time group is given first (year-month-day-hour) followed by the matching coefficient.

Selection	SV_{500}		SV_{1000}		SV_{5-10}	
1	60090612	1.00	60090612	1.00	60090612	1.00
2	60090512	0.98	65050500	1.00	58090300	1.00
3	59090812	0.98	58082900	0.98	59090200	1.00
4	60090712	0.97	58082912	0.98	58083000	1.00
5	65090100	0.97	62091912	0.98	60090412	1.00
6	60061512	0.97	59092612	0.98	59091100	1.00
7	58090100	0.97	65090212	0.98	64090912	1.00
8	59090800	0.97	65090200	0.98	59090612	1.00
9	58090300	0.95	60090512	0.98	60090512	1.00
10	61090812	0.95	60091312	0.98	58090312	1.00
	SL_{500}		SL_{1000}		SL_{5-10}	
1	60090612	1.00	60090612	1.00	60090612	1.00
2	65072000	0.98	61091712	0.97	60060712	0.97
3	59082212	0.98	63101812	0.95	62070312	0.95
4	58082712	0.98	59071512	0.93	60080212	0.95
5	64072212	0.98	62082112	0.93	65071212	0.95
6	59082200	0.98	65070112	0.93	60082712	0.95
7	58082800	0.98	63071712	0.93	60082412	0.93
8	65081400	0.97	65061912	0.92	64080212	0.93
9	63071212	0.97	60072312	0.92	64073112	0.93
10	60070812	0.97	59082212	0.92	59082312	0.93
	SD_{500}		SD_{1000}		SD_{5-10}	
1	60090612	1.00	60090612	1.00	60090612	1.00
2	63072812	0.95	58080500	0.95	59040212	0.90
3	59071300	0.90	59092400	0.93	59071600	0.88
4	60062512	0.90	60031800	0.92	64083012	0.88
5	65071400	0.90	58080412	0.92	59030112	0.88
6	59101512	0.88	58080512	0.92	63080212	0.88
7	65110212	0.88	62060612	0.92	59072800	0.87
8	64061412	0.88	62122412	0.92	60081912	0.87
9	65071500	0.88	59120400	0.90	59041100	0.87
10	58100600	0.88	59090100	0.90	59062412	0.87

Table 2 (Continued)

Selection	Total Field	
1	60090612	1.00
2	58090212	0.90
3	60090712	0.88
4	60090512	0.87
5	65082900	0.87
6	62082112	0.87
7	58090300	0.87
8	60082012	0.87
9	58090112	0.87
10	60081912	0.86

a sample of this data base is provided by Figs. 2 and 3. An immediate conclusion is that the sparseness of the data in space and time, accentuated by the naturally occurring high degree of variability of ducting conditions in space and time, is such as to make this direct approach[2] ineffective.

Accordingly a statistical approach was adopted making use of scattergrams. Figure 19 shows, for the same baseday situation (12Z, 6 September 1960), a plot of match coefficient against D-parameter for the three 1000-mb component fields. Figures 20 and 21 show the 500-mb and 5-10 thickness component fields respectively. To construct each scattergram the baseday situation was matched against every synoptic situation in the data base; all concurrent values of D were then plotted on the scattergram against the obtained value of match coefficient.

The location of this particular baseday on the scattergram is given, of course, by the coordinates D = 1.277, match coefficient = 1.00. If this were a commonly occurring type--i.e., a synoptic type associated with a high value of D--then there would be a concentration of plotted points around the baseday location. In fact the degree of pattern similarity for any of the nine component fields appears to bear no relationship to the value of the D parameter.

If the baseday situation were an unusaul event (a possibility given credence by the tropical storm seen to the south on Fig. 5, and by the reasonable supposition that any high value of D is a rare event) then the failure to identify the selected baseday as a type associated with trapping would be explained. To cover this possibility similar scattergrams were

---

[2]Although the technique could not be applied in this particular project due to data base limitations, it nevertheless is a valuable tool having applicability to other investigations requiring the establishment of synoptic types.

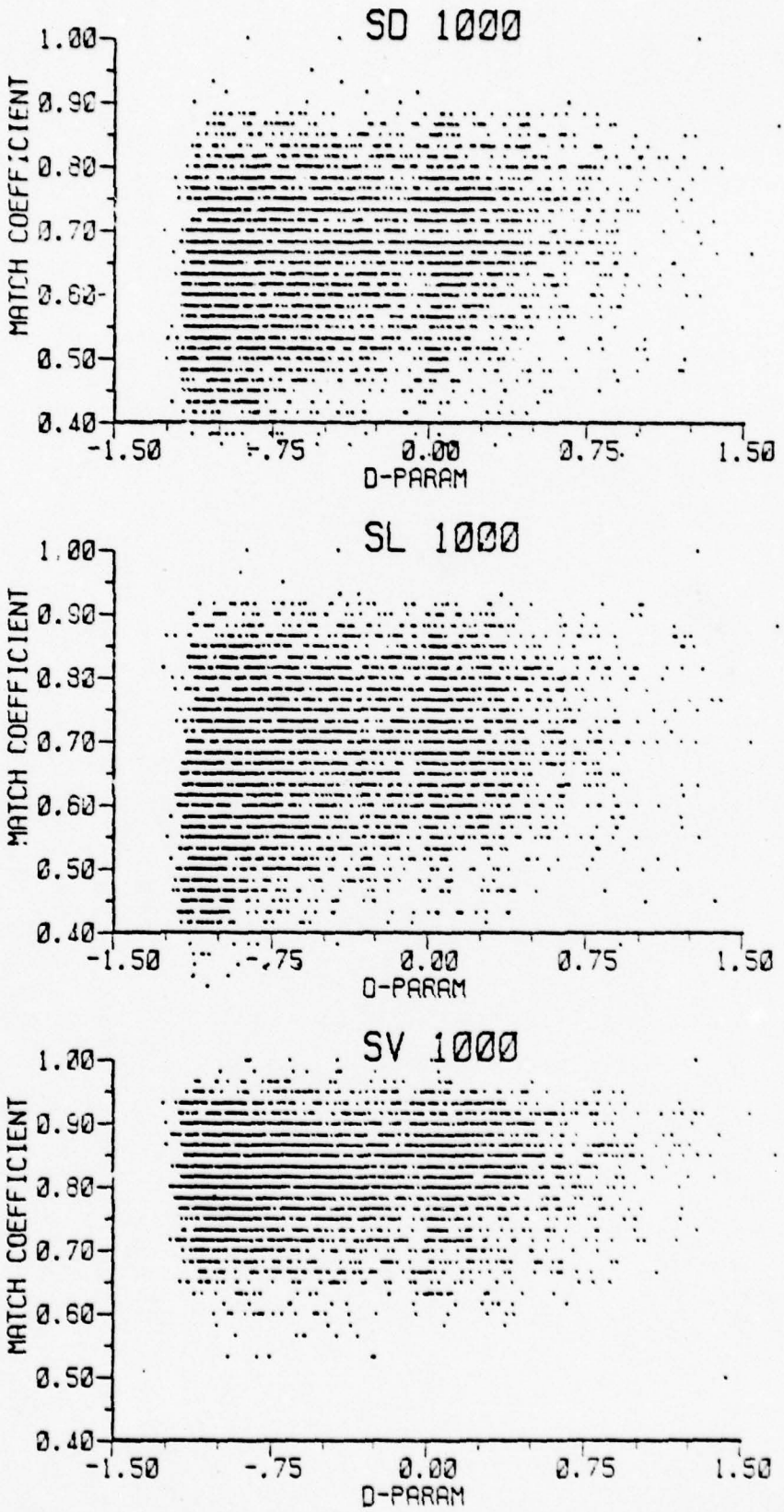

Figure 19. Plot of Match Coefficient against Value of the D Parameter for the SD, SL and SV Component Fields at 1000mb for all Available Synoptic Situations using 12Z 6 September 1960 as Baseday.

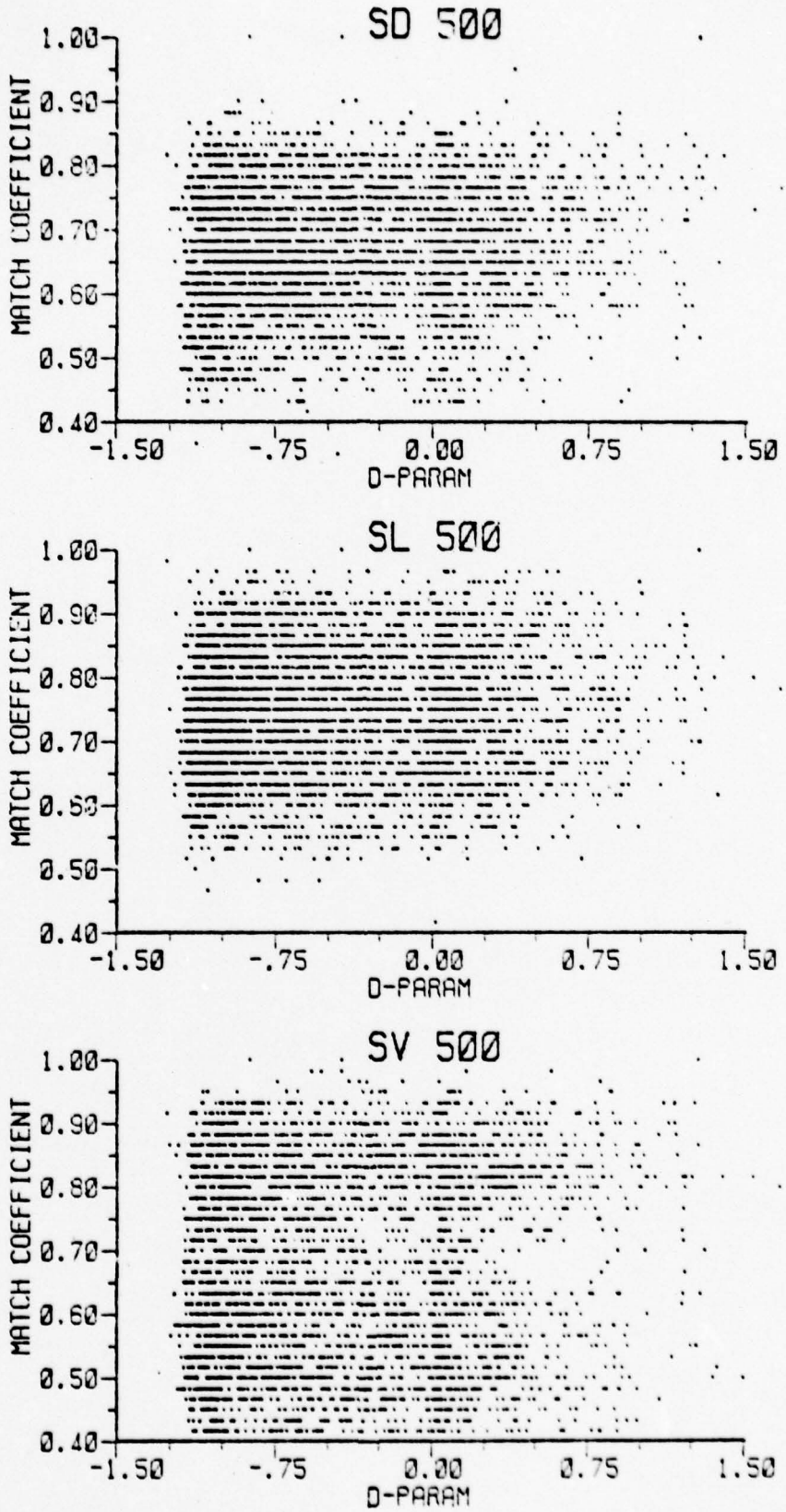

Figure 20. Plot of Match Coefficient against Value of the D Parameter for the SD, SL and SV Component Fields at 500mb for all Available Synoptic Situations using 12Z 6 September 1960 as Baseday.

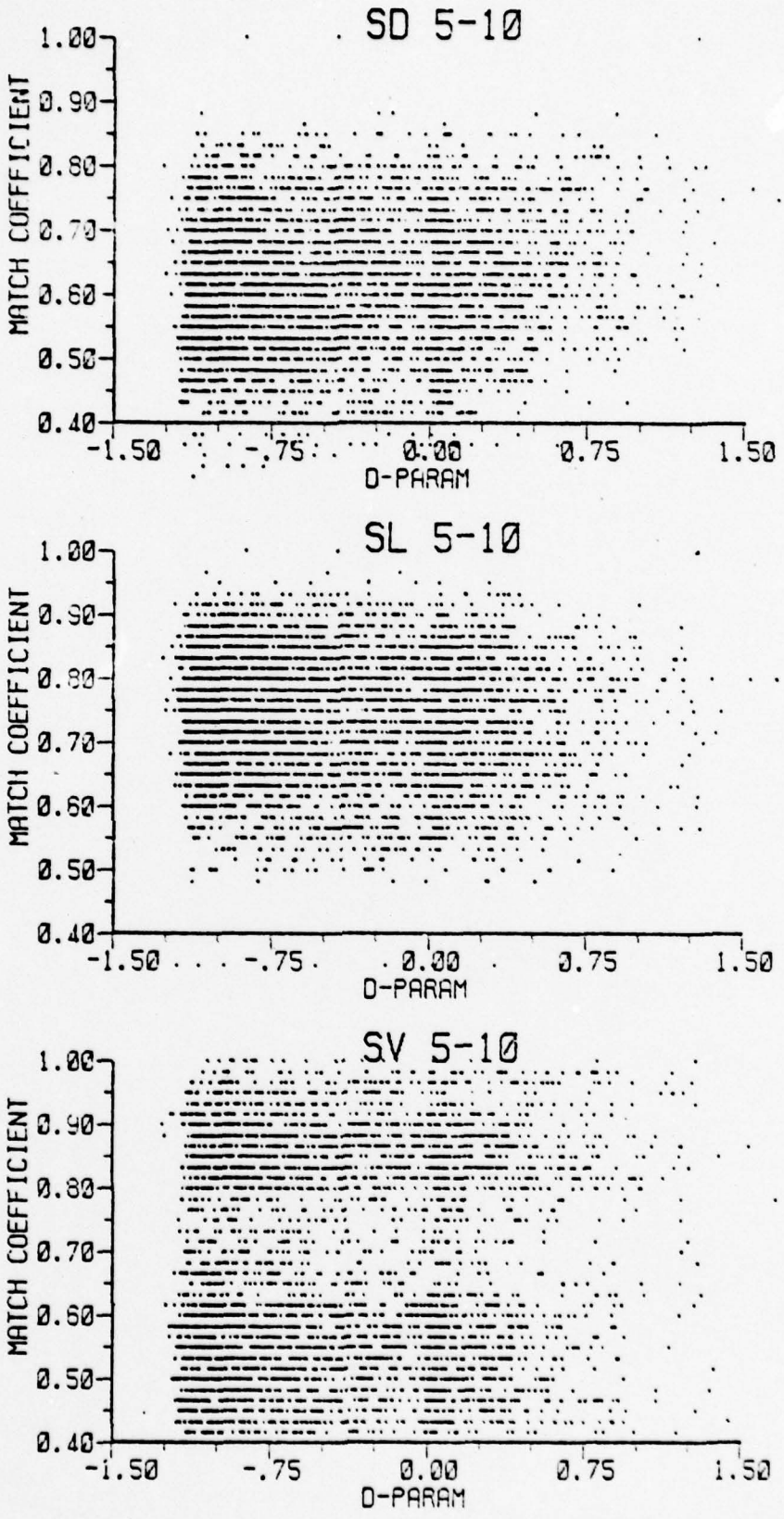

Figure 21. Plot of Match Coefficient against Value of the D Parameter for the SD, SL and SV Component Fields of 500-1000-mb Thickness for all Available Synoptic Situations using 12Z 6 September 1960 as Baseday.

prepared for 12Z 9 August 1960 with a D value in Zone 1 of 0.125. These are shown in Figs. 22-24. Again, no concentration of plotted points occurs around the baseday location of D = 0.125, match coefficient = 1.00, for any of the component fields. Several other repetitions with other basedays gave similar results.

5.3 Discussion of Results

As previously discussed (Section 5.2) certain broadscale synoptic situations are more likely to be associated with trapping than other situations--the eastern side of the Pacific anticyclone being a broadscale situation associated with a tendency toward trapping. For such situations certain qualitative relationships have been established, leading to forecasting "rules of thumb" such as "trapping should be expected when there are clear skies, little wind and high barometric conditions".

In a broadscale synoptic situation in which trapping occurs with some regularity, it seems reasonable to assume that one or more synoptic sub-types exist, falling within the broadscale typing, which are associated with a stronger tendency toward trapping than the mean. In the performance of this project it was hoped that RASS would enable these sub-types to be found and quantitatively associated with trapping probabilities. As demonstrated in Section 4.4, RASS undoubtedly has the ability to select similar patterns from the data base on even the SD range-of-scale. However, based on the results presented in Section 5.2, it must be concluded that no such synoptic sub-types have been established. It is considered that the space and time resolution capabilities required to capture and represent the naturally occurring variabilities of refractive structure on even the synoptic scale are not provided by either the data base of synoptic analyses (one or two analyses per day) or, more importantly, by the data base of refractive profiles (in general, one or two profiles per day for the area shown on Fig. 1).

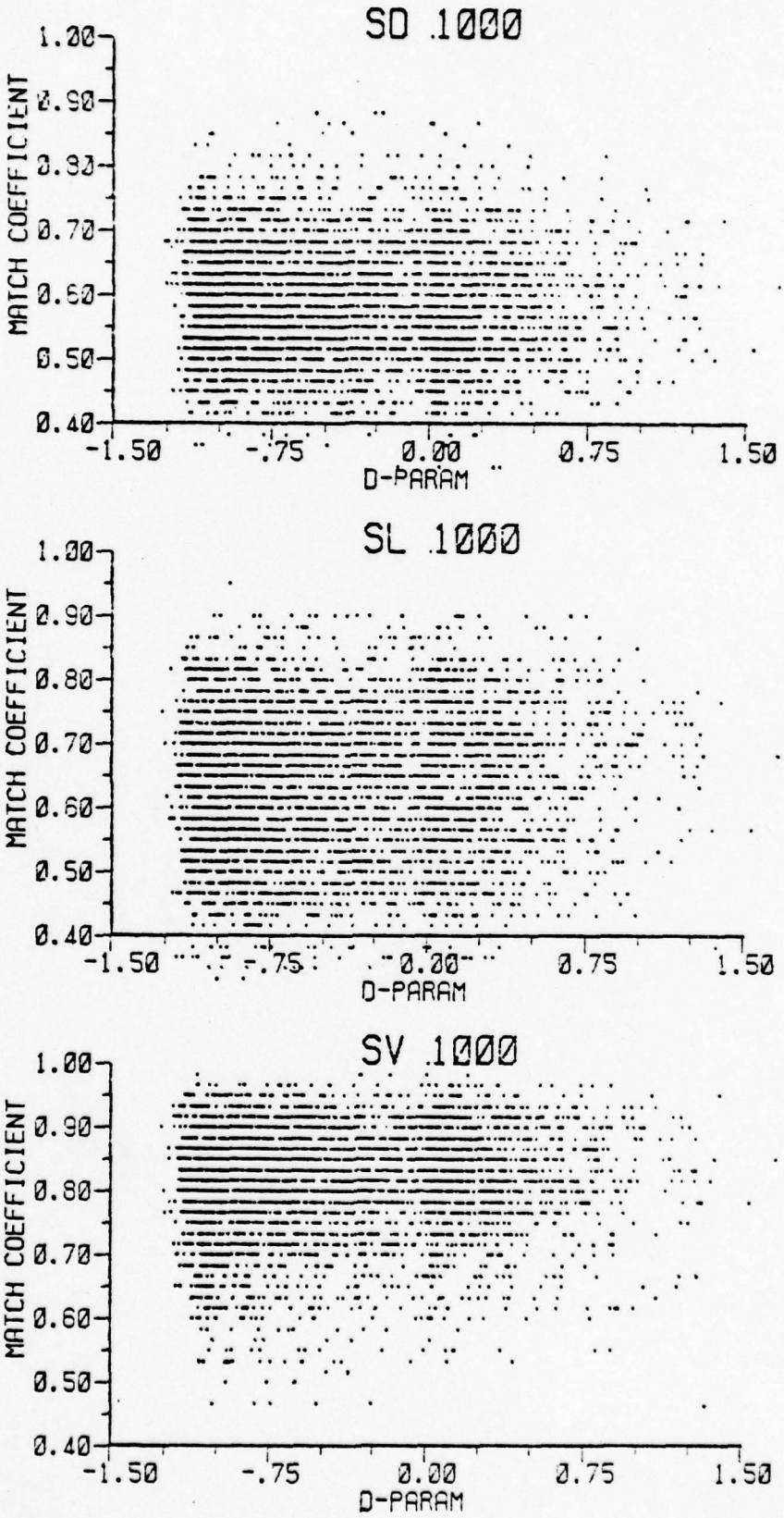

Figure 22. Plot of Match Coefficient against Value of the D Parameter for the SD, SL and SV Component Fields at 1000mb for all Available Synoptic Situations using 12Z 9 August 1960 as Baseday.

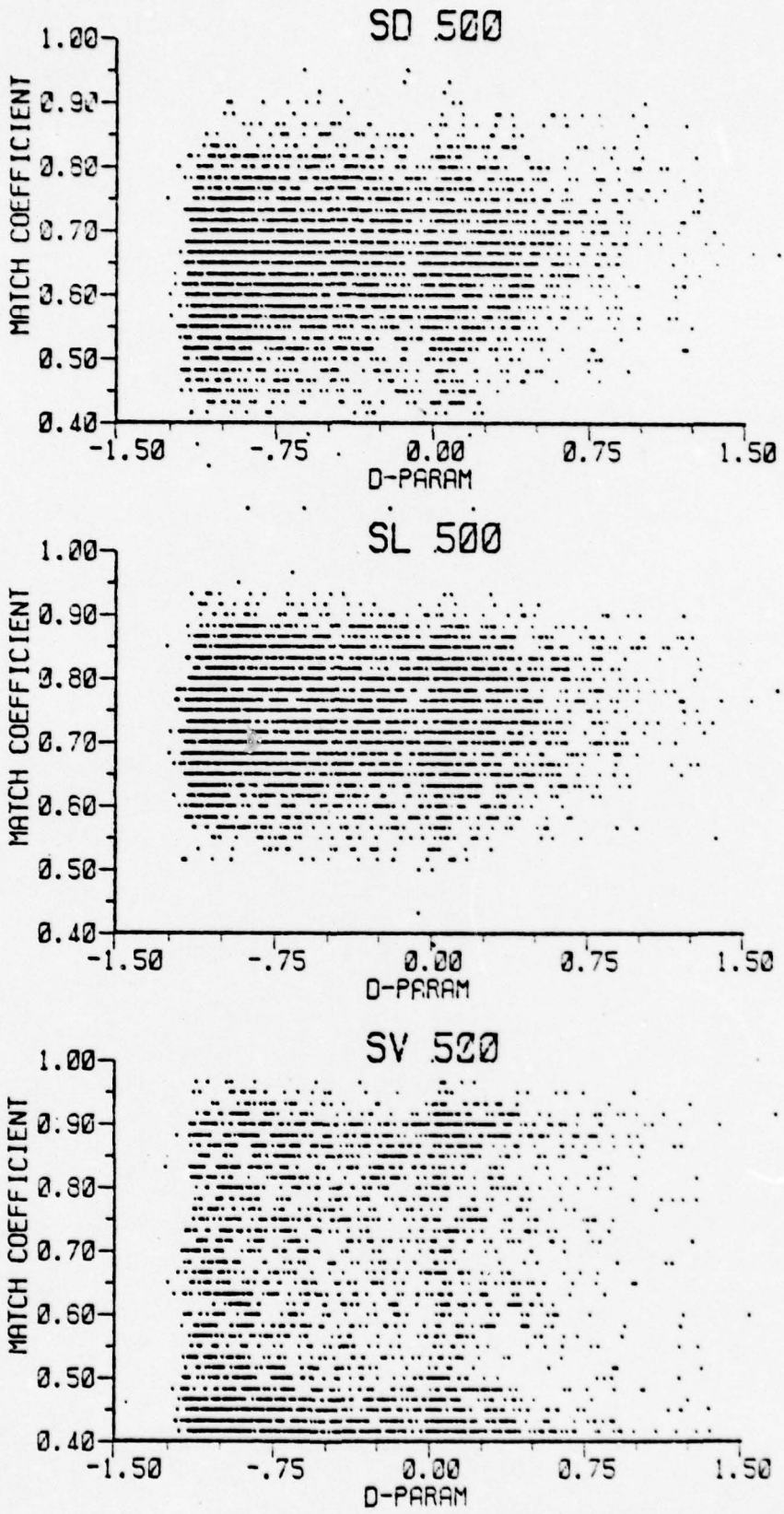

Figure 23. Plot of Match Coefficient against Value of the D Parameter for the SD, SL and SV Component Fields at 500mb for all Available Synoptic Situations using 12Z 9 August 1960 as Baseday.

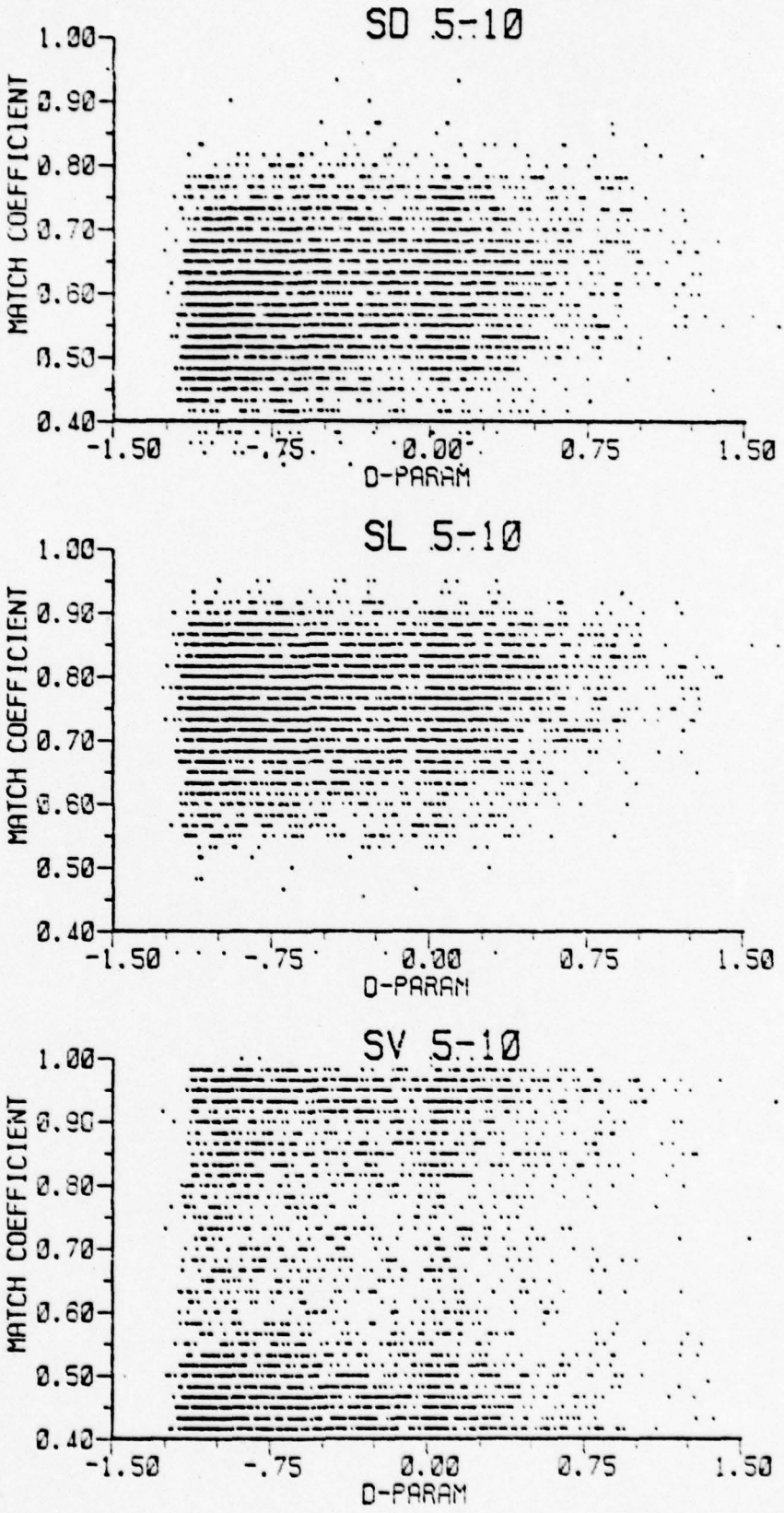

Figure 24. Plot of Match Coefficient against Value of the D Parameter for the SD, SL and SV Component Fields of 500-1000-mb Thickness for all Available Synoptic Situations using 12Z 9 August 1960 as Baseday.

The requirements of Task 3 of this project are essentially concerned with the development of a capability to assess refractive structures from synoptic patterns in probabilistic terms. It is considered that, with the demonstrated effectiveness of RASS applied to the region of interest and with the development of the various statistical techniques discussed in Section 5, such a capability has been established and is available for future use. However the data bases available at this time have not allowed a successful demonstration of the effectiveness of this capability. An alternative approach to the problem of relating refractive structure to the concurrent synoptic situation is presented in Section 6.

6. THE DEPENDENCE OF REFRACTIVE STRUCTURE ON CONCURRENT SYNOPTIC PARAMETERS

6.1 Introduction

Task 3 of this project was concerned with the development of the capability to assess refractive structure from synoptic patterns. However, although it is considered such a capability has been established, data base limitations have prevented its verification. These limitations are, in essence, that the data bases are only "samplings" of refractive structure and the concurrent synoptic situation, and that these samplings are too widely separated in space and time to allow any relationship between the two data bases to be established on even a statistical basis. The fact that ducting does indeed depend on the broadscale synoptic situation may be illustrated by comparing the percentage frequency of occurrence of total tropospheric ducting in the various zones delineated on Fig. 1--see Table 3.

Note the increase in percentage frequency of occurrence of ducting in more southerly latitudes; this increase is related, of course, to the subsidence inversion which is a feature of the Pacific anticyclone.

Table 3

Comparison of the percentage frequency of total tropospheric ducting (i.e., $D \geq 0$) for the 5 Zones shown on Fig. 1, Zones 1-3, Zones 3-5, and all Zones combined

Zone	Number of Observations in Zone	Number of Observations with $D \geq 0$	Percentage Frequency of Occurrence of $D \geq 0$
1	964	590	61
2	1508	627	42
3	1383	376	27
4	2050	380	19
5	1017	129	13
1-3	3855	1593	41
3-5	4450	885	20
1-5	6922	2102	30

It can also be shown that the probability of ducting has persistence in the synoptic time frame. For example Table 4, based on Table 56 of Ref. [1], provides the following information:

Table 4

The 24-hourly persistence of ducting and non-ducting conditions (based on 12Z observations only) for Zones 1-5, July-September

Initial conditions non-ducting:	24 hours later . . .	64% non-ducting 36% ducting
Initial conditions ducting:	24 hours later . . .	35% non-ducting 65% ducting

(Note that Table 4 does not imply, for example, that 65% of ducts persisted for 24 hours.)

The fact that such probabilistic tendencies in space and time cannot be interpreted in terms of synoptic sub-types is considered to be due to data base limitations. However, as evidenced by Tables 3 and 4, synoptic-scale space and time tendencies undoubtedly exist. In order to determine the probabilistic relationships required by Task 3 of this project, relationships between refractive structure and the concurrent synoptic parameters (see Section 6.2) have been studied; the results of the study are given in Section 6.3.

6.2 Method

Each profile in the data base (represented by values of the S and D parameters) may be associated with values of the synoptic parameters which occurred at the same point in space and time, thus:

Profile Parameters	Synoptic Parameters[1]
	SV height, 500mb and 1000mb
	SL height, 500mb and 1000mb
	SD height, 500mb and 1000mb
S	Wind speed, 500mb
D	Wind speed, 1000mb
	Wind direction, 500mb
	Wind direction, 1000mb

Values of S and D for a given profile were available from the data base of refractive conditions. Values of the synoptic parameters, interpolated to the reported location of the observing ship for that particular profile, were extracted from the FNWC 63x63 archived fields.

The relationships between the synoptic parameters and those representing the refractive profiles were investigated using statistical techniques; the results are given in Section 6.3. It should be noted that only about 5% of the profiles available showed surface trapping--an unrealistically low figure almost certainly due to the failure of conventional radiosondes to detect the majority

[1] Many other synoptic parameters could influence the values of S and D. Those listed here were used to establish methods and techniques.

of surface and low-level ducts. Therefore, in general, the statistics associated with the S parameter are considered to be non-representative and are not shown.

6.3 Results

6.3.1 The Dependence of Parameter D on Contour Height

Figures 25 through 30[2] show scattergrams for the D parameter against contour height of the SD, SL and SV ranges-of-scale for 1000mb and 500mb. Plotted points are for all profiles in the data base for which synoptic analyses were available; i.e., all zones, all months.

Using Fig. 25 as an example, height values are shown along the abscissa and D values along the ordinate. The height is expressed in terms of an anomaly from a standard height, this anomaly being measured in meters. Both height and D values are divided into ranges by dotted lines. Thus, for example, there were 43 observations with height anomalies of -120 to -060 meters with D values between -1.25 and -1.00. As well as height anomaly values, the abscissa shows, for each height range, the total number of observations in that range together with the number in which trapping occurred (i.e., $D \geq 0$). Thus, for the height anomaly range 000 to +060 meters, there were 903 occurrences of trapping out of a total population of 3016. The (truncated) percentage frequency of occurrence of trapping is also shown--in this case 29% (Each scattergram shows about 4320 plots of profile parameter:synoptic parameter, the exact number varying slightly with the availability of archived fields.)

---

[2] All figures are given at the end of Section 6.3.

Apart from the synoptic parameter represented along the abscissa, all scattergrams in Section 6 are similar in concept to Fig. 25.

As will be demonstrated, the scattergrams presented contain significant information. This will be pointed out in association with the scattergram which is most apposite, not necessarily the first scattergram to reveal such information.

Figures 25 through 30 contain all available data and thus the percentage frequency of occurrence of trapping should be about 30% (see Table 3). Figure 25 shows that the SD_{1000} height has little effect on trapping frequency unless the anomaly is less than about -060 meters (about 1.7% of the cases), in which case the trapping probability is zero (based on available data). Figure 26 shows a similar result for the SD_{500} height. In this case however, anomalies of -060 meters or less occurred on 7.8% of the occasions, with a trapping probability of only 6%.

Figure 27 shows the scattergram for the SL_{1000} height anomaly. Note in this case the marked tendency for the trapping probability to increase with SL_{1000} height. This effect is particularly pronounced on Fig. 28--the scattergram of D: SL_{500}.

Figure 28 may be used to illustrate the probability distribution of D values within height anomaly ranges. Table 5 shows this distribution,[3] obtained by normalizing the data within each height anomaly range to 100%.

Figure 28 and Table 5 show there is a positive correlation between the value of D (and hence trapping probability) and the SL_{500} height.

Figures 29 and 30 show similar scattergrams for the SV_{1000} and SV_{500} height anomaly fields respectively. Note the very marked effect (Fig. 30) of high SV_{500} values on the probability of trapping. However, because the SV_{500} field is always very zonal, a similar distribution would be obtained if a scattergram of D:latitude were to be plotted. To determine whether or not the probability of trapping increases with SV_{500} height independently of latitude requires a sufficiently large data sample obtained

---

[3]The effect of the use of a scaling height, H_*, to form a continuous measure of refractive conditions (see Section 2.3) is apparent on all scattergrams giving, in general, the following type of distribution:

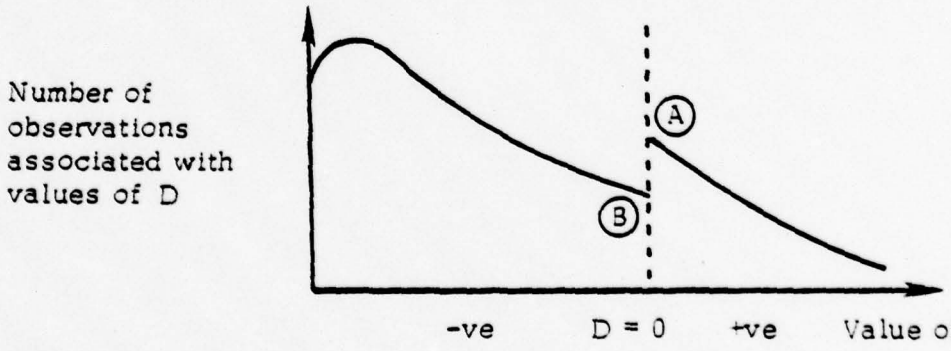

The points A and B could be made coincident (thus giving a more conventional appearance to the distribution) by re-calculating S and D values (positive values only) using a smaller value of H_*. However, since the main interest lies in determining whether or not trapping exists (i.e., D positive or negative) and this determination is not affected by H_*, positive S and D values have not been re-assessed. This should be borne in mind when studying the scattergrams and derived tables such as Table 5.

Table 5

The percentage frequency of occurrence distribution of the D parameter within selected ranges of the SL_{500} height anomaly

Range of Parameter D	Range of SL_{500} Height Anomaly						
	-180 to -120	-120 to -060	-060 to 000	000 to +060	+060 to +120	+120 to +180	+180 to +240
+1.75 to +1.50				0.2			
+1.50 to +1.25				0.2	0.4	0.4	
+1.25 to +1.00			0.3	0.9	1.2	0.2	1.2
+1.00 to +0.75			0.1	2.7	2.8	3.1	3.4
+0.75 to +0.50			0.8	2.9	5.7	5.4	1.2
+0.50 to +0.25		0.4	2.4	8.0	10.4	11.3	18.0
+0.25 to 0.00		5.5	9.5	14.9	17.6	19.2	24.1
0.00 to -0.25	7.7	4.5	5.7	8.8	10.1	9.6	16.7
-0.25 to -0.50	7.7	6.3	9.7	13.0	12.7	12.9	9.6
-0.50 to -0.75	---	10.5	16.7	15.8	14.5	16.6	10.8
-0.75 to -1.00	26.9	28.2	25.9	19.6	15.9	12.6	14.5
-1.00 to -1.25	57.7	45.0	28.8	13.0	8.6	8.7	1.2

at a fixed location--such as a weather ship. The observations in Zone 1 almost fulfill this requirement as can be seen from the geographical distribution of observation shown in Fig. 1. Figures 31 and 32 show, for Zone 1, the dependence of D on the SV_{1000} height anomaly and the SV_{500} height anomaly respectively. There is clearly a positive correlation between the value of D and these two synoptic parameters which is independent of latitude. Note also the bimodal distribution on Fig. 32, preferred ranges of the SV_{500} height anomaly being +080 to +160 meters, and +240 to +320 meters. This is a seasonal effect, also apparent on Fig. 17.

Figures 33 through 36 provide a comparison between the two extreme zones--Zone 1 and Zone 5--on the SL range-of-scale. Figure 33 shows a small decrease of trapping probability with increasing height in Zone 1. However, with the population being unevenly separated into only 3 ranges of SL height, this result is probably not statistically significant. Figures 34-36 show an increase in trapping probability with increasing SL height, the effect being more pronounced in Zone 1 than Zone 5, and more pronounced at 500mb than at 1000mb.

6.3.2 The Dependence of Parameter D on Wind Speed and Direction

Figures 37 through 40 show D:wind speed in knots at 1000mb and 500mb for Zones 1-3 and for Zones 3-5. The general trend is shown by the percentage frequencies of occurrence along the abscissa--as winds become lighter, the probability of trapping increases, the effect being more pronounced at the 500-mb level than at the 1000-mb level, and more pronounced in Zone 1 than Zone 5.

The final four scattergrams, Figs. 41 through 45, show D:wind direction in degrees at 1000mb and 500mb for Zone 1 and for Zone 5. There are clearly wind directions which are associated with higher trapping probabilities than are other directions, the effect once again being more

pronounced at the 500-mb level than at the 1000-mb level, and more pronounced in Zone 1 than Zone 5.

From Fig. 42 it is interesting to note that the 500-mb wind blows from 090°-270° (through south) for 83% of the observations with an associated trapping probability of 55%, whereas the 500-mb wind blows from 270°-090° (through north) for only 17% of the observations yet has an associated trapping probability of 76%.

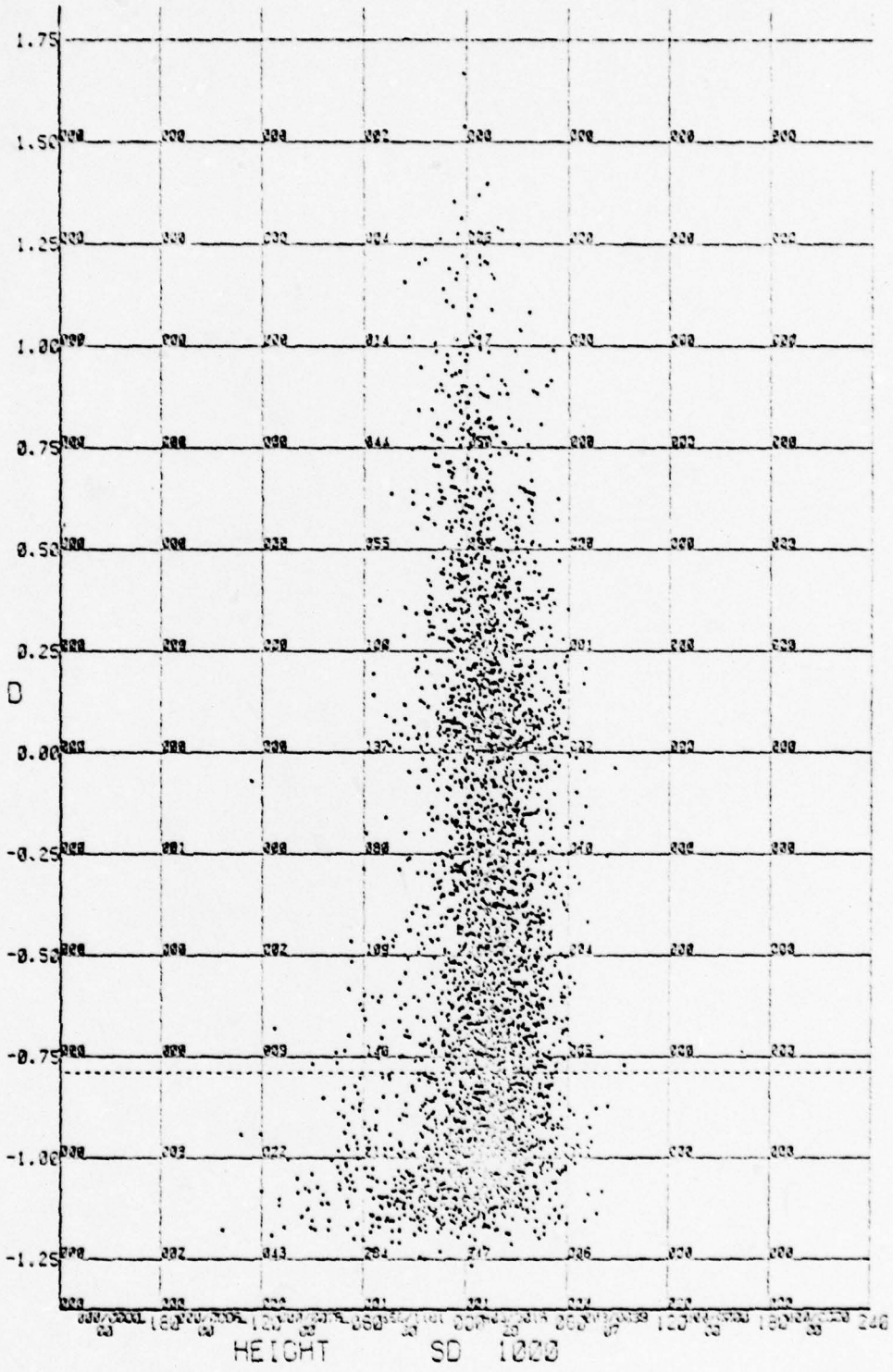

Figure 25. Scattergram of the D Parameter against the SD Height Anomaly in Meters at 1000mb for Zones 1-5.

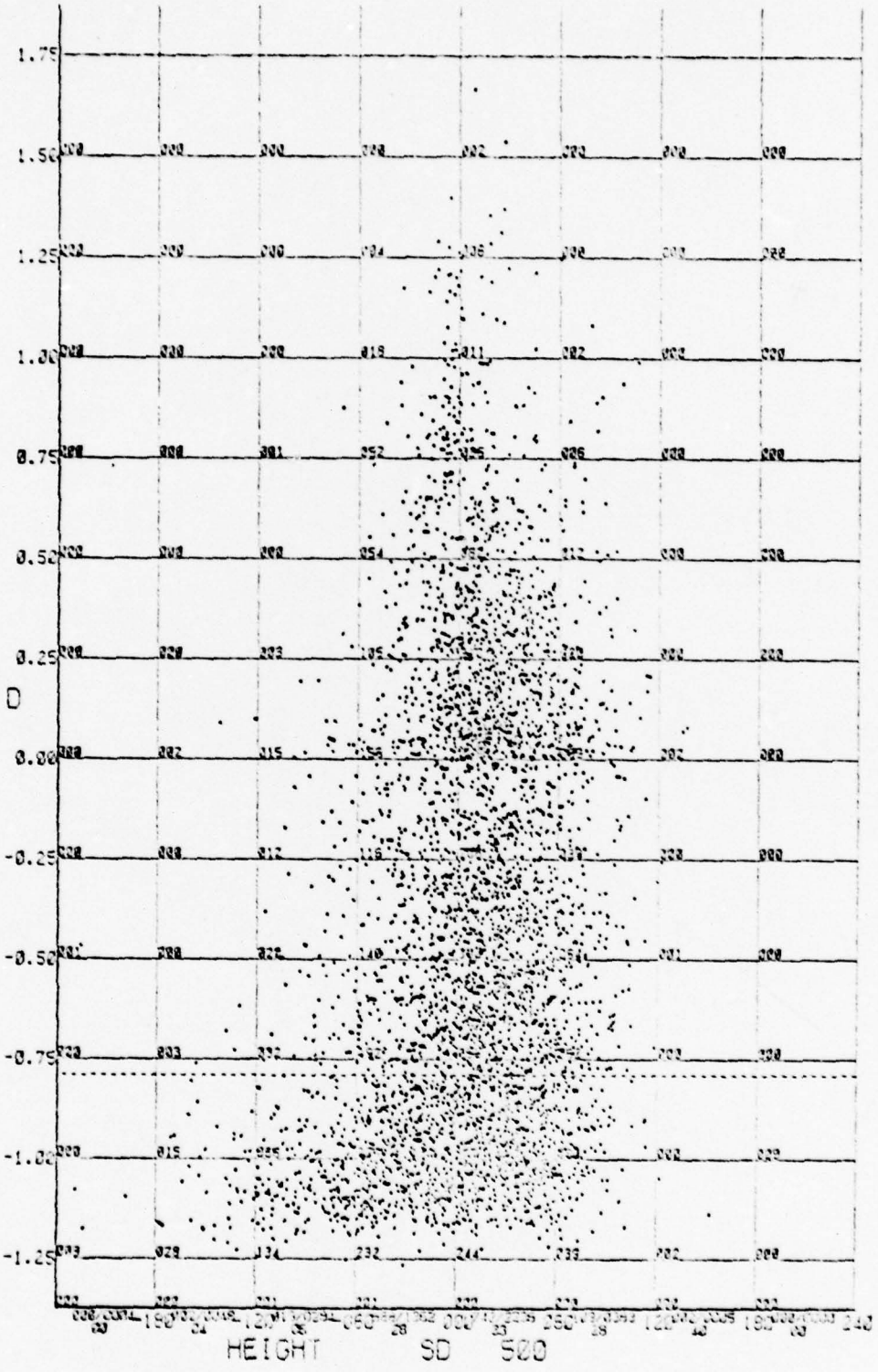

Figure 26. Scattergram of the D Parameter against the SD Height Anomaly in Meters at 500mb for Zones 1-5.

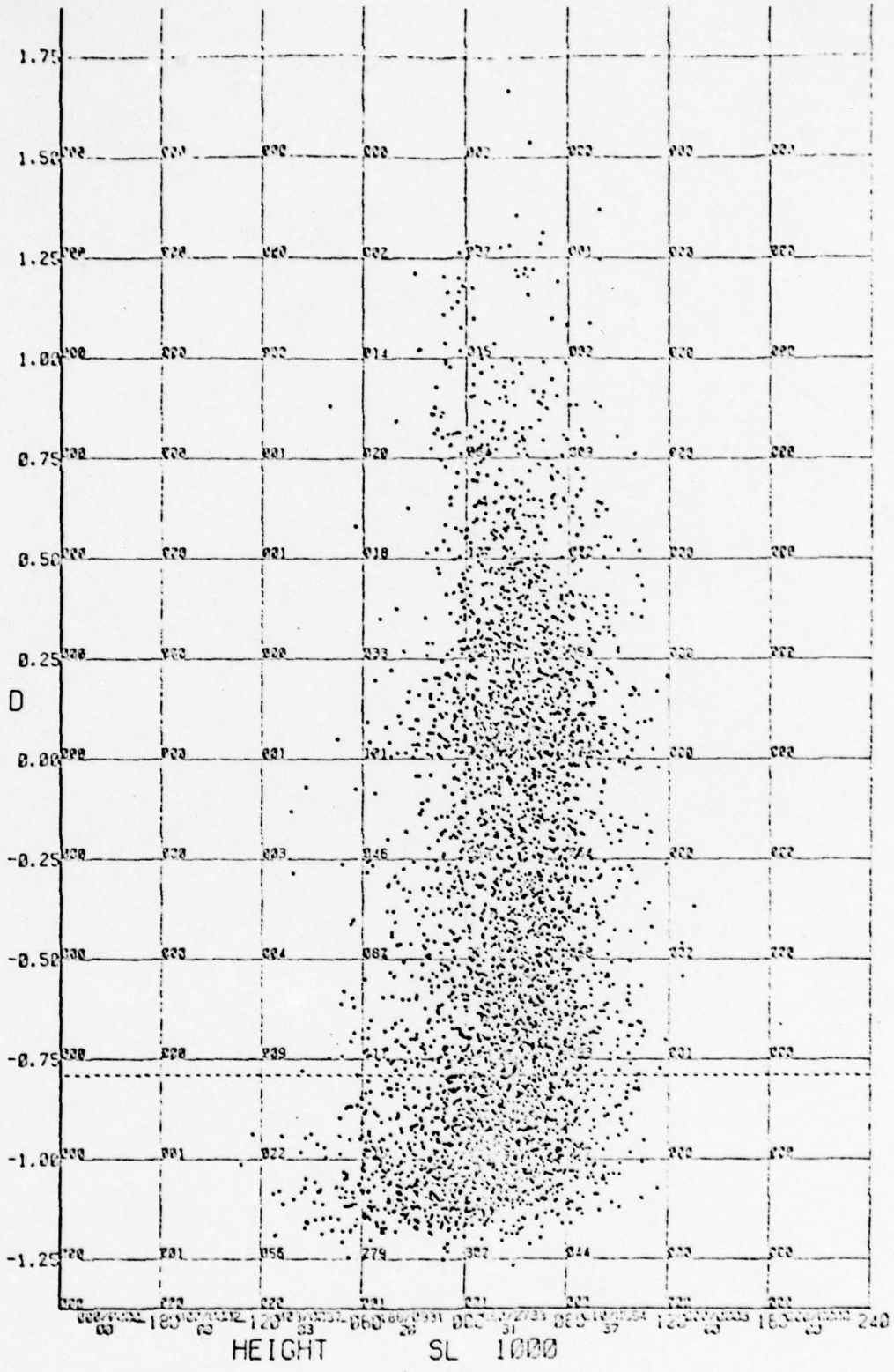

Figure 27. Scattergram of the D Parameter against the SL Height Anomaly in Meters at 1000mb for Zones 1-5.

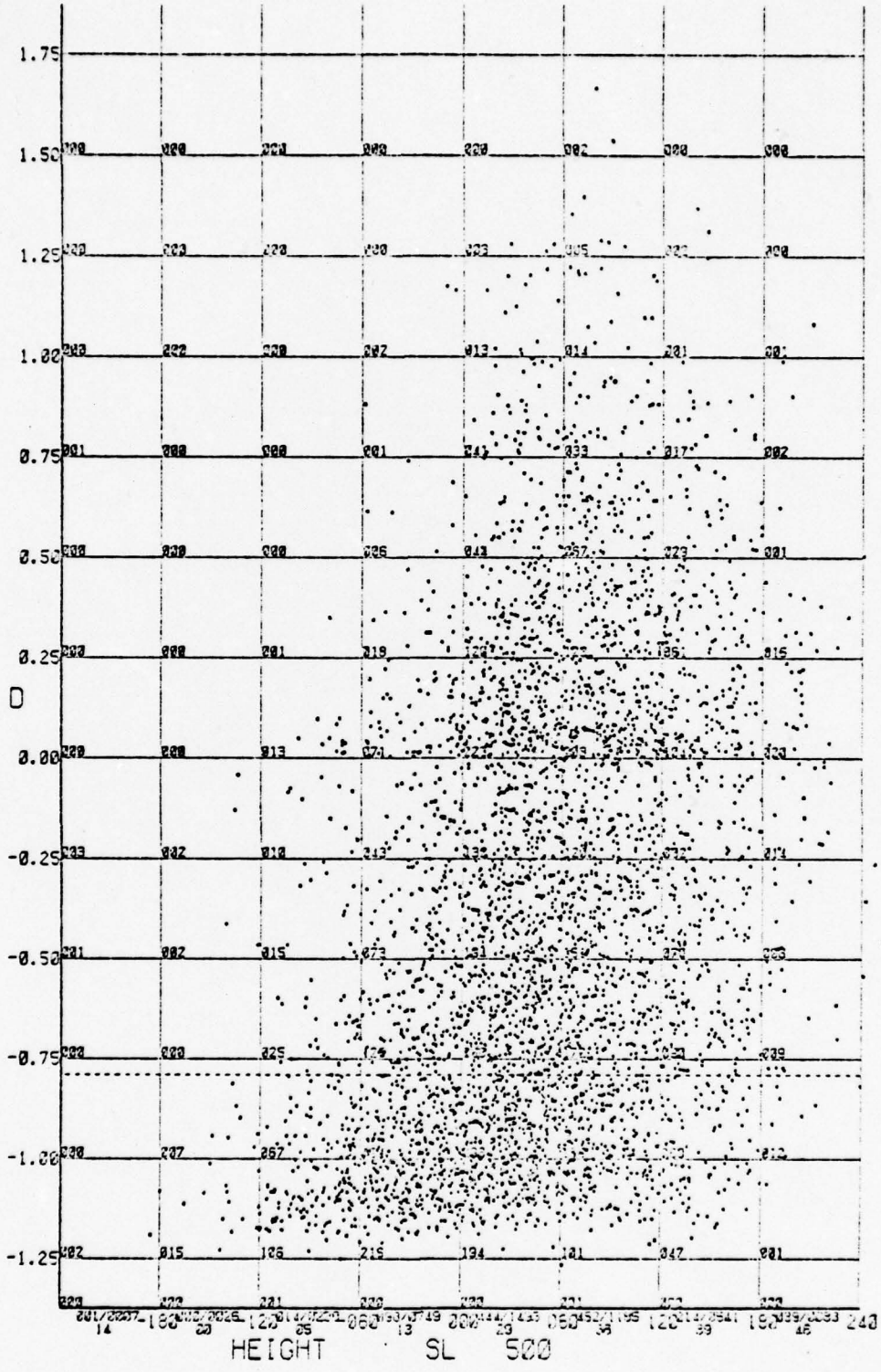

Figure 28. Scattergram of the D Parameter against the SL Height Anomaly in Meters at 500mb for Zones 1-5.

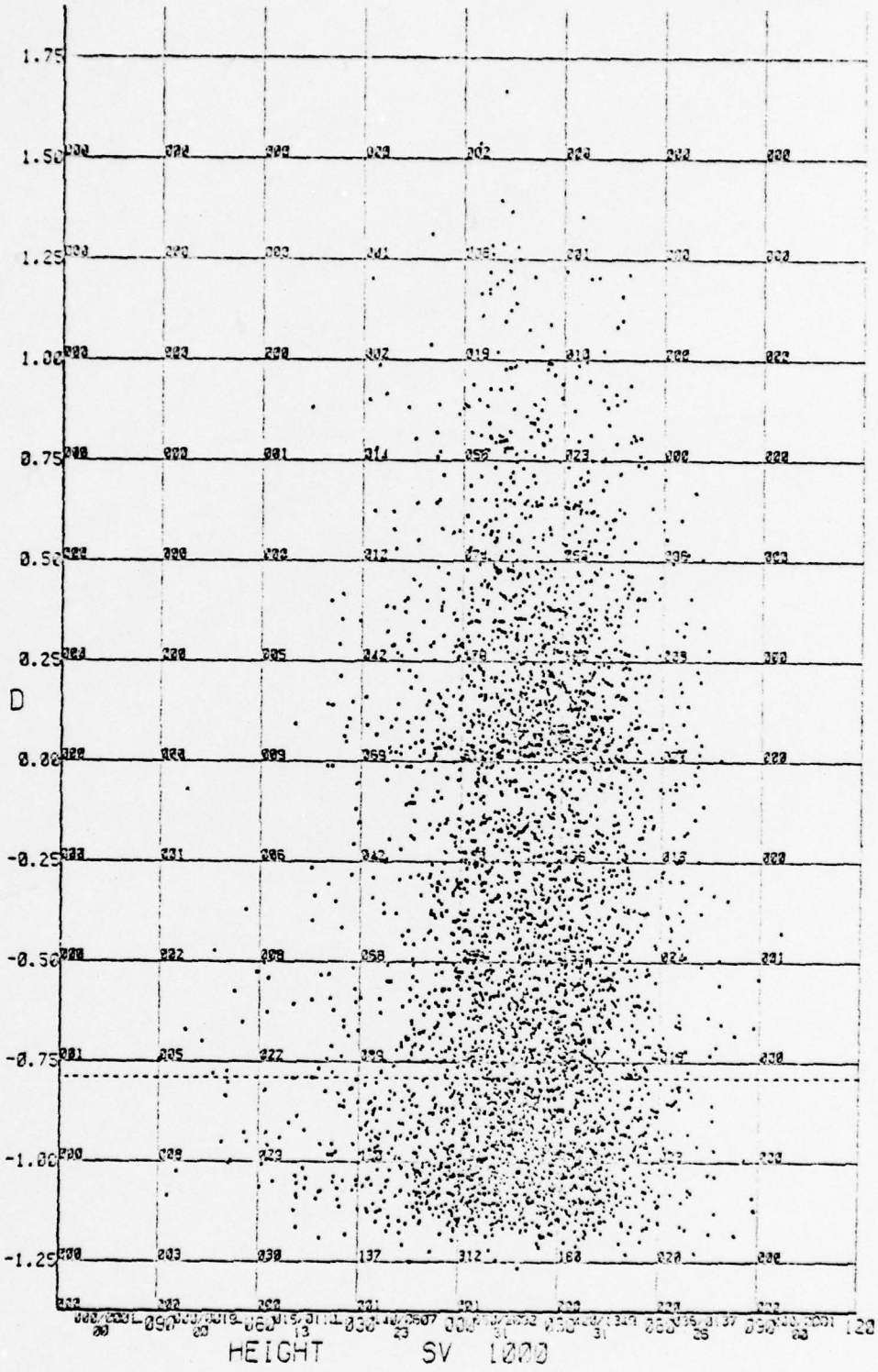

Figure 29. Scattergram of the D Parameter against the SV Height Anomaly in Meters at 1000mb for Zones 1-5.

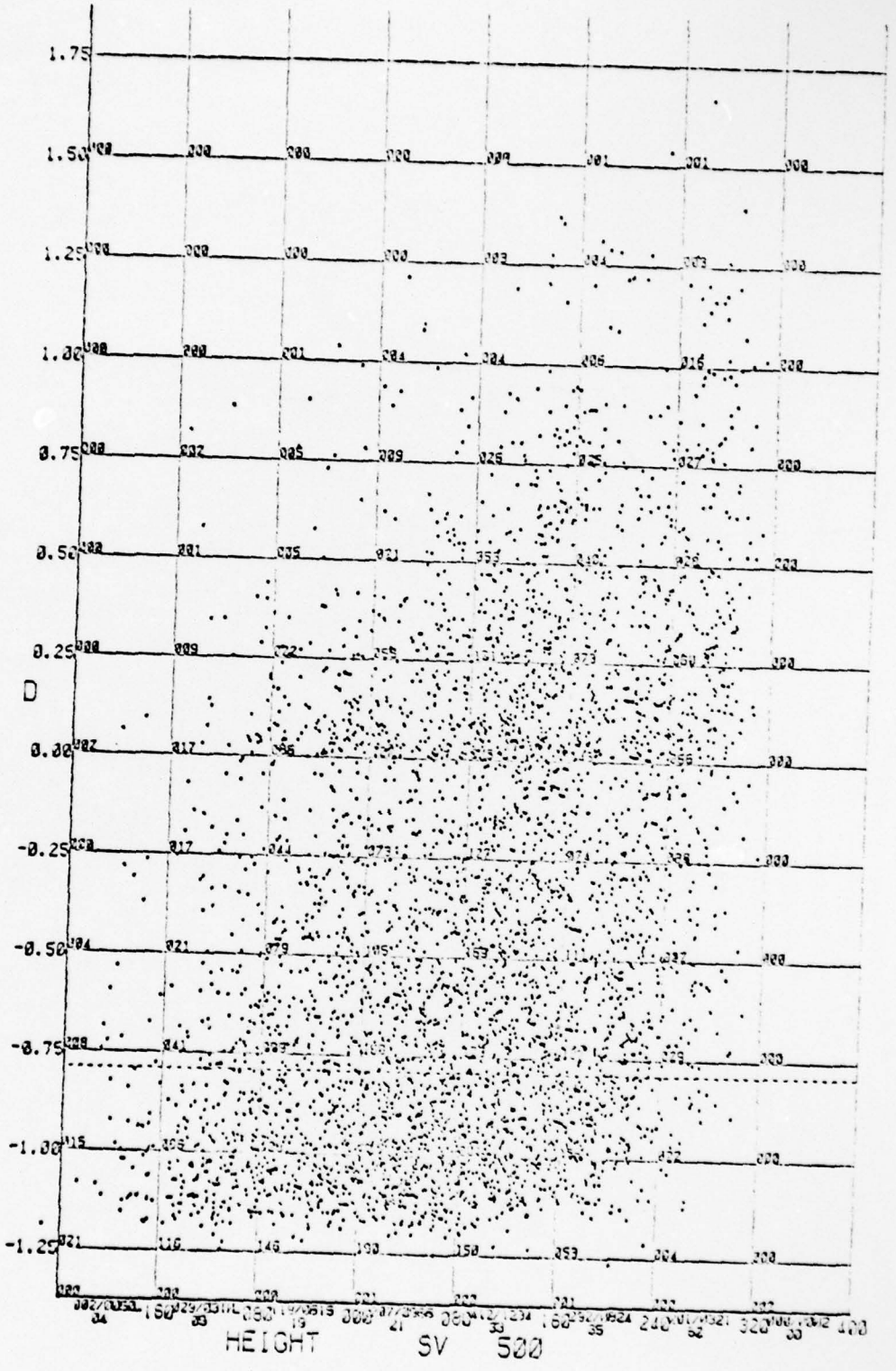

Figure 30. Scattergram of the D Parameter against the SV Height Anomaly in Meters at 500mb for Zones 1-5.

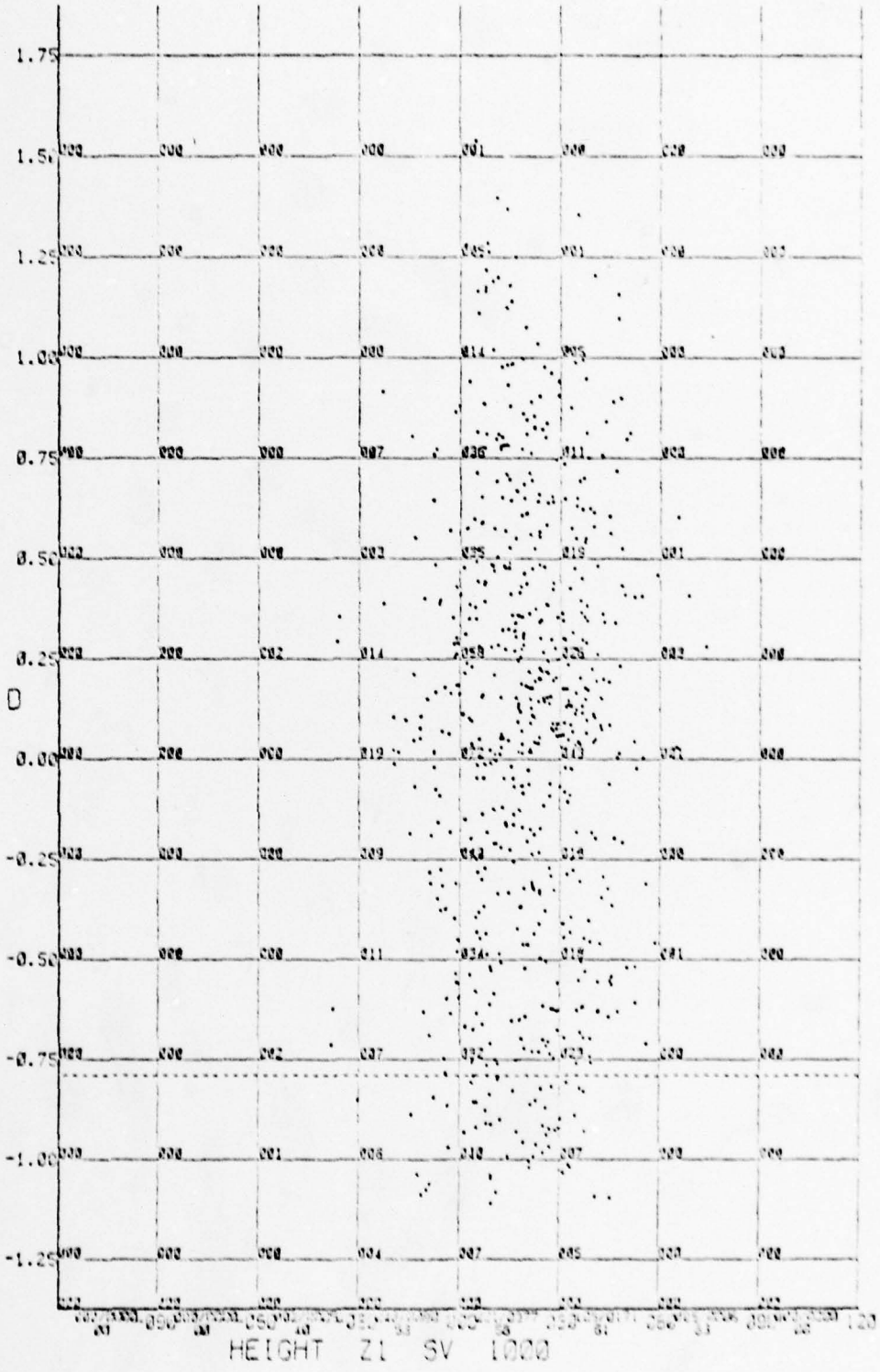

Figure 31. Scattergram of the D Parameter against the SV Height Anomaly in Meters at 1000mb for Zone 1.

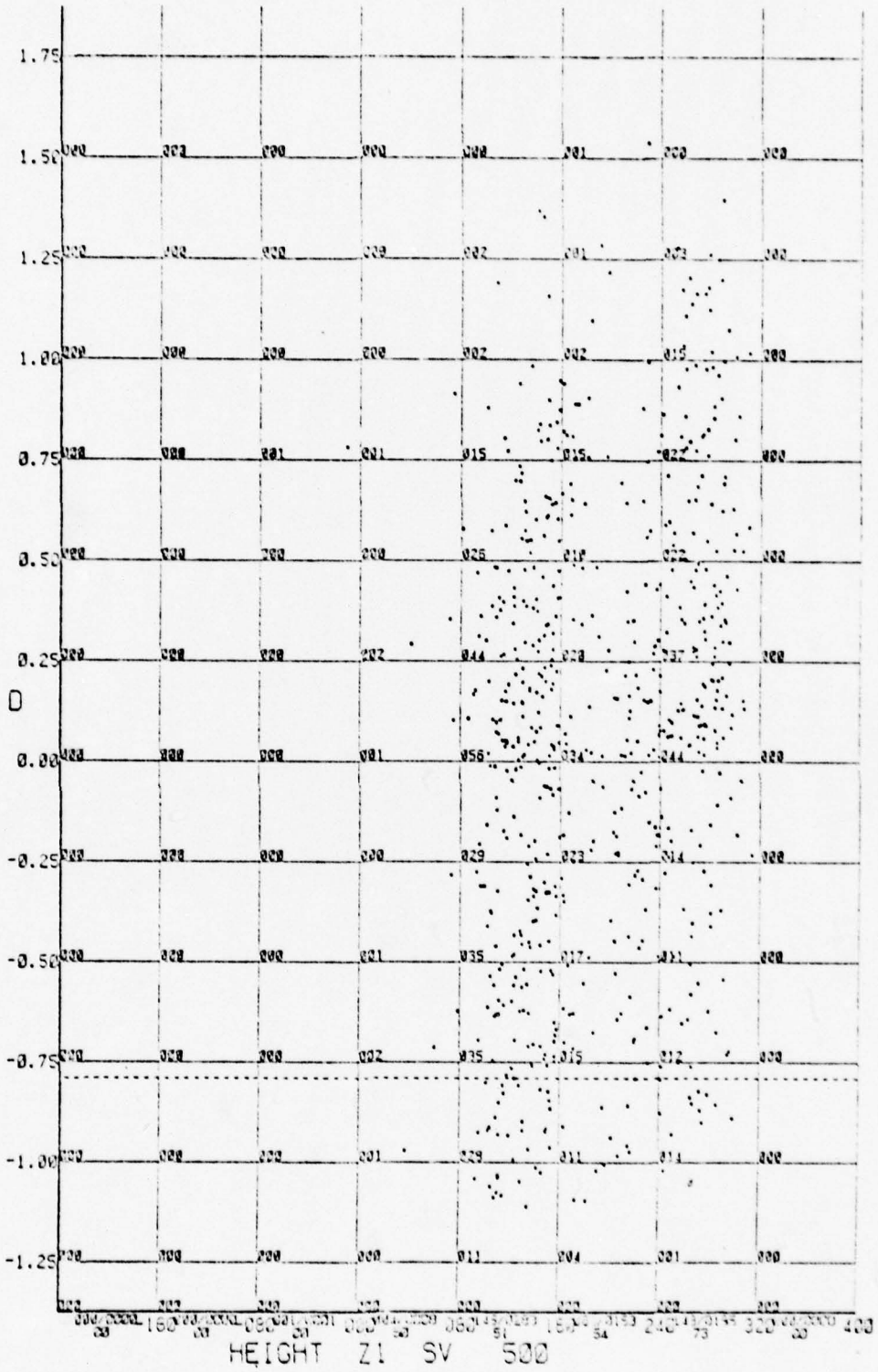

Figure 32. Scattergram of the D Parameter against the SV Height Anomaly in Meters at 500mb for Zone 1.

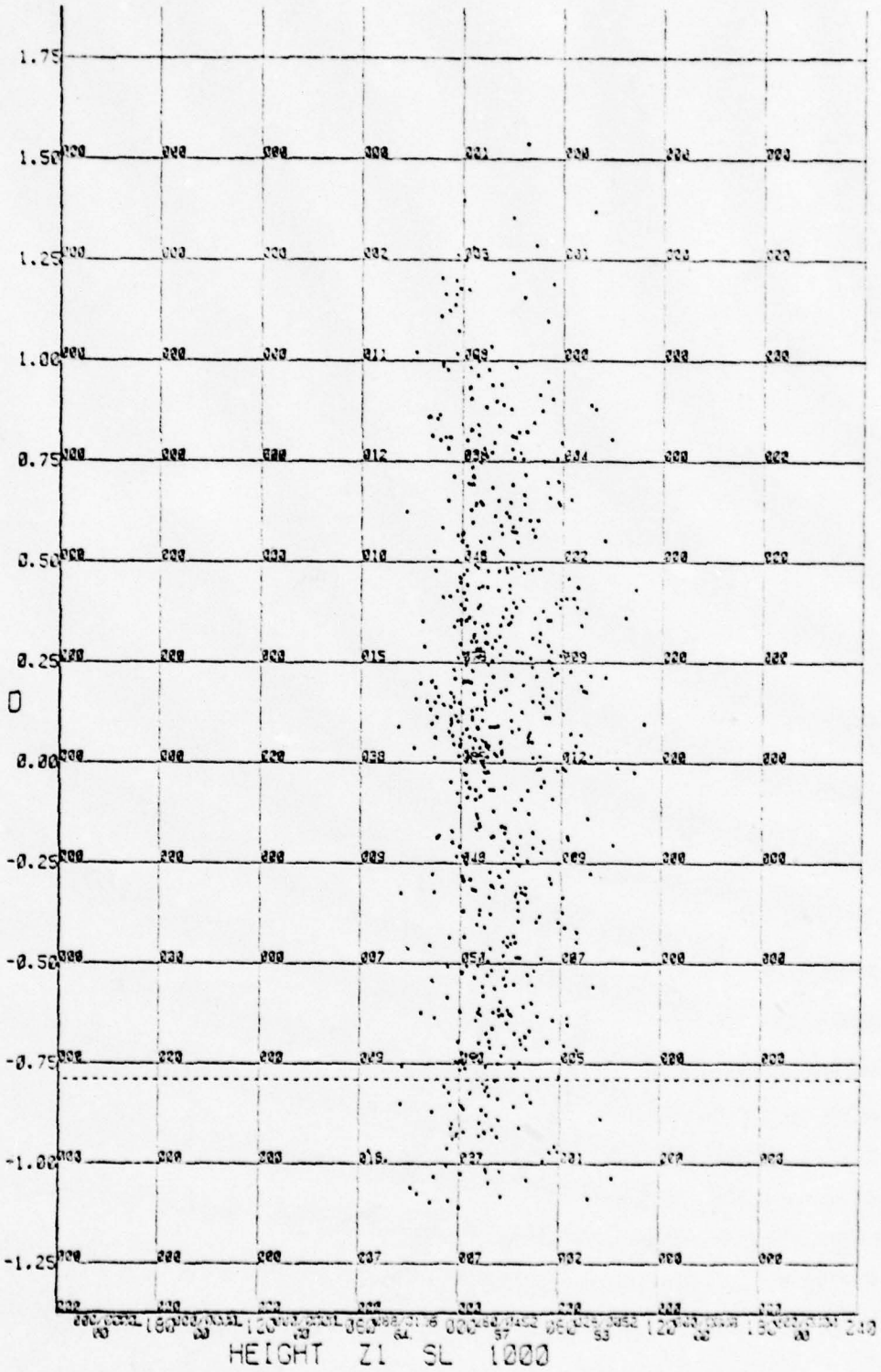

Figure 33. Scattergram of the D Parameter against the SL Height Anomaly in Meters at 1000mb for Zone 1.

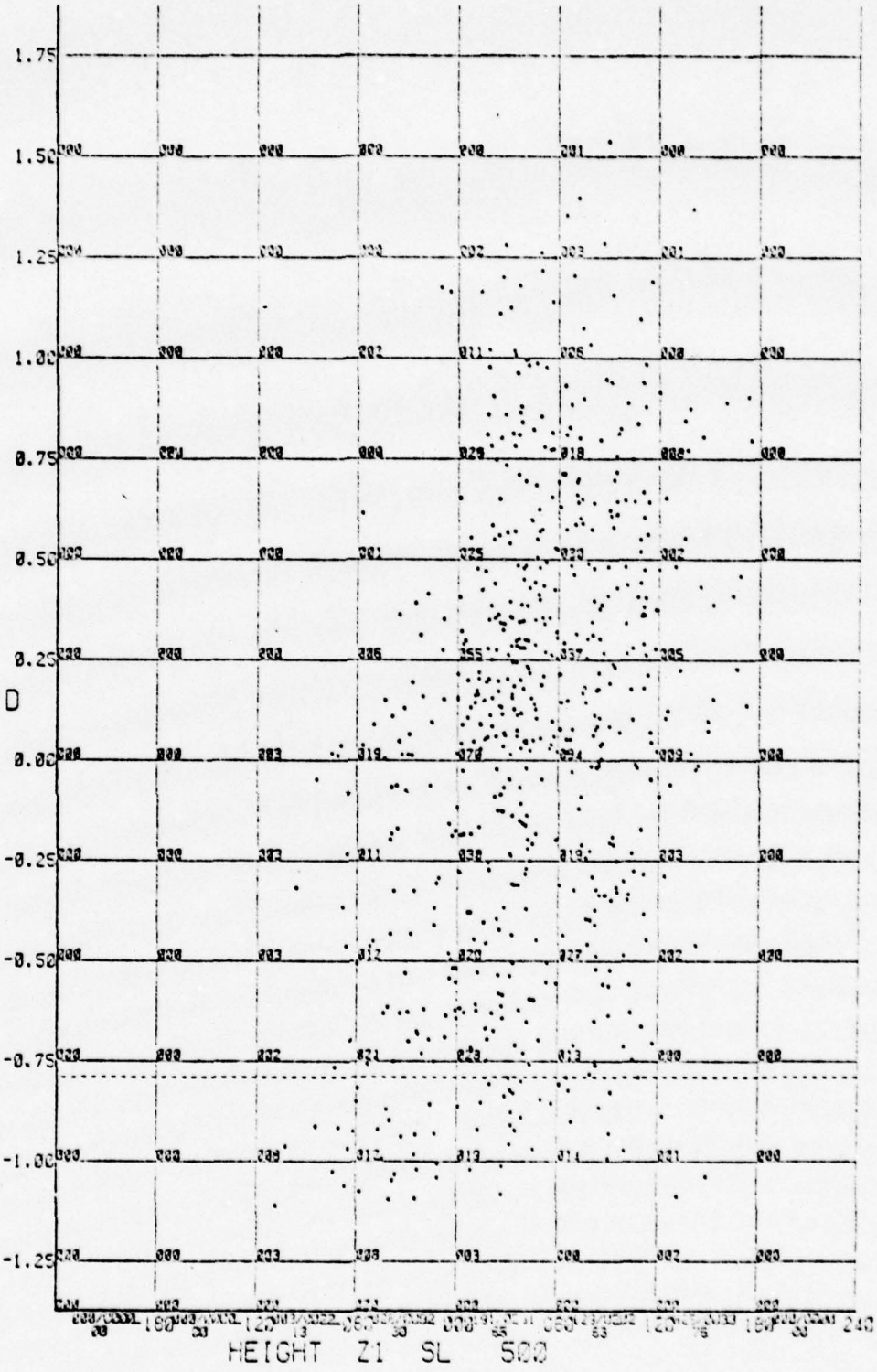

Figure 34. Scattergram of the D Parameter against the SL Height Anomaly in Meters at 500mb for Zone 1.

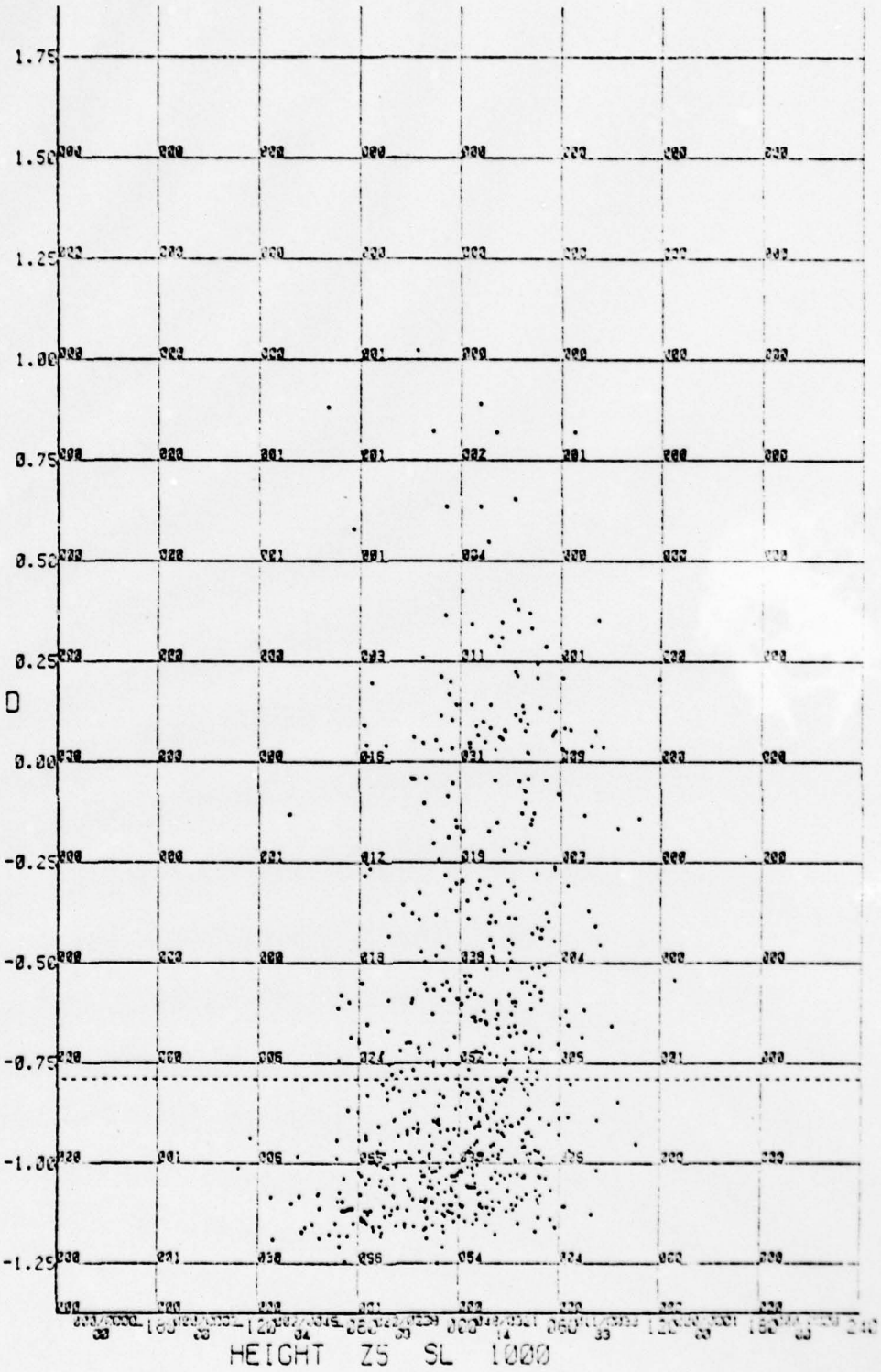

Figure 35. Scattergram of the D Parameter against the SL Height Anomaly in Meters at 1000mb for Zone 5.

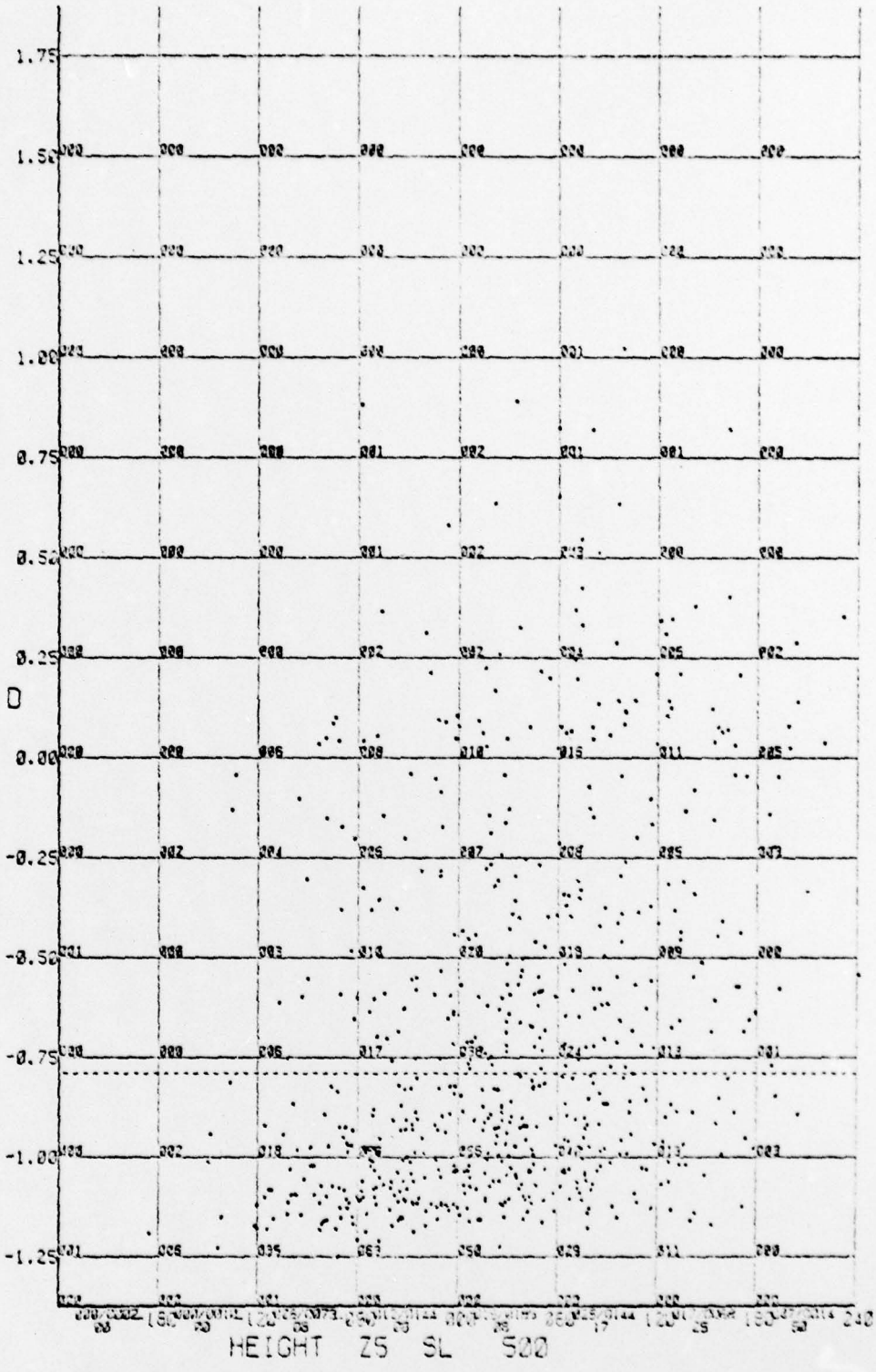

Figure 36. Scattergram of the D Parameter against the SL Height Anomaly in Meters at 500mb for Zone 5.

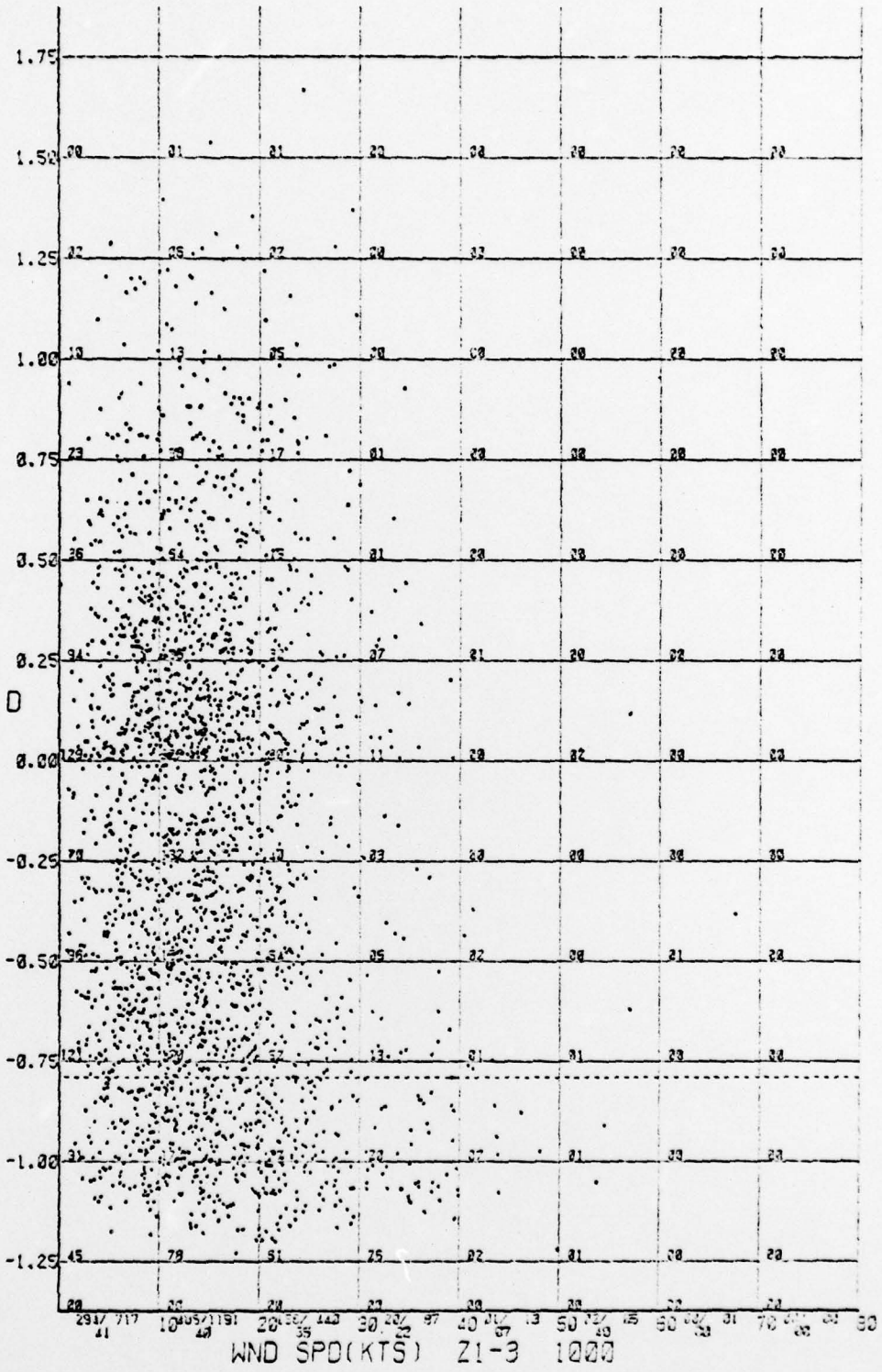

Figure 37. Scattergram of the D Parameter against the Wind Speed in Knots at 1000mb for Zones 1-3.

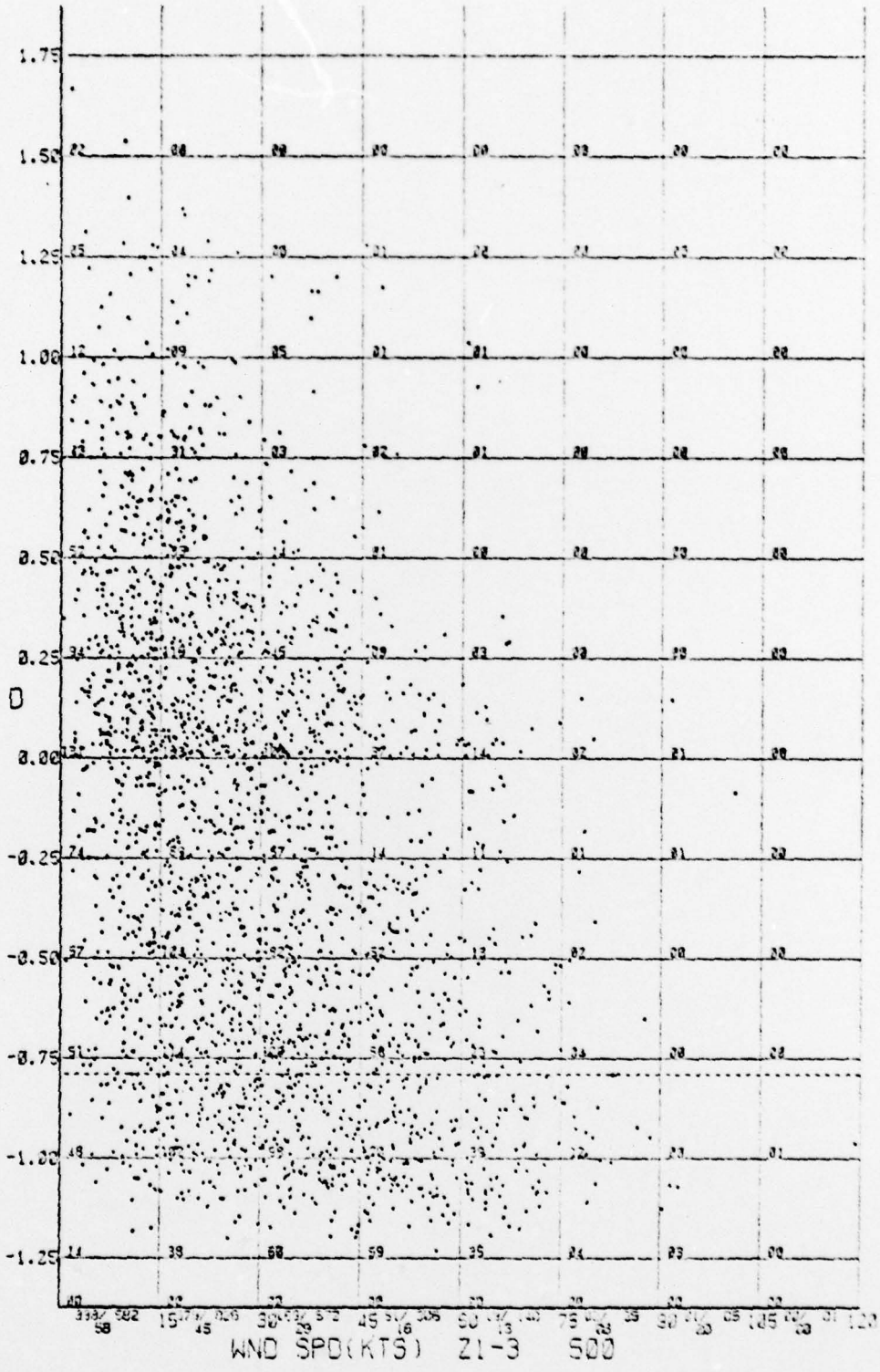

Figure 38. Scattergram of the D Parameter against the Wind Speed in Knots at 500mb for Zones 1-3.

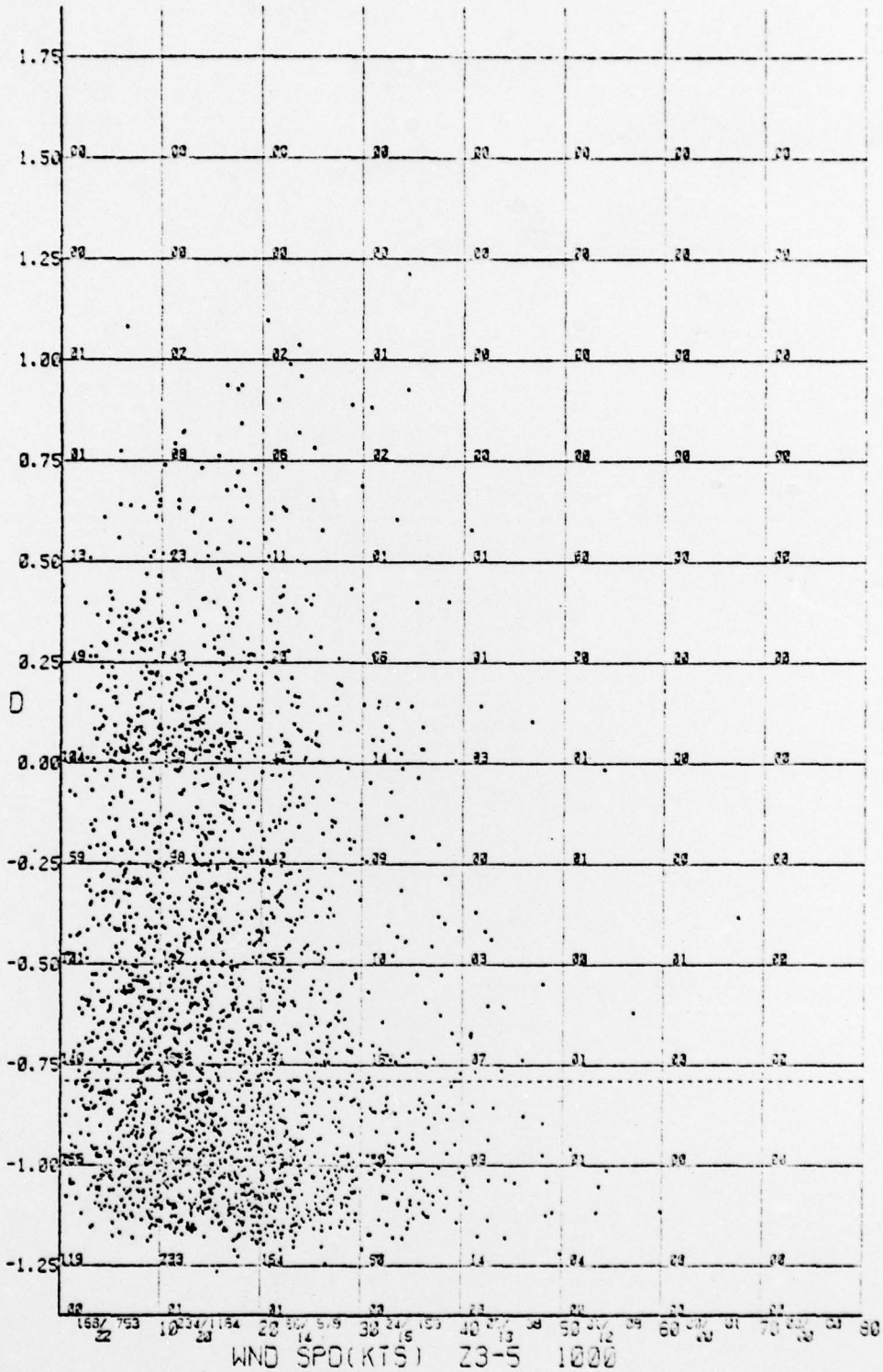

Figure 39. Scattergram of the D Parameter against the Wind Speed in Knots at 1000mb for Zones 3-5.

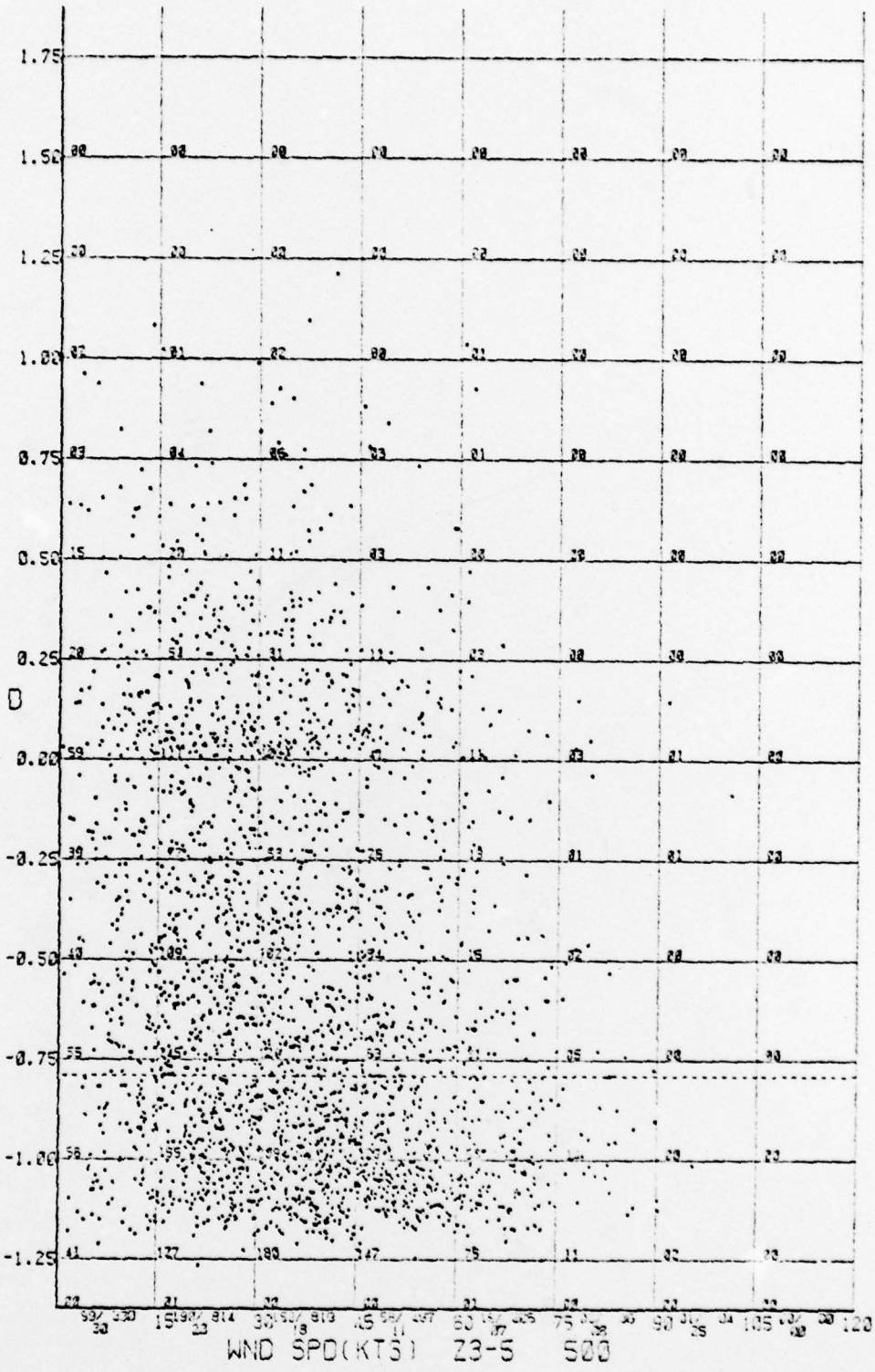

Figure 40. Scattergram of the D Parameter against the Wind Speed in Knots at 500mb for Zones 3-5.

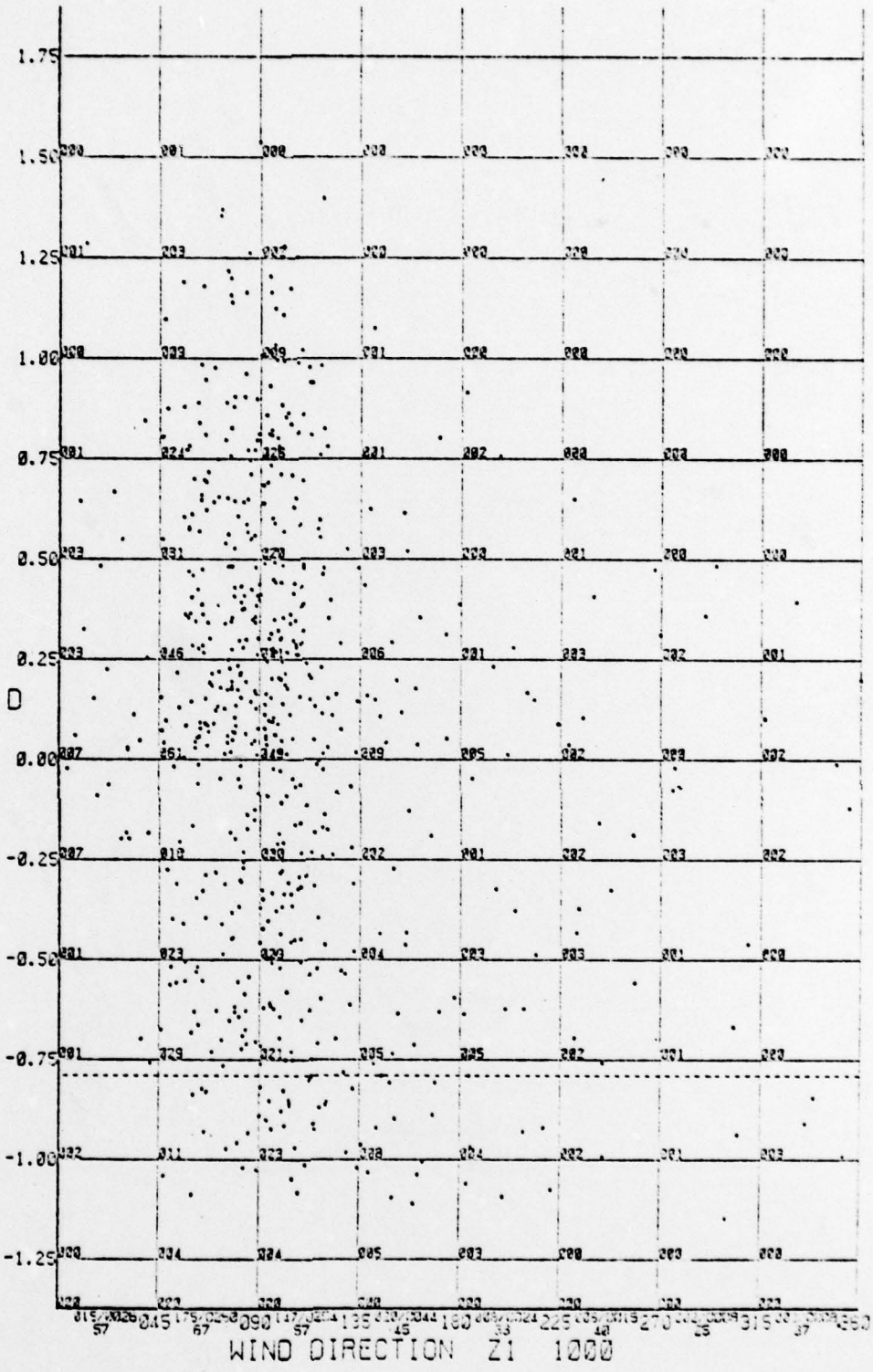

Figure 41. Scattergram of the D Parameter against the Wind Direction in Degrees at 1000mb for Zone 1.

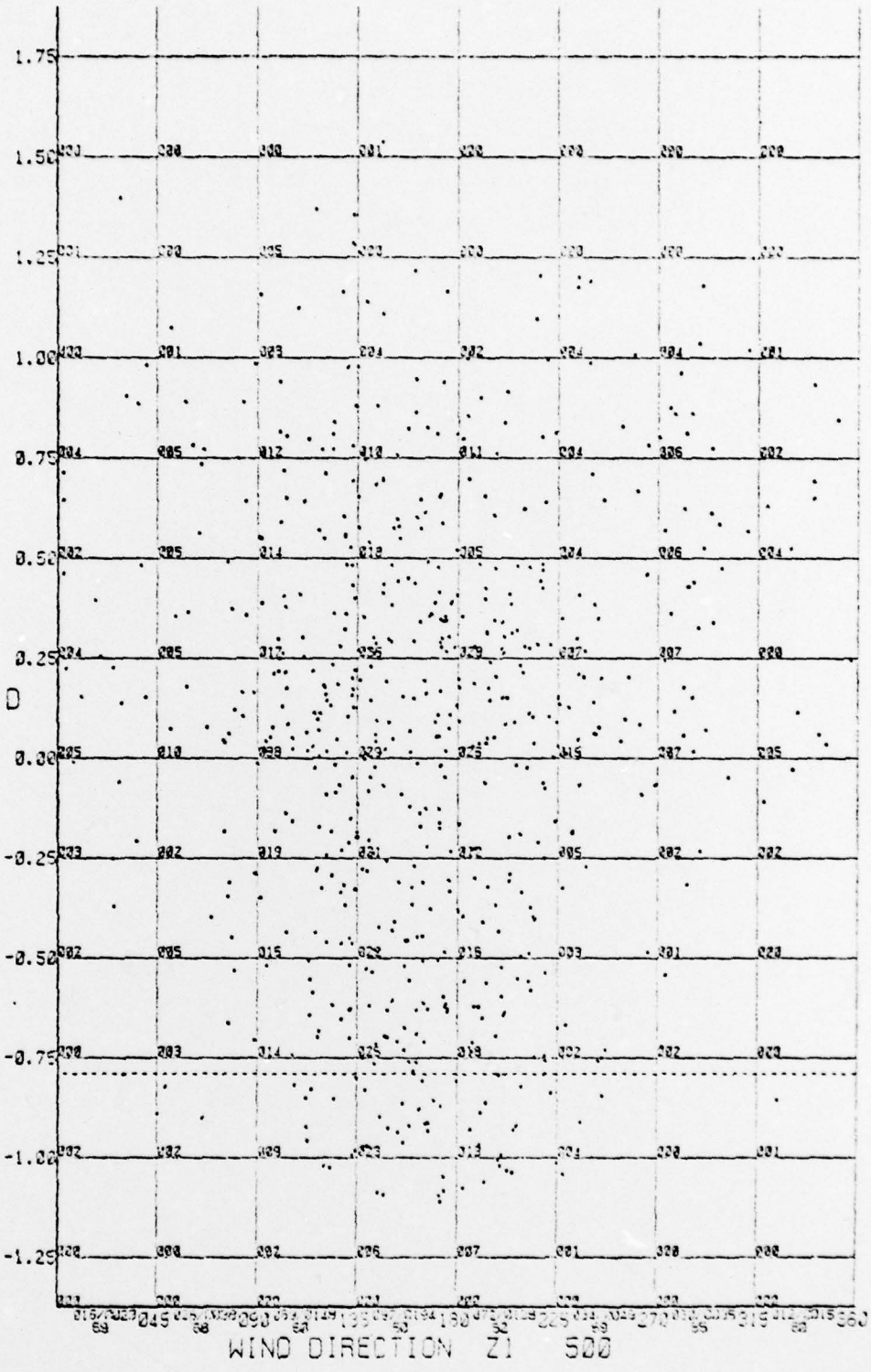

Figure 42. Scattergram of the D Parameter against the Wind Direction in Degrees at 500mb for Zone 1.

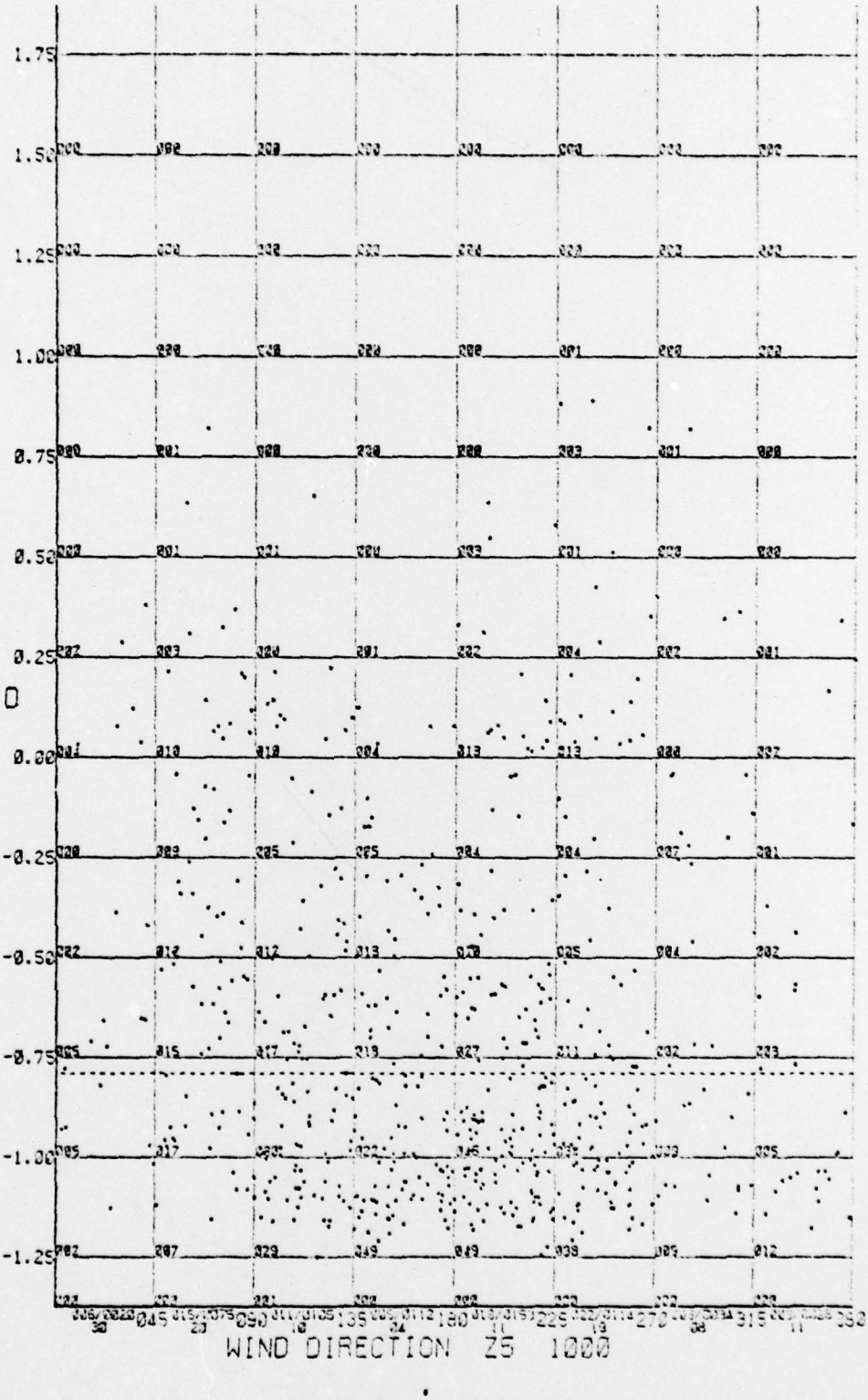

Figure 43. Scattergram of the D Parameter against the Wind Direction in Degrees at 1000mb for Zone 5.

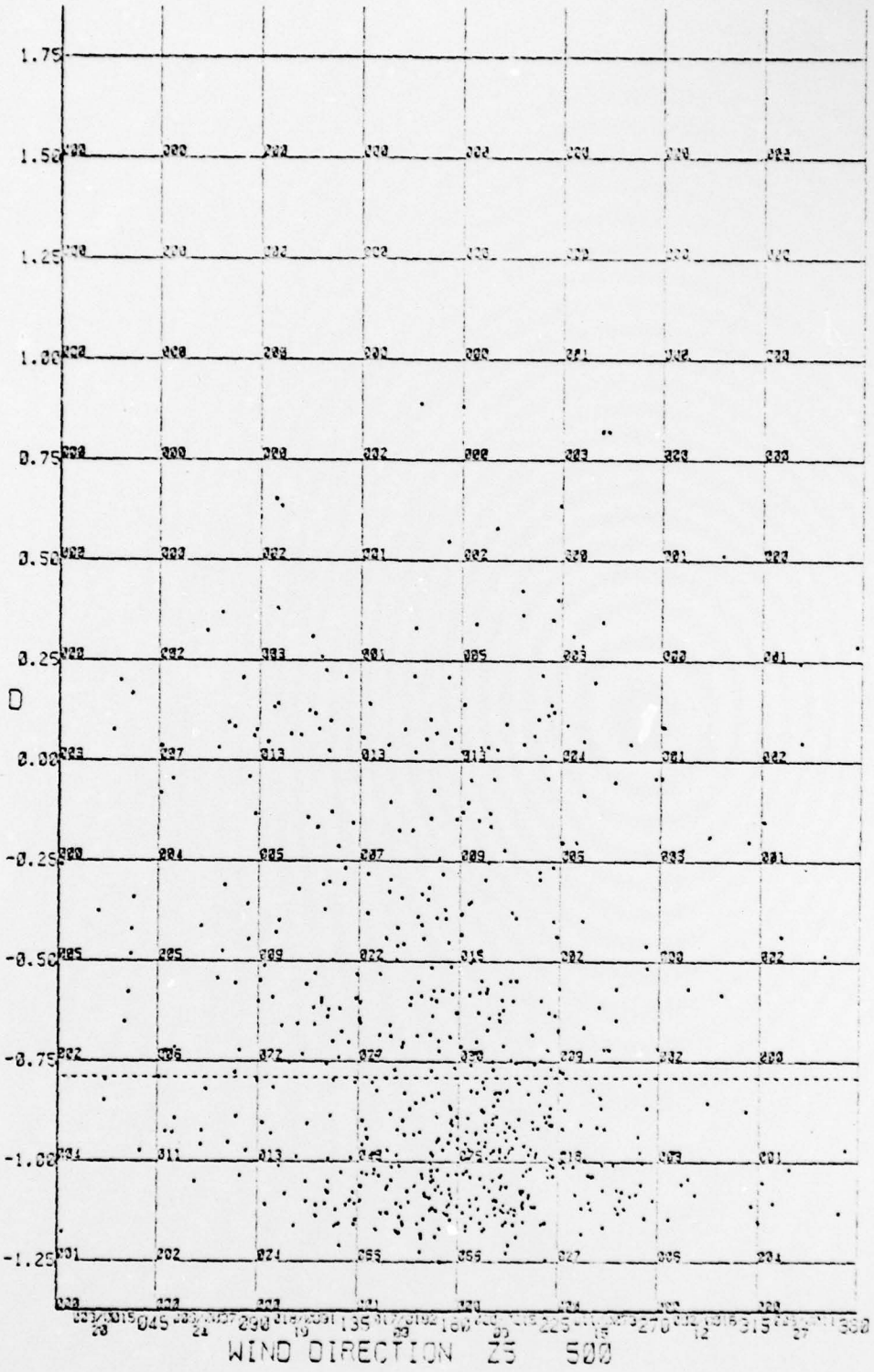

Figure 44. Scattergram of the D Parameter against the Wind Direction in Degrees at 500mb for Zone 5.

6.4 Discussion of Results

The scattergrams and derived statistics presented in Section 6.3 clearly indicate that a correlation exists between refractive structure and the prevailing values of synoptic parameters. Scattergrams of the type shown may be used to determine not only the probability of trapping to be associated with a selected synoptic parameter, but also the probability of occurrence of any desired range of the intensity of refraction. The probability of occurrence of a selected range of D may be determined in relation to a chosen synoptic parameter by using the numbers of occurrences printed on the appropriate scattergram.[4]

It should be noted that the scattergrams given in Section 6.3 represent only a selection of the large number prepared during the course of this investigation. The results shown were chosen to demonstrate that refractive structure does indeed depend on the synoptic situation (as represented by values of synoptic parameters) and that the dependency is capable of statistical representation. Of course, the relationships demonstrated are not independent relationships--for example, low wind speeds are often associated with anticyclonic conditions reflecting, in turn, high values of SL height. Thus, for Zone 1, although a SL_{500} height anomaly of +120 → +180 meters is associated with a trapping probability of 75% (Fig. 34), a 500-mb wind speed of 0 → 15 knots is associated with a trapping probability of 58% (Fig. 38),[5] and a 500-mb wind direction of 270° → 315° is associated with a trapping probability of 85% (Fig. 42), these

---

[4] For operational use these probabilities could be presented in the form of histograms or tables such as Table 5.

[5] Figure 38 shows the wind speed relationship for Zones 1-3.

probabilities cannot be used to determine the probability of trapping if all three conditions are satisfied simultaneously.

Statistical techniques could be applied to determine the amount of covariance explained by each synoptic parameter. In this respect it is likely that synoptic parameters associated with atmospheric levels nearer to the mean trapping height would show a stronger relationship--the 850-mb level for example. The stronger correlations found in Zone 1 compared with more northerly zones reflect, of course, the greater space and time variability of synoptic conditions associated with increasing latitudes; it is likely that more covariance would be explained in terms of small-scale disturbances in the higher latitudes.

7. CONCLUSIONS AND RECOMMENDATIONS

Section 6 establishes that the refractive structure at a given point is related to the values of concurrent synoptic parameters at the same location. Section 5 indicates that, within the limitations of the refractive data base and the resolution capabilities of the analysis techniques, there is no marked relationship between refractive structure and the prevailing synoptic-scale pattern. However the synoptic pattern(s) representing a synoptic situation are essentially isopleths (or gridded fields) of the same synoptic parameters; it must be concluded that the space and time variability of refractive structure is too great to be captured within the imposed limitations. It is possible that a long time-series of refractive profiles and concurrent analyses at, say, 6-hourly intervals would allow a relationship to be established. However, it would seem that the best approach at this stage would be to investigate more thoroughly the relationships between refractive structure and synoptic parameters, applying statistical techniques to radiosonde observations. Such an investigation should utilize the full range of synoptic parameters observed and reported by the radiosonde ascent--not the values derived from analyzed fields. In this way, for example, all reported levels and their associated synoptic parameters could be considered with regard to their contribution toward determining the refractive structure which existed at the time the ascent was made. Having determined the most significant synoptic parameters, quantitative estimates in probabilistic terms could be made for the refractive structure at a location given the actual (or forecast) values of these parameters.

8. REFERENCES

[1] Kalinyak, Paul P., 1977; "Development of a Synoptic Climatology of Tropospheric Refractive Conditions for the Eastern Pacific Ocean off the West Coast of the United States, Tasks One and Two", Final Report (Contract N00228-76-C-3139, Naval Environmental Prediction Research Facility), Meteorology International Incorporated, Monterey, California, 174 pp.

[2] Holl, Manfred M., 1963; "Scale-and-Pattern Spectra and Decompositions", Technical Memorandum No. 3 (Contract N228-(62271)60550), Meteorology International Incorporated, Monterey, California, 28 pp.

[3] Caton, Francis G. et al., 1977; "Technical Description of the Rapid Analogue Selection System including Regionalized Capabilities Applied to the Mediterranean Sea", Final Report (Contract N00228-76-C-3189, Naval Environmental Prediction Research Facility), Meteorology International Incorporated, Monterey, California, 164 pp.

[4] Air Ministry, Meteorological Office, 1962; "Weather in the Mediterranean", London, Her Majesty's Stationery Office, Vol. I, 362 pp., Vol. II, 372 pp.

[5] Palmen, E. and C. W. Newton, 1969; "Atmospheric Circulation Systems", Academic Press, New York, New York, 603 pp.

[6] Byers, H. R., 1959; "General Meteorology", McGraw-Hill Book Company, Inc., New York, New York, Third Edition, 540 pp.

[7] Neiburger, M. et al., 1961; "Studies of the Structure of the Structure of the Atmosphere over the Eastern Pacific Ocean in Summer. I. The Inversion over the Eastern North Pacific Ocean", University of California Press, Berkeley, California, 94 pp.